Steelwork Partially Protected From Post-Flashover Fires In Gypsum Plasterboard Lined Compartments

By

Nick Brown

Supervised by

Dr Charles Clifton (HERA)

Professor Andy Buchanan

Fire Engineering Research Report 07/3
2007

A project submitted in partial fulfilment of the requirements for the degree of Master of Engineering in Fire Engineering

Department of Civil Engineering
University of Canterbury
Private Bag 4800
Christchurch, New Zealand

For a full list of reports please visit http://www.civil.canterbury.ac.nz/fire/fe_resrch_reps.shtml

Abstract

This report extends the step-by-step method of thermal analysis of unprotected steel, to a multi mass system and includes radiant heat transfer between elements.

The analysis was applied to i) partial protection of a beam and to ii) a light-gauge radiation shield around a steel beam. Both the partial protection of the bottom flange, and the light-gauge steel radiation shield improved performance but did not give useful protection against a realistic fire in a gypsum plasterboard lined fire compartment.

The report also formulates a method of thermal analysis for gypsum plasterboard ceilings. This analysis was applied to a gypsum plasterboard ceiling giving protection to a steel beam within the ceiling space. Gypsum plasterboard ceilings were found to give useful protection to steelwork in the ceiling space. The analysis method can be implemented using a spread-sheet analysis, or by using a simplified approach based on the ‘equal area concept’.

Three compartment experimental tests, along with previous furnace data, validates the analysis.

The report also compares the time-temperature curves of the three compartment experimental tests with the Eurocode (and modified Eurocode) Parametric design fires.

Acknowledgements

This research was conducted under the guidance of Dr Charles Clifton (HERA) as my industry supervisor and Dr Andy Buchanan as my University supervisor. I wish to thank both of them for their support and guidance.

I am thankful for the funding by HERA, which enabled the three compartment test fires to be undertaken. I also wish to thank Winstone Wallboards Ltd for their donation of the Gyspum Wallboard used in the tests, and for the release of previous furnace test data used in the analyses. The staff at BRANZ were very helpful and supportive during the compartment testing.

I wish to express a special thanks to Dr Peter Collier, who released his Firebarrier model to me for my use, and who worked diligently on the tedious and painstaking thermocouple installation for the compartments tests. Peter also shared with me his insight into the behaviour of gypsum plasterboard exposed to fire. Peter never failed to respond to my questions and was always constructive with his critique. Hans Gerlich also gave useful comment.

Lastly, but definitely not least, I wish to thank my wife, Shirley, for her patient endurance while, for four and a half years, I have been preoccupied with study.

Table of Contents

Chapter 1 – Introduction

General

The development of a fire in a room or compartment can be separated into the following development stages (Fire Engineering Design Guide[19]): -

- Incipient phase: this is the stage before the onset of flaming, where fuel, close to a heat source, begins to smoulder.
- Growth phase: After the development of flame, a fire typically grows at an exponential rate during the growth phase.
- Flashover: Flashover is the point in time when the fire rapidly spreads to all exposed fuel surfaces throughout the compartment. It is associated with a very rapid rise in temperature throughout the compartment, to temperatures in the order of 1000°C.
- Fully developed stage: After flashover, the fire is controlled by the flow of air entering the compartment through the openings. This is also called the ventilation-controlled phase. The fully developed stage continues while there is sufficient fuel, and sufficient fuel surface area, to consume all the oxygen entering the compartment.
- Decay Stage: The decay stage starts when the oxygen entering the compartment through the openings is only partially consumed by the fire. This stage is also called the fuel-controlled stage.

The pre-flashover stages are important when assessing a safe available escape time from the firecell of origin. The post-flashover stages impact the compartment's structural elements. The post-flashover stages of fire are the focus of this project report.

The ISO[24] standard fire is a time-temperature curve that has been widely used to test materials and components. While ISO standard furnace testing provides a way of classifying and grading fire rated systems and components, the ISO time-temperature curve does not represent typical temperatures of a fire within a gypsum plasterboard lined compartment. Ventilation-controlled fires in gypsum plasterboard lined compartments may be hotter than the standard ISO curve, particularly in well ventilated compartments during the first sixty minutes. As a consequence, the impact on the compartment's fire rated components and structural members may also be more severe.

Fire severity is a concept where a realistic compartment time-temperature curve (design fire) is compared to the standard ISO fire. A fire is said to have an equivalent fire severity of 'X' minutes, when the temperature rise of a fire rated steel member is the same as that for 'X' minutes exposure to the ISO standard fire. If the equivalent fire severity can be established by calculation, then materials and components can be chosen to give the structural elements the required performance during fire, based on standard ISO furnace tests.

Background

Unprotected steel can be analysed using a lumped mass, step-by-step method (Buchanan[6]). The rise in temperature during a small time step is calculated by equating *the energy flow from the fire into the lumped mass* with *the increase in energy (function of temperature) of the lumped mass*. The calculation is repeated for each time step for the full duration of the fire. Once the maximum elevated temperature of the steel has been calculated, the yield stress associated with the elevated temperature can be determined (for instance, using NZS 3404[32], the New Zealand Steel Structures Standard) and then the structural capacity of the steelwork calculated. If the steelwork can support the fire emergency dead and live load (NZS 4203[33]), then the steelwork has an adequate fire resistance rating (FRR).

Typically unprotected steelwork will achieve a fire resistance rating (FRR) of between 15 and 25 minutes. A 30 minute fire resistance rating is difficult to achieve, unless the steelwork has considerable over-strength capacity.

Scope of Research

The objective of the research report is to: -

- Develop a method of analysis that would enable partially protected beams to be analysed, and
- Develop a method of analysis for gypsum plasterboard, to establish the protection that structural steelwork above a gypsum plasterboard ceiling, receives from the ceiling.

The focus of the project is: -

1. Insulation protection of only a portion of the cross-section of a steel beam.
   The lumped mass step-by-step method of analysis is developed into a multi-lumped-mass step-by-step method (typically three masses – top flange, web & bottom flange). To achieve this, the analysis includes radiative heat transfer between the relevant surfaces (beam and compartment surfaces and the fire). The analysis is applied to a 200UB25 universal beam with the bottom of the bottom flange protected with 50mm thick timber.
2. The protection of a steel beam with a thin radiation shield.
   The multi-lumped-mass step-by-step analysis is applied to a 200UB25 universal beam wrapped in a 0.55mm light-gauge steel shield.
3. The protection of a steel beam with a gypsum plasterboard suspended ceiling.
   An energy based analysis of gypsum plasterboard is developed. The analysis is applied to a 13mm GIB ® standard suspended ceiling and a 13mm GIB Fyreline® suspended ceiling.

The protection proposed above is not new and has been proposed previously in the literature: -

- Gibboard Ceilings, Feeney[17]
- Plaster or Mineral Fibre Ceiling Tiles, Proe & Bennetts[38]
- Horizontal or Vertical (Radiation) Screens, Technical Note No 1.7[16]

Three compartment fire experiments were carried out testing each of the above systems. The experimental results are compared with the calculated results. Recommendations for design are suggested.

Project Report Overview

- Chapter 2 presents an overview of the design of unprotected steelwork (NZS 3404[32]). The rational behind the recent increase in the required firecell FRR (Approved Document, Acceptable Solution C/AS1, Department of Building and Housing (DBH), Acceptable Solution[2]) is included in the overview.

- Chapter 3 describes the compartment experiments and summarises the compartments and beam time-temperature results.

- In chapter 4, a multi-lumped-mass step-by-step steel beam analysis is developed both for partially protected steel beams and for steel beams protected with a light-gauge steel radiation shield.

- Chapter 5 compares the calculated and experimental results for the partially protected steel beam.

- Chapter 6 compares the calculated and experimental results for the steel beam protected with a light-gauge steel radiation shield.

Because the minimal protection offered by partial protection, or a light gauge steel radiation shield, is of limited use to the construction and fire-protection industries, chapters 4, 5 & 6 have been kept brief. Chapter 7 is the most relevant section of this report.

- In chapter 7 a gypsum plasterboard analysis model is developed.

- Chapter 8 compares the calculated and experimental results for steel beams protected with a gypsum plasterboard ceiling.

- Chapter 9 discusses design fires, comparing the Eurocode Parametric fires with the time-temperature curves from the three compartments test fires.

- Chapter 10 summarises the conclusions and recommendations.

Chapter 2 – Background

Fire Ratings

Fire ratings are provided to elements of buildings for three main reasons: -

1. To limit fire spread and thus ensure that the occupants have time to escape and that the fire fighters have time to carry out search and rescue operations,
2. To contain the fire, thus preventing the spread of fire to adjacent firecells.
3. To ensure that the structural elements have the capacity to support the fire emergency design load, thus preventing collapse of the building.

The prescriptive fire design code, which is applicable in New Zealand, is the Acceptable Solution, C/AS1[2]. This code prescribes an "F rating", or firecell rating, to meet the first objective above, and an "S rating", or structural endurance rating, to meet the second and third objectives, where the spread of fire, or collapse of the structure, would endanger a neighbour's property. The F rating is based on the time required for fire fighters to respond to an emergency and carry out search & rescue operations. The S rating is based on the burnout time of the firecell.

Prior to the October 2005 amendment, C/AS1 required F ratings as follows: -

- Roofs and single storeyed buildings: 0 minutes,
- Intermediate floors: 15 minutes,
- Two to four level buildings (top level less than 10 metres above, or below, ground level): 30 minutes or 15 minutes if sprinkler protected,
- Escape height up to 25 metres: 45 minutes or 23 minutes if sprinkler protected,
- Escape height up to 58 metres: 30 minutes (must be sprinkler protected), and
- Escape height over 58 metres: 60 minutes (must be sprinkler protected).

ISO Fire

The ISO standard fire[24] is a time-temperature curve that is used to test the fire resistance of building elements or components. An element that fails at 47 minutes in the standard ISO furnace test is said to have a 47 minute FRR (fire resistance rating). The ISO standard fire provides a repeatable method of testing, and comparing, building elements. However, the performance of a building element in the standard ISO furnace may not necessarily model the element's performance in a realistic compartment fire.

Realistic Compartment Fires & Equivalent Fire Severity

For gypsum plasterboard lined compartments, the compartment temperatures typically reach 900°C within a minute or so after flashover and climb to over 1000°C within 10 to 15 minutes. The ISO standard fire, by comparison, reaches 735°C at 15 minutes and 840°C at 30 minutes. Fires within gypsum plasterboard lined compartments tend to be significantly harsher, than the standard ISO fire, on building elements that have a fire resistance rating (FRR) of less than 60 minutes.

Different fires are said to have the same equivalent fire severity if they have the same impact on a building element. Thus, if a building element, which fails at say 60 minutes in the standard ISO furnace, is on the point of failure, at some instant, during a compartment fire or a design fire (i.e. a time-temperature curve: growth, fully-developed and decay stages), then the given time-temperature curve fire is said to have an equivalent fire severity of 60 minutes. 15 minutes of a quickly developing, intense, short-duration fire may therefore potentially have an equivalent fire severity of up to 40 minutes.

Revised F Ratings

In October 2005, the New Zealand prescriptive fire design code, C/AS1, recognised that fires in modern construction consisting of gypsum plasterboard lined compartments are significantly more severe than the standard ISO fire. Accordingly the required F rating for buildings was increased. To ensure an actual survival time for Fire Service search and rescue a higher FRR is now required. The basis and background of the increase in the F ratings is given by Nyman[31], Gerlich et al[21], and also in the BIA's 'Proposed Changes to The Approved Documents for Fire Safety Clauses of the Building Code'[5]. The new F ratings depend on the compartment's fire load, as well as purpose group and building height. The prescribed F ratings are now as follows: -

- Roofs and single storeyed buildings: 0 minutes,
- Intermediate floors: 30 minutes, or 15 minutes if sprinkler protected.
- Two to four level buildings (top level less than 10 metres above or below ground level): between 45 and 60 minutes (or between 22 and 30 minutes if sprinkler protected),
- Escape height up to 25 metres: between 45 and 90 minutes (or between 23 and 45 minutes if sprinkler protected),
- Escape height up to 58 metres: between 30 and 45 minutes (must be sprinkler protected), and
- Escape height over 58 metres: between 60 and 90 minutes (must be sprinkler protected).

If a compartment, and it's supporting members, can survive the burnout period of a compartment, then unlimited time is available for the fire fighter's search and rescue operations. However, because of the uncertainty involved in analysis and design, the DBH's Acceptable Solution, C/AS1, requires that a steel beam be designed for the higher of the F rating and the S rating. If an Alternative Solution includes a more thorough and

rigorous analysis, then, with the approval of the authority having jurisdiction, the lesser of the F rating and the S rating could be used for design.

Steel Beam Design

Steel beam design involves firstly a thermal analysis to determine the temperature(s) in the beam and then secondly a structural analysis to determine whether the steel beam can support the fire emergency load.

The thermal analysis can be based on either: -

- The ISO standard fire, using the equivalent fire severity concept, or
- A design fire based on the fuel load, the ventilation, and the properties of the compartments linings. Examples of design fires are the Swedish curves[35] or one of the Eurocode parametric fire [13, 9, 37].

Further, the thermal analysis may either be a simplified analysis, calculating the average temperature of the steel beam, or it may be a more thorough analysis, calculating the temperature distribution across the cross-section.

The yield stress of steel is a function of temperature. The yield stress of steel and thus the section capacity can be calculated following the thermal analysis. If the steel beam capacity can sustain the fire emergency loads then the beam has an adequate fire resistance rating. The fire emergency load is specified in NZS 4203[33] as the dead load plus the long-term live load.

NZS 3404 [32], the Steel Design Code, uses a simplified design approach. Firstly the ratio of fire emergency load to ambient beam capacity is calculated. Based on this ratio, a limiting beam temperature is calculated, which is the temperature at which the steel beam supporting the fire emergency load will fail. The time for the beam to heat up to this limiting temperature is then evaluated based on an empirical formula. The empirical formula is based on the ISO standard fire and is a function of the Hp/A factor (heated

perimeter/cross sectional area). The lower the Hp/A factor, the slower the rate of temperature increase. The Hp/A ratio may be lowered by using a heavier or stockier member or by reducing the surface area that is exposed to the fire, for instance by burying the beam within the depth of a floor so that only the bottom flange is exposed.

A more sophisticated analysis would: -

1. Select a design fire based on a realistic or representative time-temperature curve, such as one of the Eurocode Parametric fires [13, 9, 37],
2. Calculate the distribution of temperature across the steel beam cross-section (possibly by dividing the steel cross section up into elements, as in a finite element analysis),
3. Calculate the steel yield stress across the cross-section,
4. Calculate the section moment capacity, based on a plastic analysis, and
5. Compare the section moment capacity at the elevated temperature with the required moment capacity associated with the fire emergency load.

The section moment capacity may need to be calculated at various times throughout the duration of the fire to ensure that the worst possible instant has been considered.

An Example

The experiments carried out as part of this project involved 200UB25 steel beams in a 2.400m wide by 3.600m long by 2.400m high compartment with a 1.200m wide by 2.000m high opening. The fire load for tests 1 and 3 was 400 MJ/m^2 (Fire Hazard Category 1).

The Acceptable Solution, C/AS1[2]

1. The required F rating, for a compartment on a second or third floor is 45 minutes.

2. The S rating is calculated as follows: -
    - Ah/Af = 0.00
    - Av/Af = 0.28
    - The S rating from table 5.1 is 30 minutes.

The required FRR (Fire Resistance Rating) is either the F Rating or the S Rating, as required by the Acceptable Solution, C/AS1. The F rating is required to give adequate time for fire-fighting search and rescue operations. The S rating is required for support of the building and the exterior walls.

Gypsum Plasterboard Protection

1. To achieve the required fire rating, the steel beam could be wrapped in a GIB® plasterboard product. The GIB® Fire Rated Systems booklet[45] requires the beam to be wrapped in two layers of 13mm GIB Fyreline®, to achieve a 60/-/- FRR.

2. Alternatively the steel beam could be positioned above a fire rated ceiling. Options are: -
    - 45/45/45 FRR: one layer of 13mm GIB Fyreline® on timber joists to Winstones Wallboards Ltd specification GBFC 45.
    - 60/60/60 FRR: two layers of 13mm GIB Fyreline®, or one layer of 16mm GIB Fyreline®, on a suspended ceiling system to Winstones Wallboards Ltd specification GBSC 60a or GBSC 60b respectively.
    - 45/45/45 FRR: two layers of 13mm GIB Fyreline on any supporting system to Winstone Wallboards Ltd specification GBUC 45.

Unprotected Steelwork - NZS 3404 Analysis

For our example 200UB25s will be assumed to be at 3.5m centres, spanning 5.400m supporting a classroom or cafeteria. Calculations, based on NZS 4203 [33] and NZS 3404 [32], are as follows: -

- Dead load 0.5 kPa
- Live Load 3.0 kPa
- Ultimate Limit State Load = 1.2 G & 1.6 Q = 5.4 kPa
- Fire Emergency Load = G & Qu = G & ψ_l Q = 1.7 kPa (ψ_l = 0.4)
- The ratio of design actions r_f = 1.7/5.4 = 0.314
- The limiting Temperature = 906 – 690 r_f = 688 °C = 961 K
- Exposed surface area of a 200UB25 = 0.793 m^2/m (3 sided exposure)
- Mass of 200 UB25 = 0.0254 tonnes/m
- SF = exposed surface area to mass ratio = 31.2 m^2/tonne
- t, the time at which the limiting temperature is reached

  = -5.2 + 0.0221 T_l + 0.433 T_l / SF = 19.6 minutes.

Alternative Thermal Analysis: Step-By-Step Method: ISO Standard Fire

The step-by-step method of thermal analysis is more accurate than using the NZS 3404 empirical formula that relates time to Hp/A and temperature rise. This analysis uses the standard ISO fire and thus it still relies on the equivalent fire severity concept. Figure 2.1 illustrates the Step-By-Step method of analysis of the 200UB25 subjected to the ISO fire.

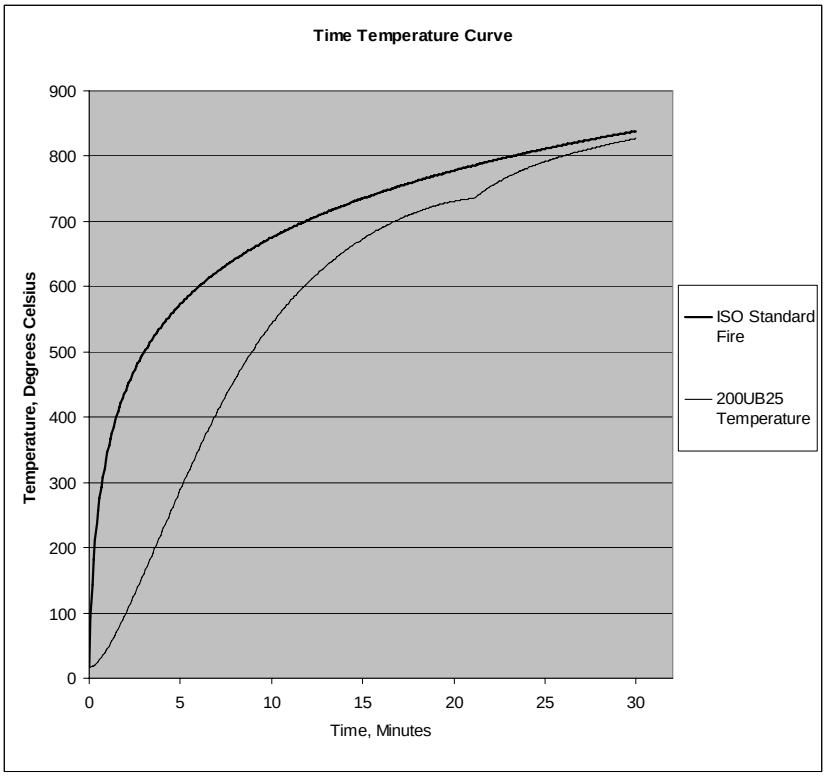

Figure 2.1 Time Temperature Curve for 200UB25 Subjected to the ISO Fire

The limiting temperature of 688 °C was reached at a time of 15.9 minutes (cf 19.6 minutes using the NZS 3404 regression formulae).

Alternative Thermal Analysis: Step-By-Step Method: Eurocode Parametric Fire

This design method is more rigorous both in terms of the design fire and the thermal analysis. Possibly, such an analysis would allow the lesser of the F Rating and the S rating to be used in the proposed construction. Figure 2.2 graphs the result of the Step-By-Step method on the 200UB25 subjected to the Eurocode Parametric Fire (2001) (the fuel load and ventilation is given on page 10). The limiting temperature of 688 °C was reached at 11.6 minutes. The maximum temperature reached was 1042 K (767 °C). If the weight of steel section was increased so that the ratio of design actions was 0.2, then the steel beam would survive the Eurocode Parametric design fire.

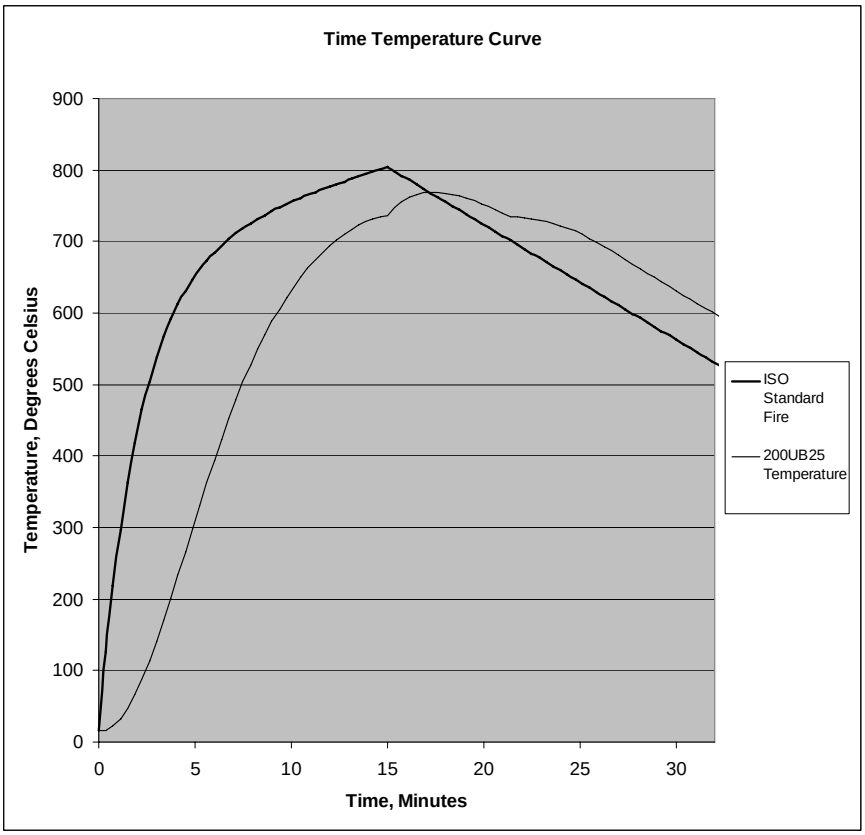

Figure 2.2 Time Temperature Curve for 200UB25
Subjected to the Eurocode Parametric Fire

Summary

Analysis of the unprotected 200UB25, using either the NZS 3404 design method, the step-by-step method with the ISO fire, or the step-by-step method with the Eurocode Parametric fire, gives the same result. The unprotected 200UB25 will not achieve a 30 minute (or 45 minute fire rating) thus the 200UB25 will require additional protection.

Chapter 3 - Full Scale Compartment Experiments

Introduction

Three full scale compartment tests were carried out as part of this study. The tests were to simulate a hotel room or a small office in a multi-storey building, where steel beams supporting the floor above, have protection from a suspended gypsum plasterboard ceiling. The first test, FQ5013_1, had a 13mm GIB® Standard ceiling, with a design fire load of 400 MJ/m^2. The second test, FQ5013_2, had a 13mm GIB Fyreline® ceiling, with a design fire load of 800 MJ/m^2. The third test, FQ5013_3, had a 13mm GIB Fyreline® ceiling, with a design fire load of 400 MJ/m^2.

The construction details and other test details follow in the next paragraph. The tests were loosely based on the experiments by Nyman[31], so that the test data would complement Nyman's data. The gypsum plasterboard wall lining was designed to be more robust that the ceiling, so that the compartment ventilation conditions would not change when the ceiling collapsed.

General

Enclosure Construction

The compartment was constructed in concrete blockwork with a 150mm precast concrete roof and a 100mm insitu concrete floor on grade as shown in Figures 3.4 and 3.5. The internal dimensions were 2.600m wide by 4.000m long by 2.800m high. Openings were constructed in each wall primarily for access, but also for the future versatility of the compartment.

Within the block enclosure a room 2.400m wide by 3.600m long by 2.400m high was framed out and lined with gypsum plasterboard. The geometry and drywall linings were similar to the tests by Nyman[31]. The walls were framed with 100x50 timber framing at 600 centres and were lined with 13mm GIB Fyreline®, from floor to the underside of the concrete roof above.

The GIB® Standard (or GIB Fyreline®) ceiling was fixed to a suspended Rondo grid, the Rondo battens running across the width of the compartment at a maximum of 600mm centres. The gypsum plasterboard sheets ran along the length of the building. There was one end joint on each side of the compartment. The side edges of the plasterboard were butted together without back-blocks. All joints were stopped.

The ceiling space was divided into two spaces with a 13mm GIB Fyreline® bulkhead running along the length of the compartment. On the left hand side, four 125mm diameter holes were cut in the ceiling. These represented unprotected openings such as down-lights or ventilation grills. On the right hand side, the ceiling was a sealed barrier to smoke and hot gases.

Fuel

Nyman[31] started his fires with methylated spirits on tissue paper on a mock sofa. The same steel-framed sofa, with olefin covered polyurethane cushions, was used for these tests. The fuel load of the sofa was approximately 314 MJ which equates to 36 MJ/m^2 fire load. The remainder of the fuel was made up with timber cribs, which again matched the tests by Nyman[31] with respect to timber stick size and spacing. After the slow growth rate of the first fire test, additional polyurethane foam was

used for both the second and third tests. Details of the fuel are given below in each of the test descriptions.

The design fire load energy density (FLED) was 400 MJ/m^2 for the first and third tests. This is the appropriate FLED for fire hazard category 1 firecells, as defined in the Department of Building and Housing's (DBH's) Acceptable Solution, C/AS1[2]. Fire hazard category 1 applies to residential dwellings, apartments, hotels, etc.

The design FLED for the second test was 800 MJ/m^2, which is the design FLED that applies to fire hazard category 2 firecells. Offices are categorized as fire hazard category 2 in the Acceptable Solution, C/AS1[2].

Steel Beams

In each test, four short lengths of 200UB25 Universal Beam were bolted to the concrete so that the temperatures of the flanges and webs could be measured.

- Beam A was above the gypsum plasterboard ceiling on the right hand side of the ceiling space bulkhead.
- Beam B was above the gypsum plasterboard ceiling on the left hand side of the ceiling space bulkhead, where the four 125mm dia holes were cut in the ceiling.
- Beam C was erected below the gypsum plasterboard ceiling towards the front. A 0.55mm light gauge galvanised steel shield was placed around the steel beam.
- Beam D was erected below the Gib® ceiling towards the rear. 150x50 timber was bolted to the underside of the bottom flange of this beam.

Thermocouples

Thermocouples were placed to measure the temperature of the steels beams and the air and surface temperatures each side of the beams. The thermocouple position is shown in Figures 3.1 and 3.2. The thermocouple numbers are listed in Appendix 1, Table A1.1.

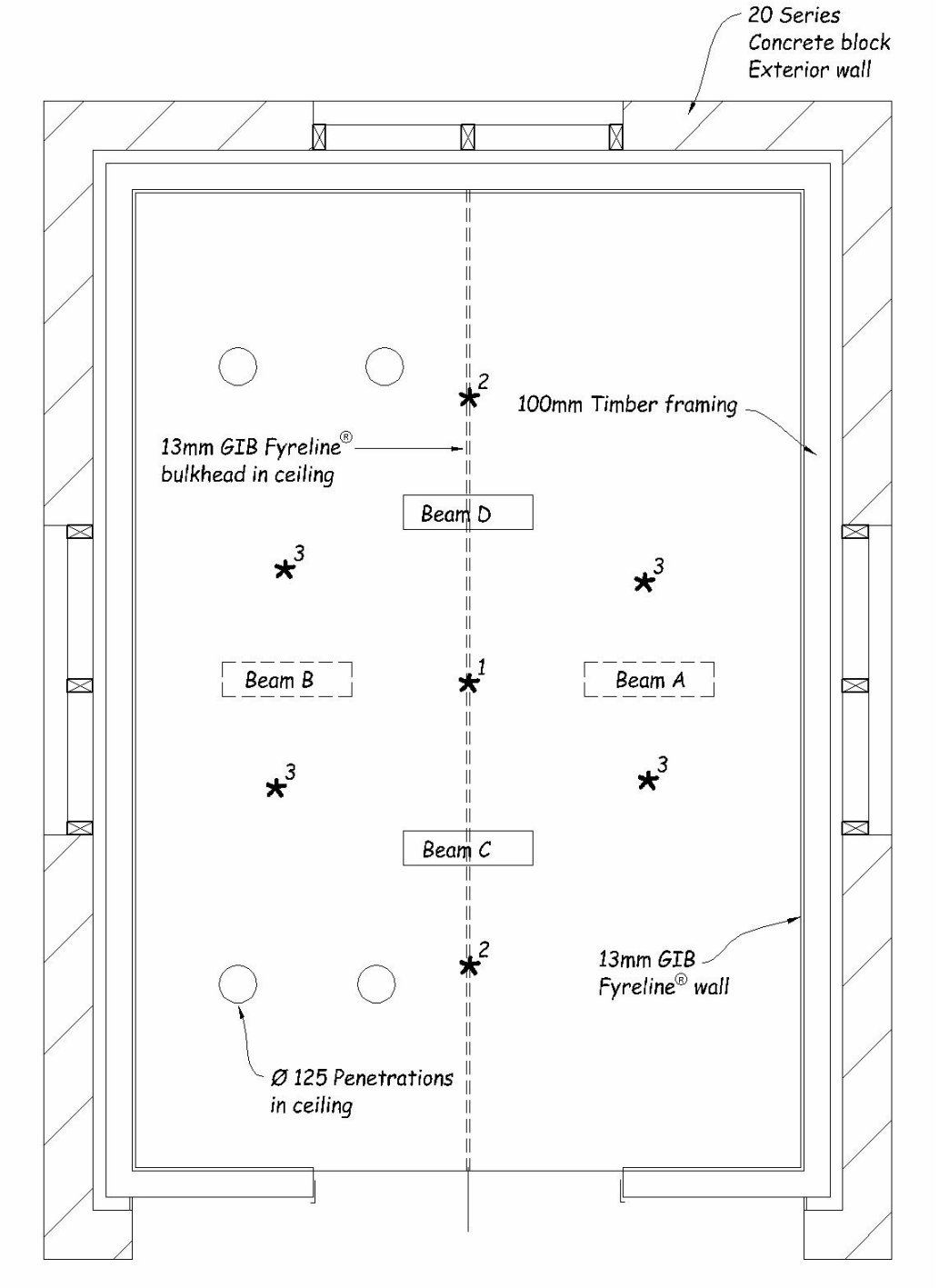

Figure 3.1 Reflected Ceiling Plan Showing Thermocouple Locations

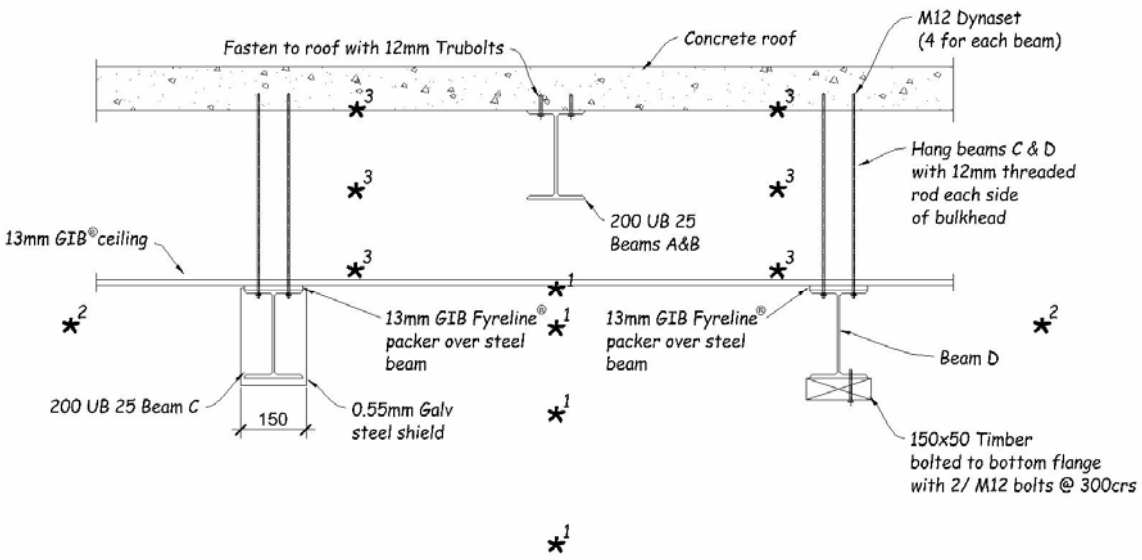

Figure 3.2 Section Through Beams Showing Thermocouple Locations

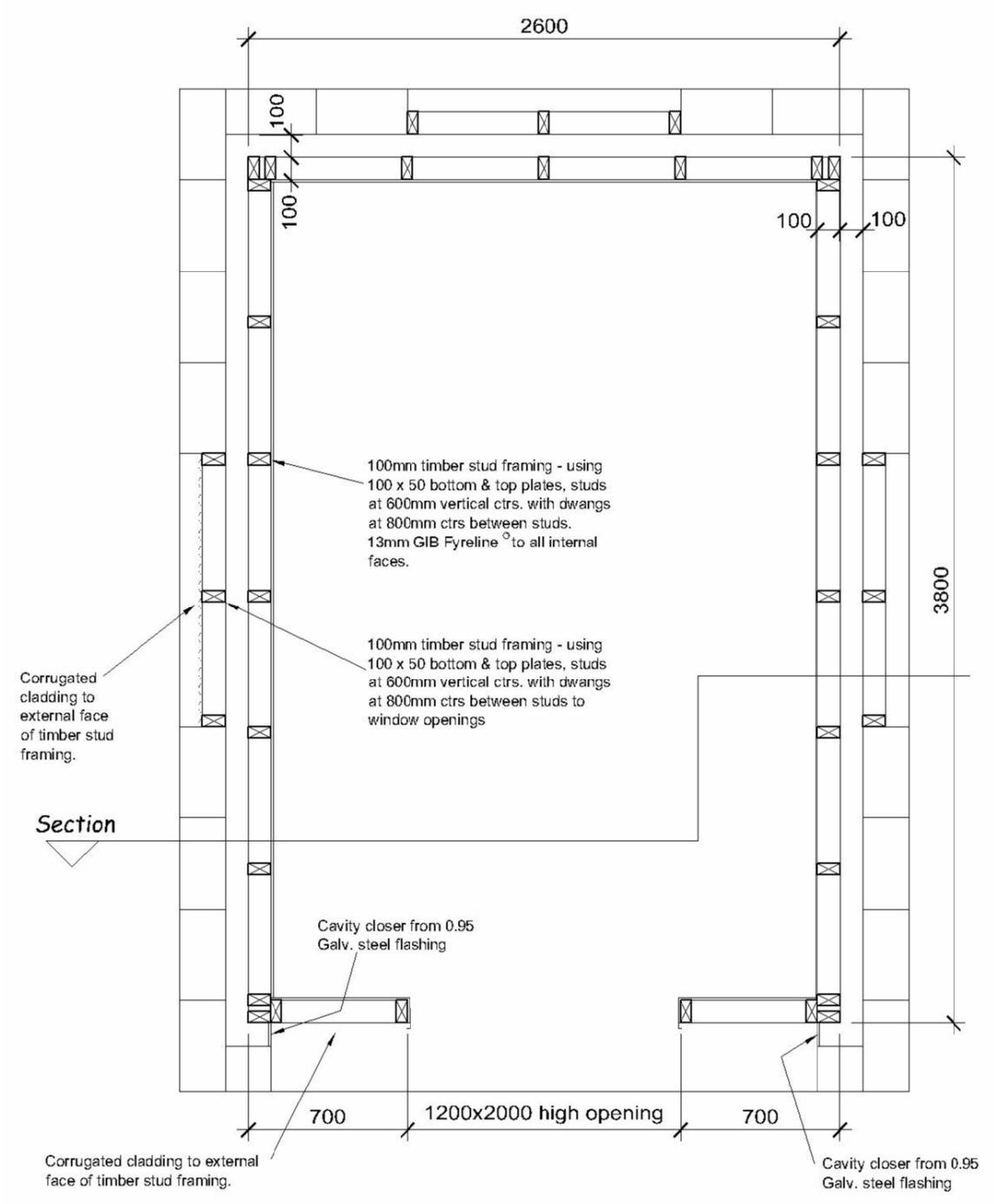

Fig 3.3 Compartment Plan Showing Construction

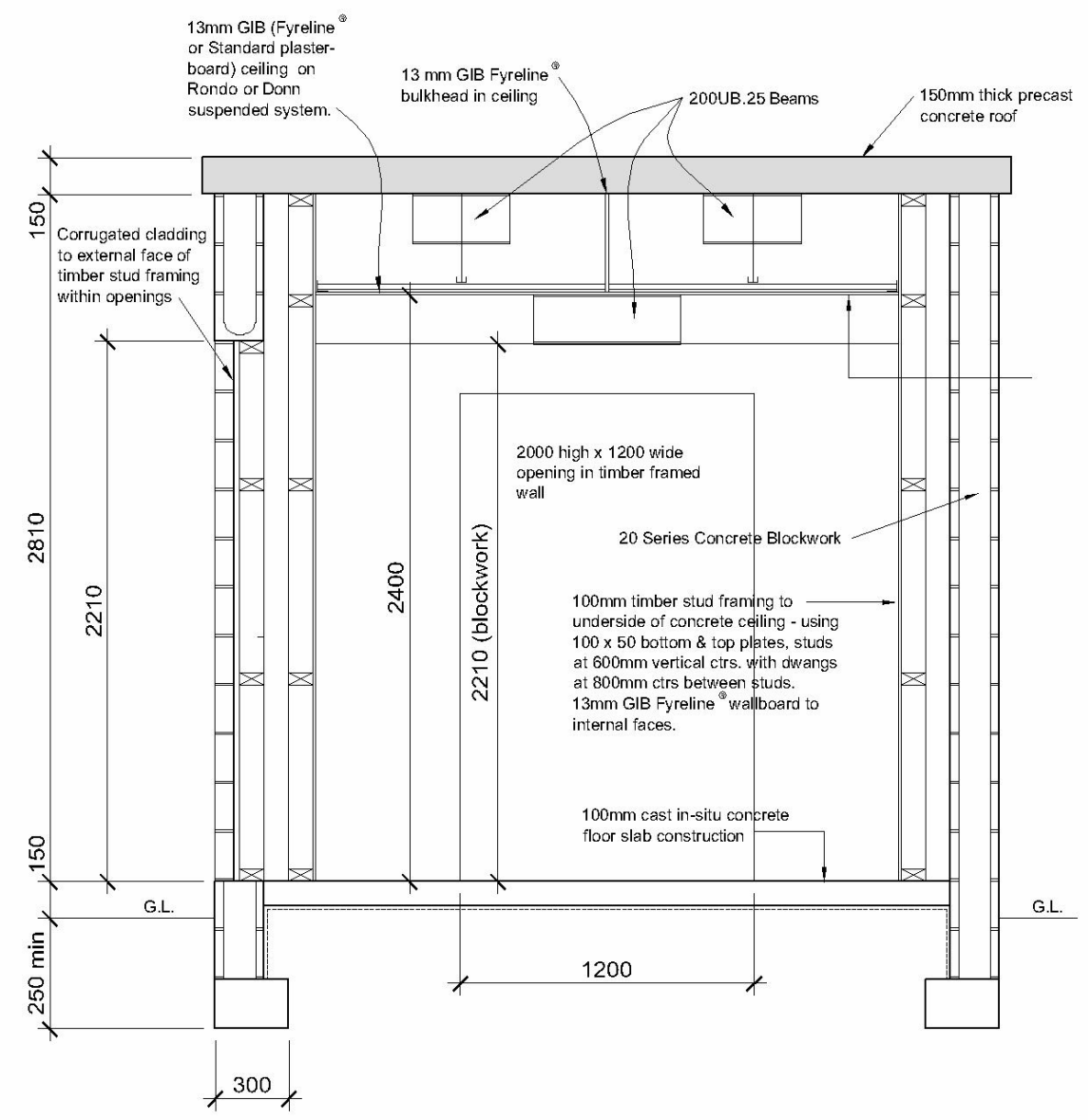

Figure 3.4 Compartment Section Showing Construction

Test 1 (FQ5013-1)

Construction

13mm GIB® Standard was used for the ceiling in Test 1. The joints at the end of the gypsum plasterboard sheets were located between battens and were back-blocked.

Fuel

The fuel consisted of: -

- 9.02 kg of polyurethane foam and 2.65 kg of Olefin fabric. The fuel load was 11.7kg at 26.9 MJ/kg = 314 MJ.
- 224 kg of timber crib
    - 12.9% moisture content (14.8% of the dry weight)
    - Calorific Value (Buchanan[6]) = 16.2 MJ/kg
    - 3627 MJ

The total fuel was 3941 MJ, which equates to 456 MJ/m^2. Refer to Fig 3-5 for the fuel layout. In addition to the above: -

- the ceiling bulkhead was constructed with a 100x50 top and bottom plate and jack studs at 600 centres,
- two lengths of 100x50 timber were inserted into the fire compartment during the test,
- a 400mm length of 150x50 timber was bolted to the underside of beam D, and
- the timber wall framing, supporting the GIB Fyreline® wall lining,

This timber contributed to the fuel only during the latter stages of the fire after the ceiling and wall linings had collapsed.

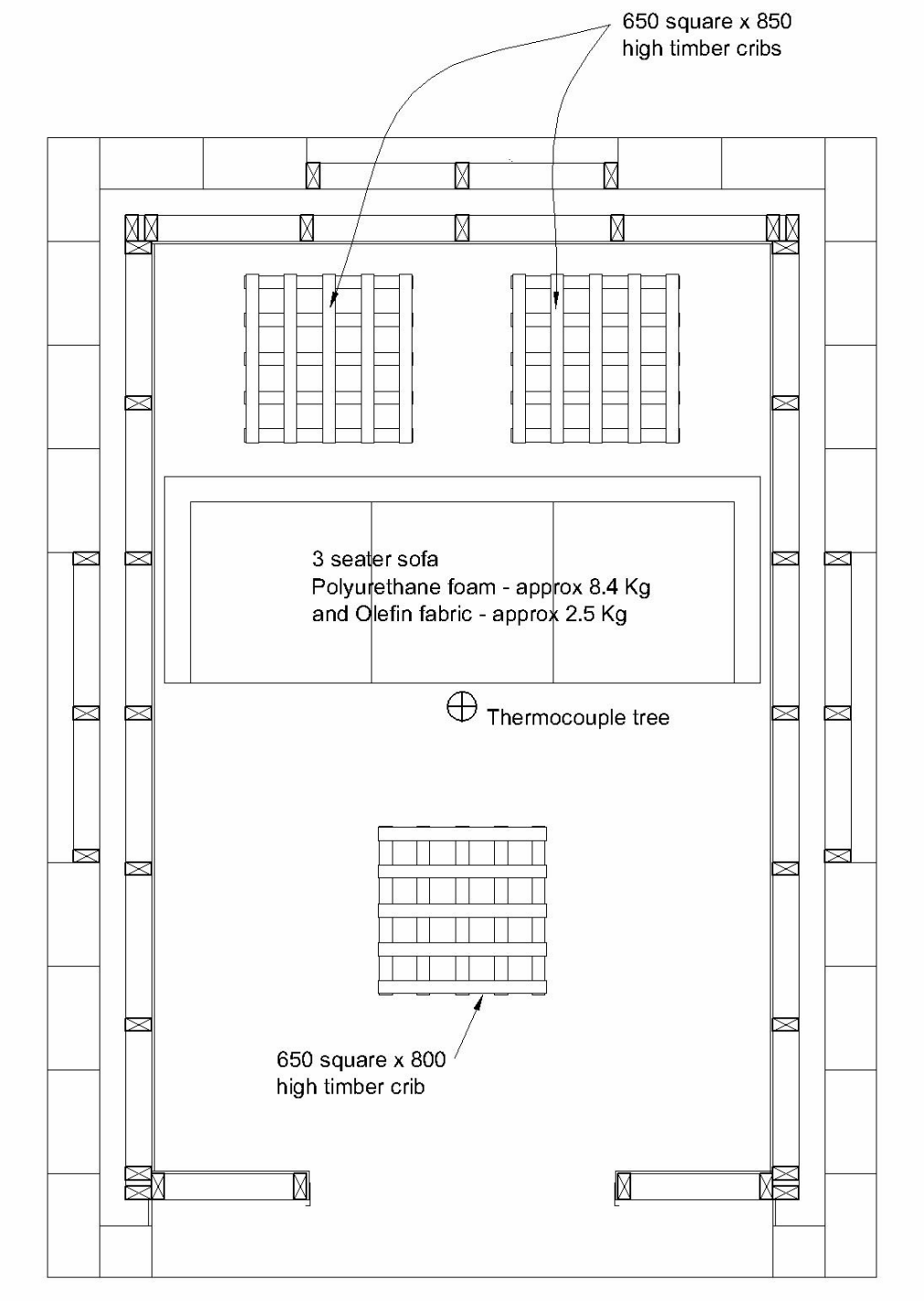

Figure 3.5 Test #1 Fuel

Observations

Observations of Test 1 are described in Appendix 2. Of particular interest was that the timber, bolted to the bottom of Beam D, was observed to be burning well into the test at 27 minutes, 45 seconds, when the decay period started.

Time-Temperature Curves

Fig 3.6 shows the measured temperature at the top of the thermocouple tree, the web of Beam D, and the average temperatures above the ceiling.

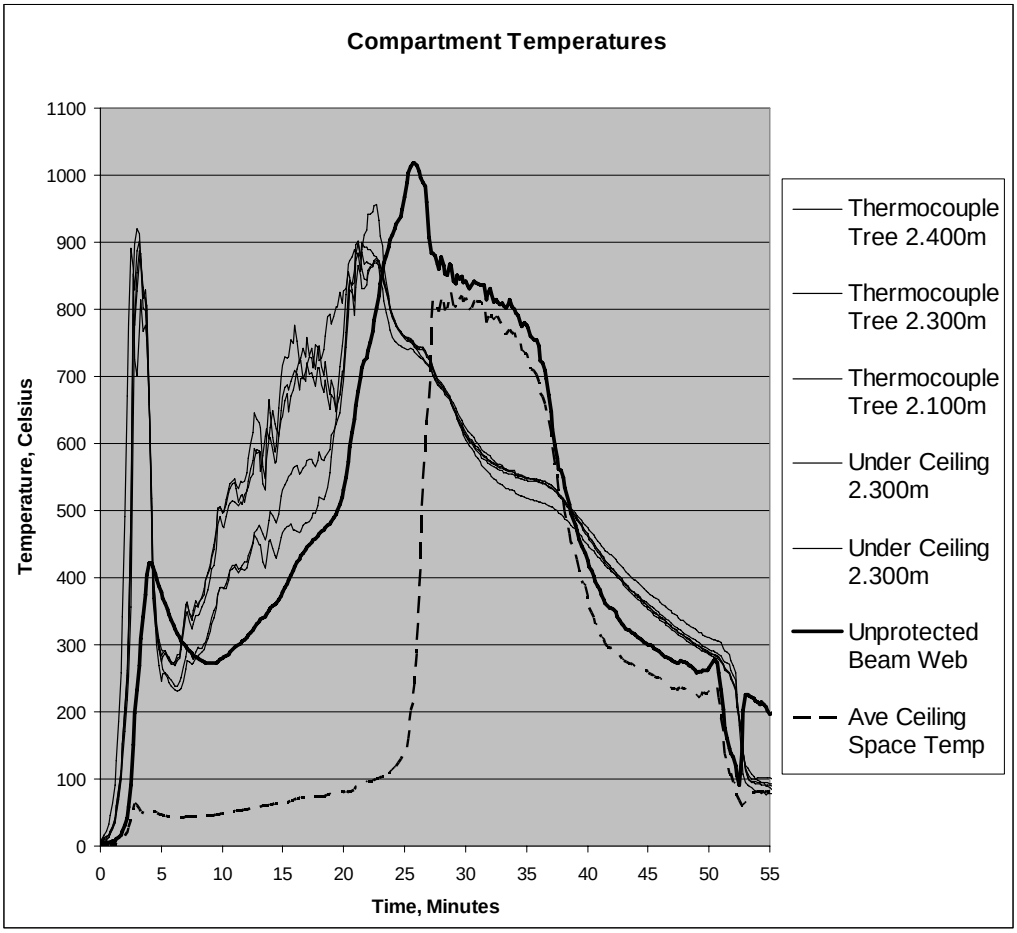

Figure 3.6 Compartment Temperatures for Test #1

It can be seen that after approximately 22 minutes, the thermocouple tree (compartment) temperatures began to decline while the ceiling space temperatures and the beam temperatures continued to climb. In addition, after the front crib at the base of the thermocouple tree began to collapse, the tree thermocouples all record the same temperature, within a narrow band. It was concluded that after 22 minutes, the thermocouple wires at the base of the thermocouple tree were damaged by the fire and that the recorded temperatures were the temperature at the base of the collapsed front crib. After the ceiling collapsed at 26 minutes, the ceiling space thermocouples give a good indication of the compartment temperature. Between 22 minutes and 26 minutes, the compartment temperature has been estimated based on the web temperature of Beam D. The maximum temperature of over 1000ºC is consistent with the second and third tests, which reached peak average temperatures of 1030ºC and 955ºC respectively.

The resulting compartment temperature and beam temperatures are shown in Figures 3.7 and 3.8, the temperature between 21 minutes and 26 minutes being estimated rather than measured.

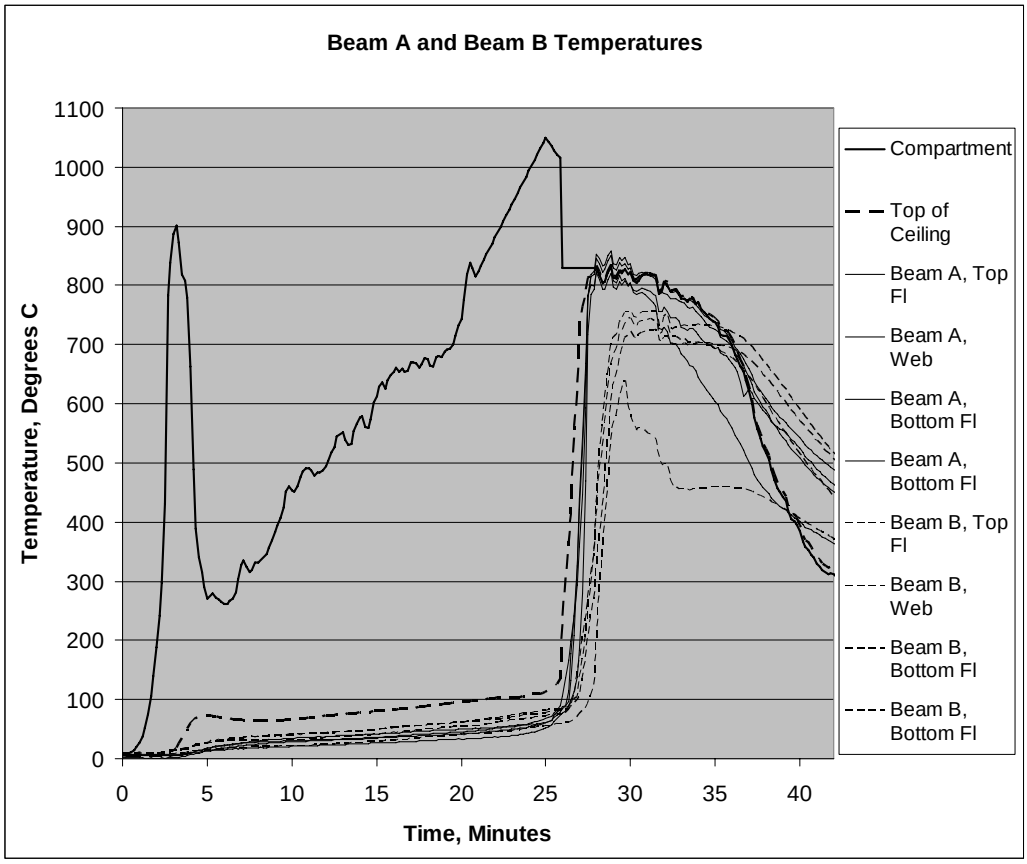

Figure 3.7 Compartment and Beam A & Beam B Temperatures for Test #1

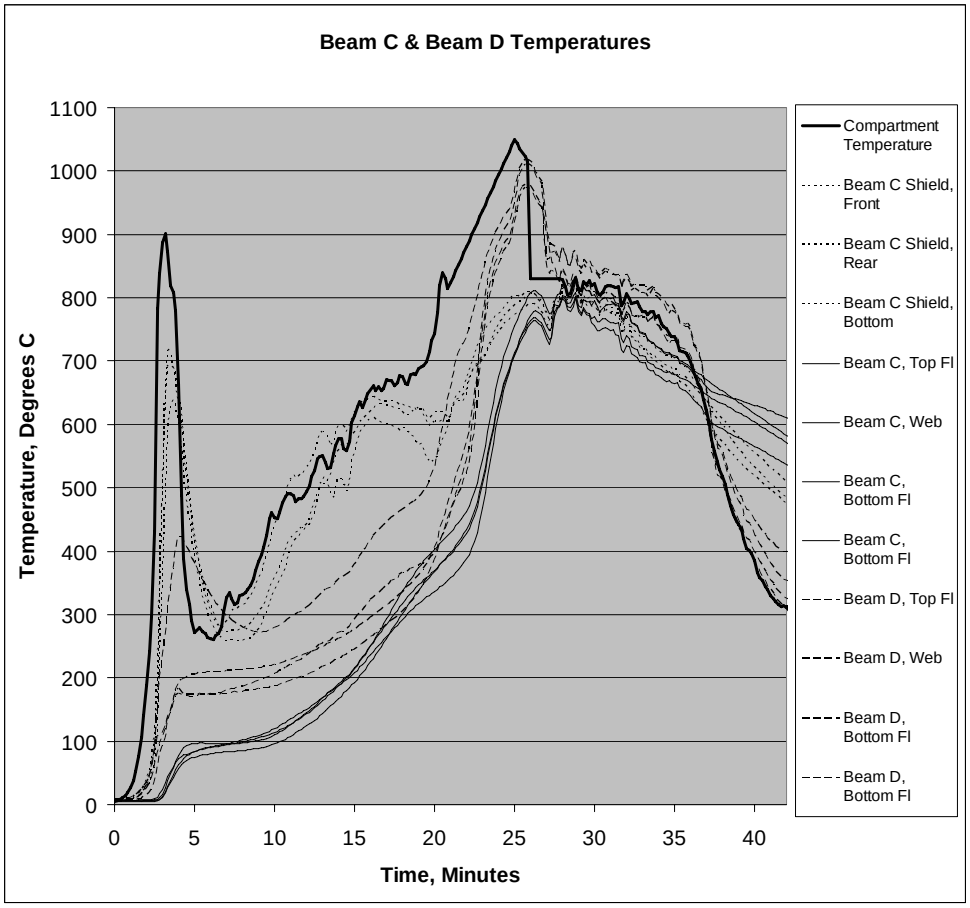

Figure 3.8 Compartment and Beam C & Beam D Temperatures for Test #1

Comments

1. At 26 minutes the compartment temperatures dropped markedly. This was when the ceiling collapsed, exposing the cooler surfaces of the concrete roof to the fire compartment. The increase in heat loss to the compartment linings results in cooler compartment fire temperatures. The decay stage of the fire also started at approximately this time.

2. Flames were observed around the timber bolted to Beam D at the rear of the compartment at 28 minutes, well after the start of the decay period. The front crib at this stage had collapsed to a pile of embers. This observation was considered interesting, in that a small piece of

timber located in the hottest part of the compartment would survive significantly longer than timber in one of coolest parts of the compartment. The following explanation is offered. Char requires oxygen to come in contact with the fuel surface before it can pyrolyse (burn). For the timber bolted to the beam at the top of the compartment, this can only occur when the equivalence ratio of the compartment gases reduces to less than 1.0, i.e. when there is free oxygen in the compartment gases. The front crib char burns before the start of the decay phase, because it is in the draft of the fresh air entering through the compartment opening.

Test 2 (FQ5013-2)

Construction

13mm GIB Fyreline® was used for the ceiling for the second test. The end joints at the end of the gypsum plasterboard ceiling sheets were located between battens and were back-blocked. The side joints were butted and stopped.

Fuel

To encourage the timber cribs to catch alight in the early stages of the fire additional polyurethane foam was used. Some timber crib was placed below the sofa foam and some polyurethane foam was placed within the timber cribs. This was regarded as being more representative of an office or hotel room, where the hydrocarbon and cellulose fuels are generally in close contact with each other. Much of the fuel load in an office consists of files &/or library type fuels. 250x50 timber in the form of two ‘book

cases' were used to represent this type of fuel. The 'book cases' were fixed to the wall. The fuel consisted of: -

- The mock sofa: 8.23 kg of polyurethane foam and 2.39 kg of Olefin fabric, plus ten slabs of 700x700x100 polyurethane foam weighing 14.7kg. The fuel load was
  25.3kg at 26.9 MJ/kg = 682 MJ.
- 178 kg of timber crib
  - 12.9% moisture content (14.8% of the dry weight)
  - Calorific Value (Buchanan[6]) = 16.2 MJ/kg
  - 2894 MJ
- 221 kg of 250x50 (book case)
  - 13.0% moisture content (14.9% of the dry weight)
  - Calorific Value (Buchanan[6]) = 16.2 MJ/kg
  - 3576 MJ

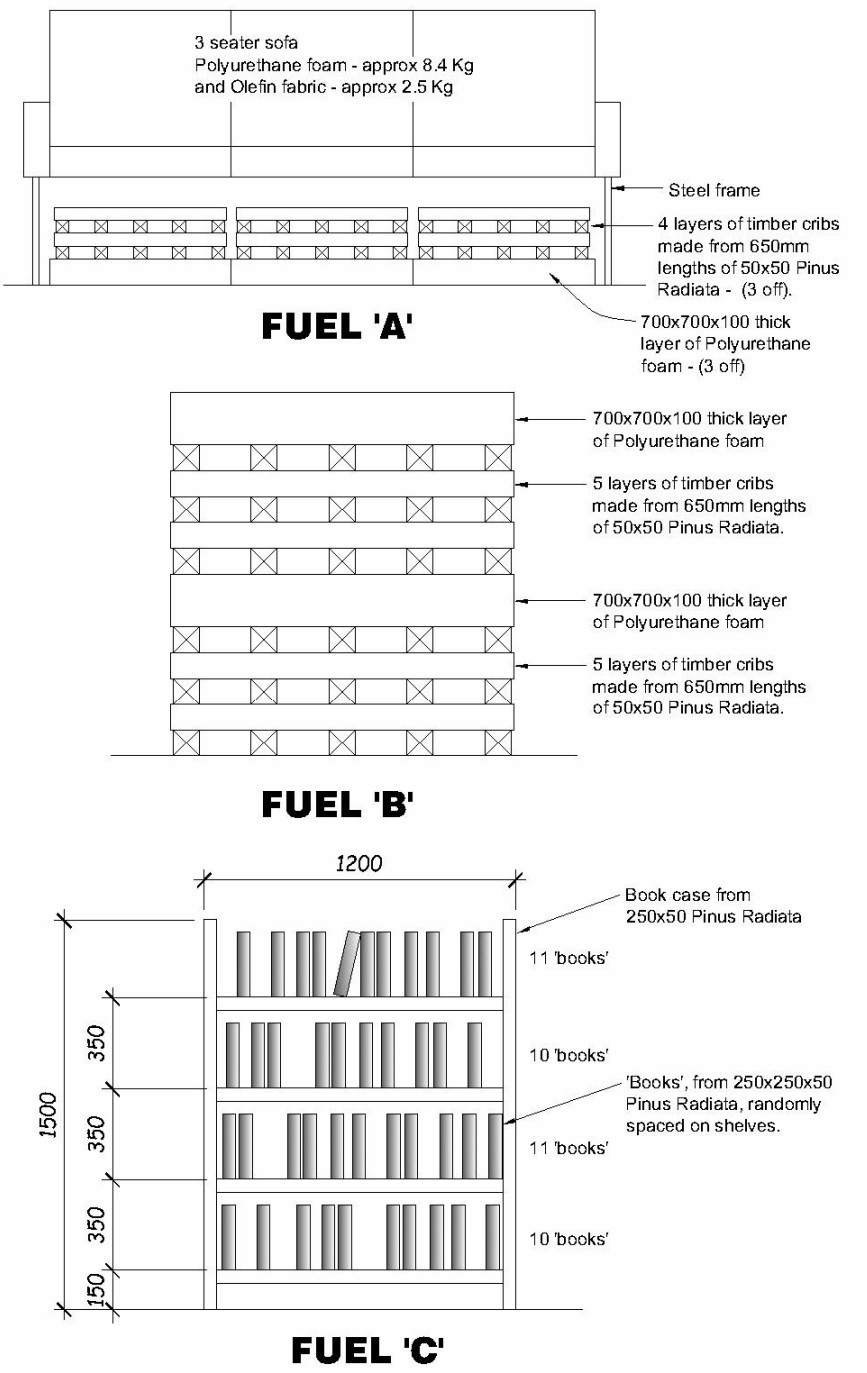

Figure 3.9 Fuel Used in Test #2

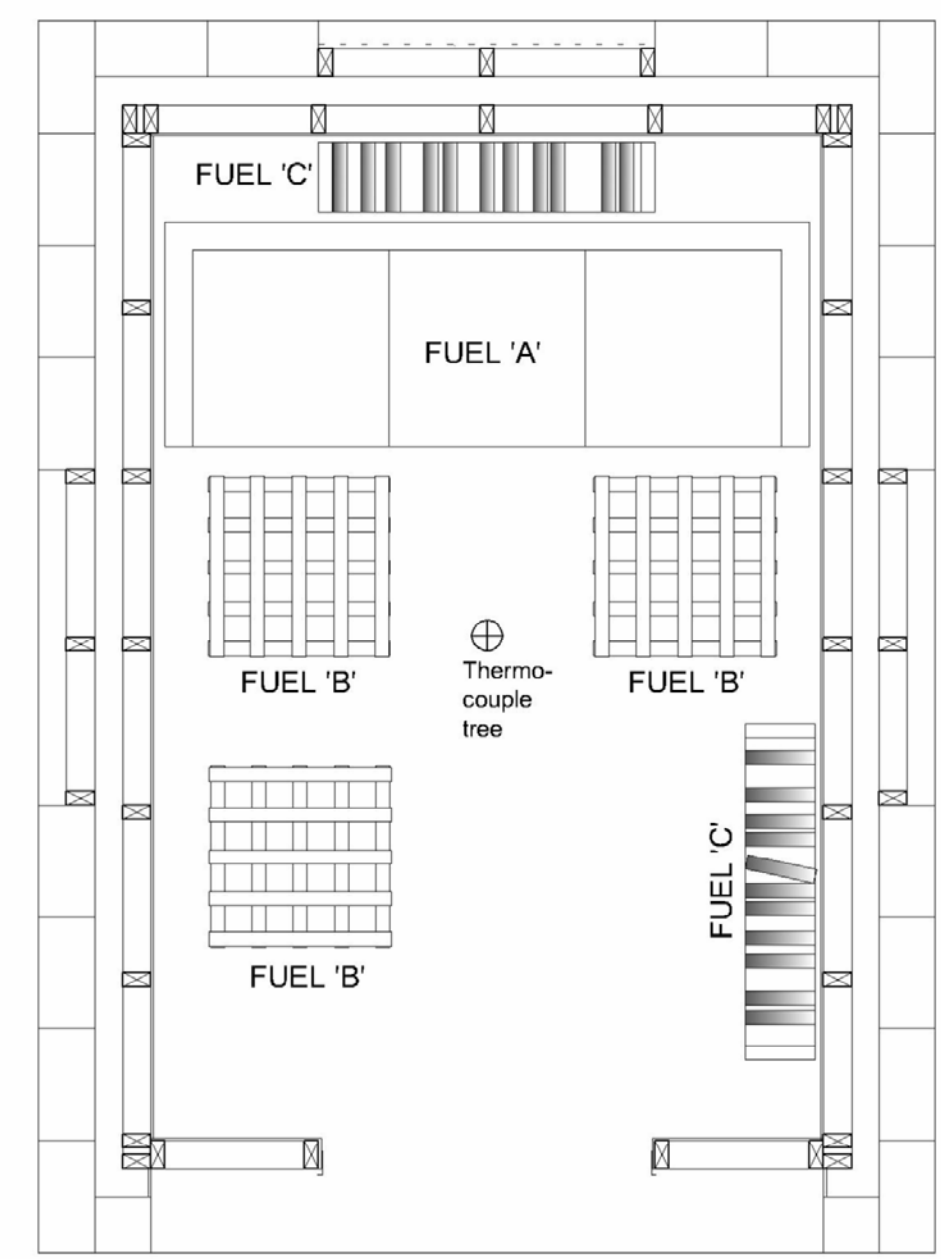

Figure 3.10 – Fuel for Test #2

The total fuel was 7152 MJ, which equates to 828 MJ/m^2. Refer to Figures 3.9 and 3.10 for the fuel layout. In addition to the above: -

- the ceiling bulkhead was constructed with a 100x50 top and bottom plate and jack studs at 600 centres,
- a 400mm length of 150x50 timber was bolted to the underside of beam D, and
- the timber wall framing, supporting the gypsum plasterboard wall lining.

This timber contributed to the fuel only during the latter stages of the fire after the ceiling and wall linings had collapsed.

Time-Temperature Curves

The compartment temperatures are shown in Figure 3.11. Ceiling space thermocouples failed &/or became dislodged at around 35 minutes. The ceiling space thermocouple readings after this time should be disregarded. Beam temperature graphs are shown in Figures 3.12 and 3.13.

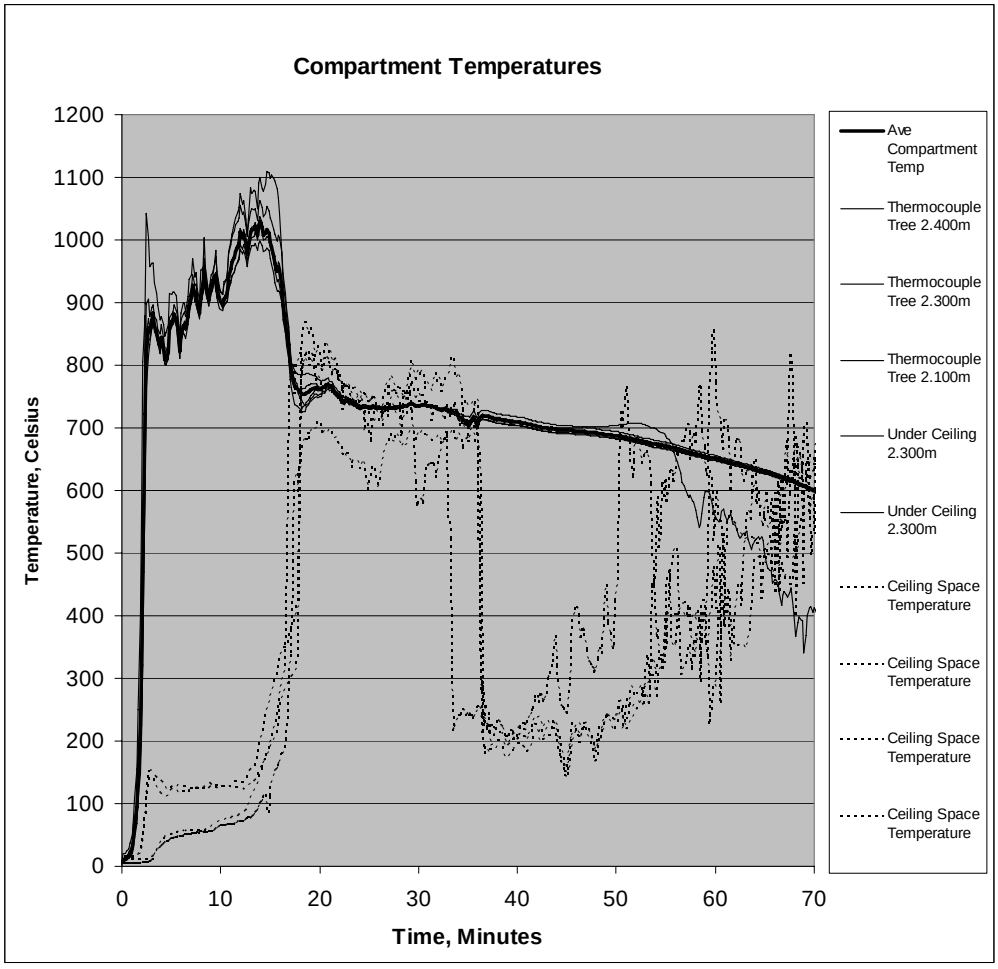

Figure 3.11 Compartment Temperatures, Test #2

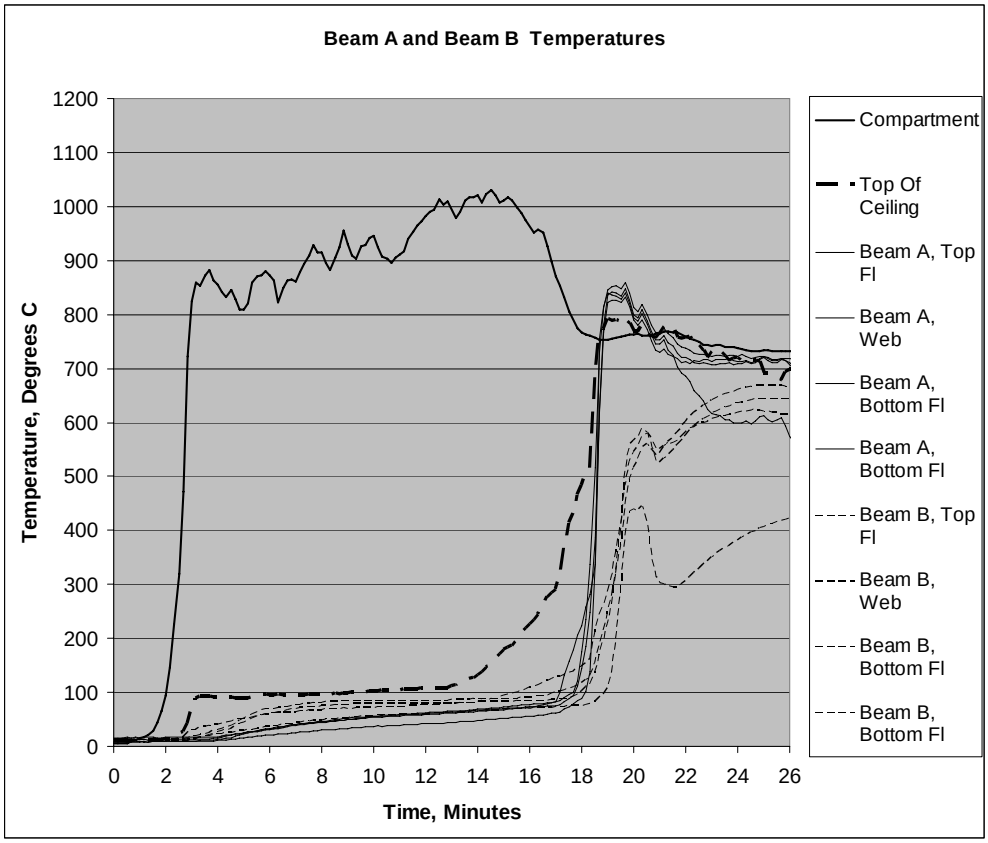

Figure 3.12 Test #2 Beam A & Beam B Temperatures

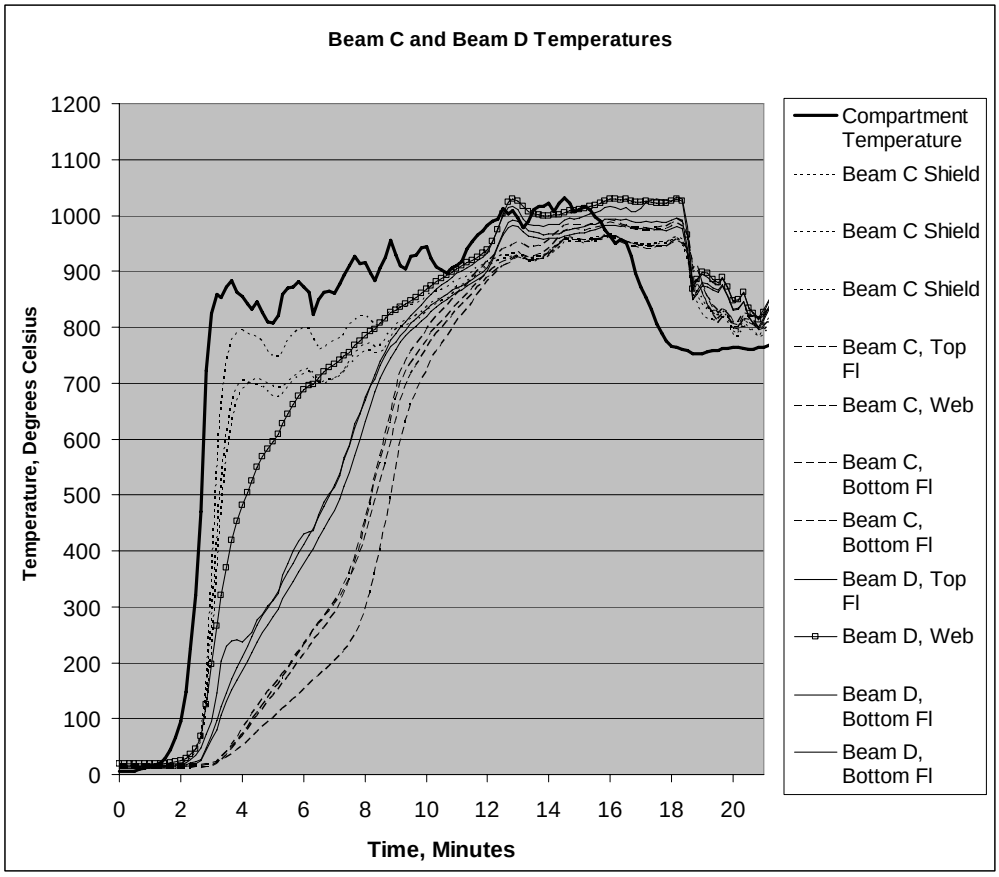

Figure 3-13 Test #2 Beam C & Beam D Temperatures

Observations

The observations for test 2 are described in Appendix 3.

Comments

As in the first test, when the ceiling collapses, the compartment fire temperature drops markedly. As previously, this is due to the cooler concrete roof temperatures absorbing energy from the compartment. As in the first test, the decay period begins at this time or shortly afterwards. The rate of temperature decay is much slower because of the concentrated Fuel C fire load, which continues to burn for a long time after the other fuel has been consumed.

Test 3 (FQ5013-3)

Construction

13mm GIB Fyreline® was used for the ceiling in the third test. The joints at the end of the gypsum plasterboard sheets were located on a batten.

Fuel

The fuel was similar to the second test, except that there were no 'book-cases' in this test. The fuel consisted: -

- The mock sofa: 9.06 kg of polyurethane foam and 2.56 kg of Olefin fabric, plus nine slabs of 700x700x100 polyurethane foam weighing 13.1kg. The fuel load was
  24.7kg at 26.9 MJ/kg = 665 MJ.
- 178kg of timber crib
  - 13.4 moisture content (15.4% of the dry weight)
  - Calorific Value (Buchanan[6]) = 16.1 MJ/kg
  - 2865 MJ

The total fuel was 3529 MJ, which equates to 408 MJ/m^2. Refer to Figure 3-14 for the fuel layout. In addition to the above a 400mm length of 150x50 timber was bolted to the underside of beam D, which contributed to the fire load.

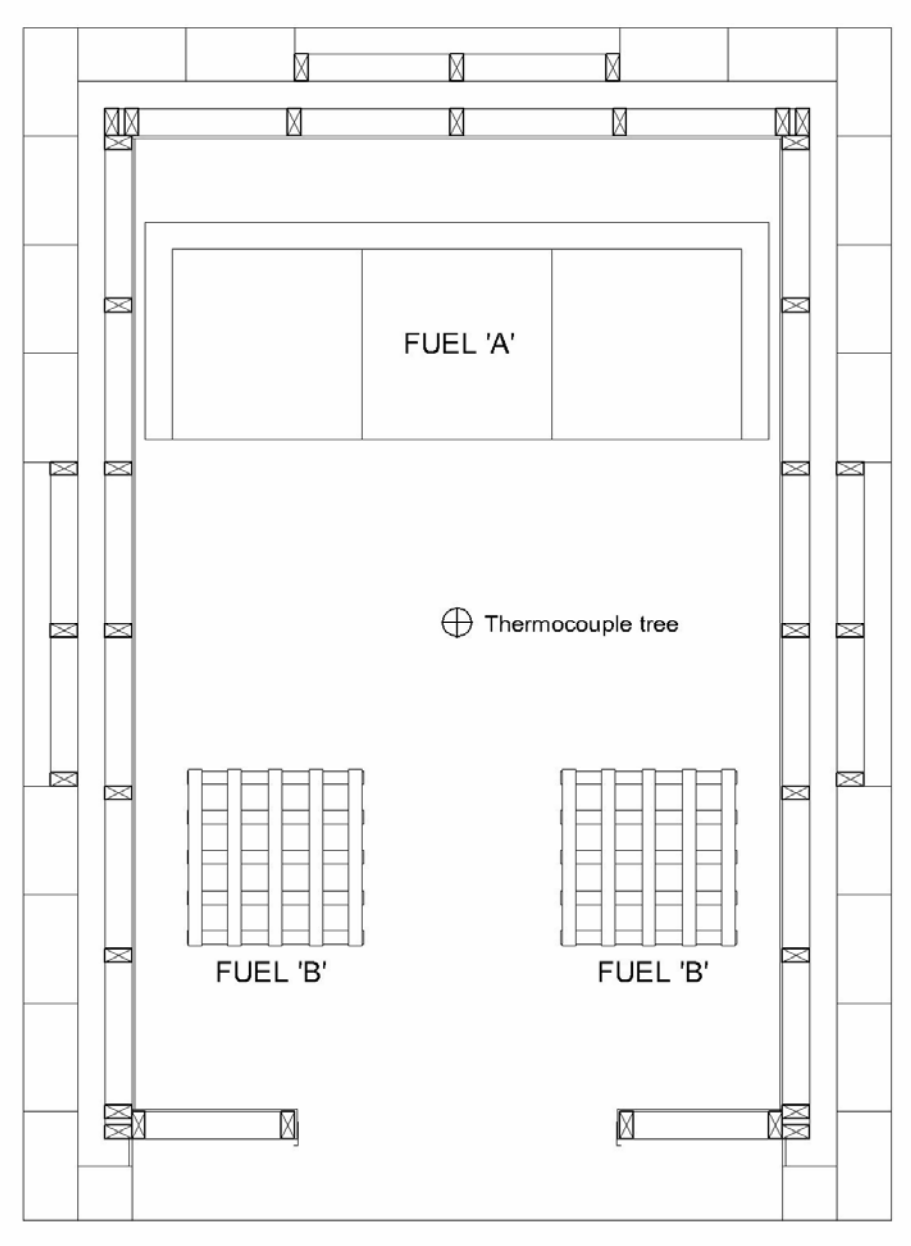

Figure 3.14 Test #3 Fuel

Observations

The observations for Test 3 are described in Appendix 4. The timber on the bottom of beam D started to burn at 11’10”, the start of the decay stage.

Time-Temperature Curves

Figure 3-15 shows the compartment temperatures. Figures 3-16 and 3-17 show the beam temperatures.

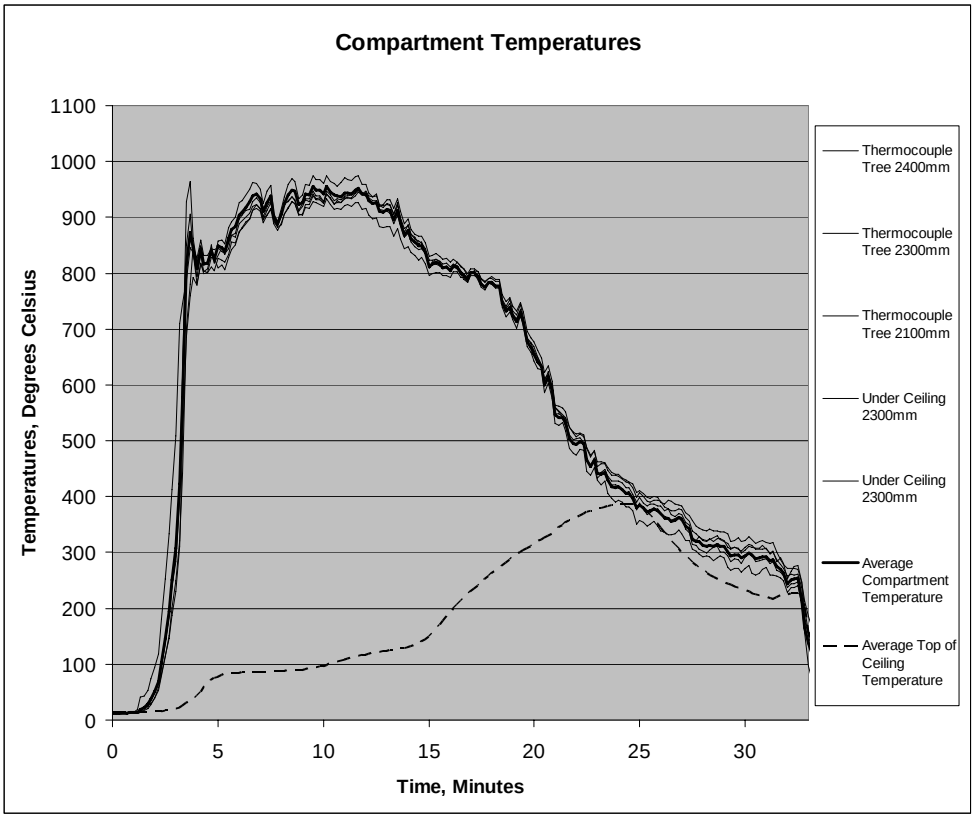

Figure 3.15, Compartment Temperatures for Test #3

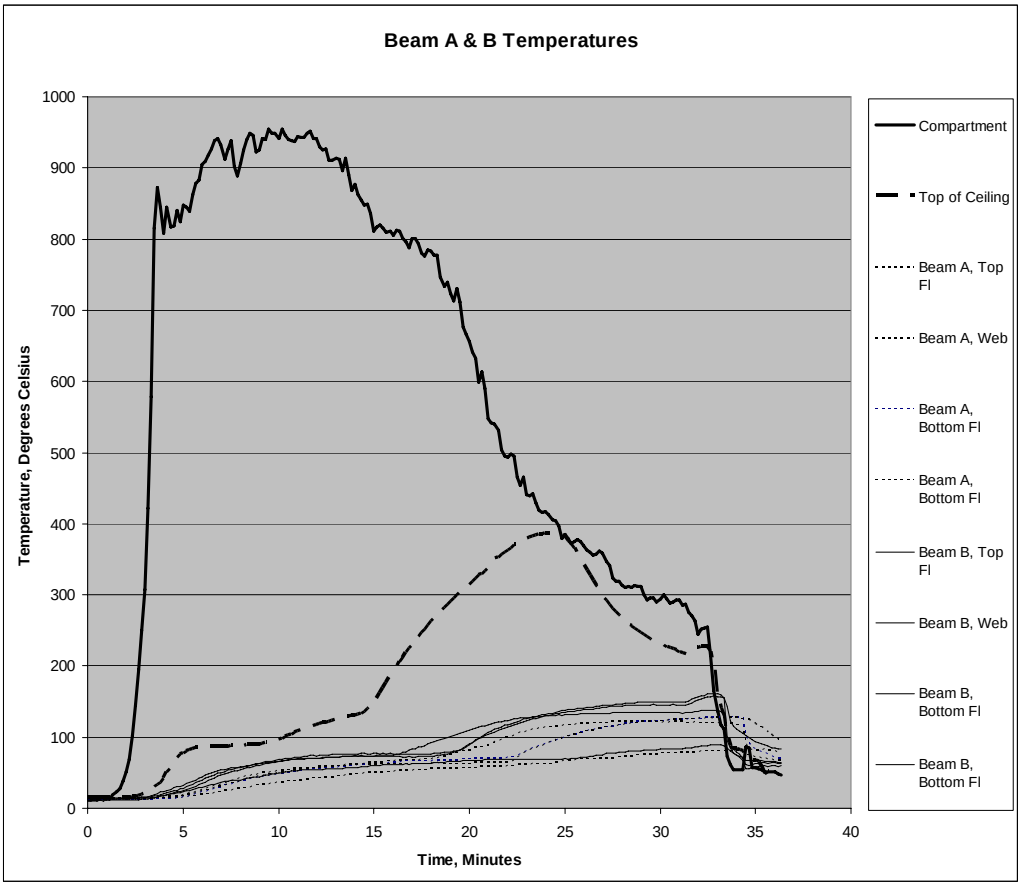

Figure 3.16, Beam A & Beam B Temperatures for Test #3

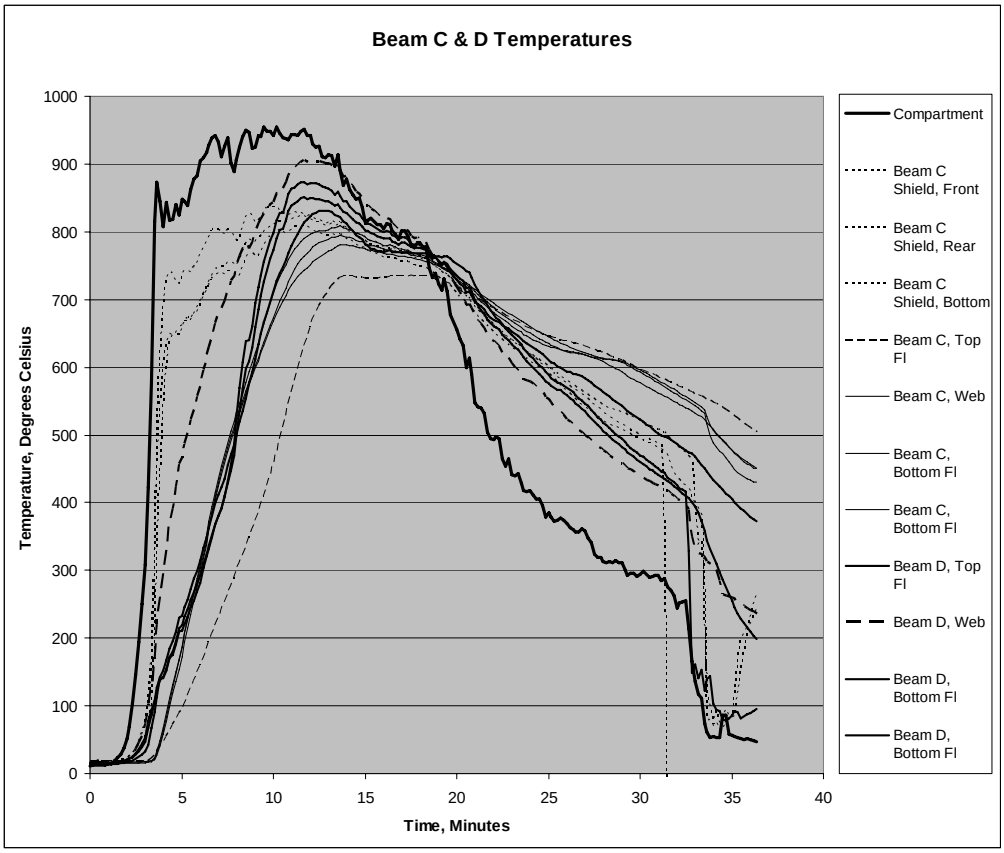

Figure 3.17, Beam C & Beam D Temperatures for Test #3

Comments

1. Small sections of gypsum plasterboard fall from the ceiling when the fire is well into the decay stage (compartment temperatures approximately 400ºC).

2. As in tests #1 & #2, the charred timber on the bottom of Beam D was observed to be burning once the decay stage has started (i.e. once the equivalence ratio reduces below 1.0, i.e. once oxygen comes in contact with the char).

Conclusions

- The three tests gave good data for the study and analysis of heat transfer into steel beams.

- If the suspended gypsum plasterboard ceiling remains intact, the steel beams within the ceiling space stay at temperatures well below the fire compartment temperatures.

- When a steel beam is exposed to the compartment fire, the steel beam temperature rapidly climbs to match the compartment temperature.

- The 125mm diameter penetrations in the suspended ceiling do not make a significant difference to the beam temperatures.

- The surface char of timber burns when oxygen is present at the surface of the char. This occurs when timber is located in the draught of an opening. Char remote from an opening burns during the decay stage (when the equivalence ratio is less than 1.0).

Chapter 4 - Multi-Lumped-Mass Step-By-Step Analysis of Steel Beams

Background

Calculations to analyse the heat transfer into unprotected steel beams have been well established for many years. Pettersson et al[35] wrote a comprehensive paper in 1976 outlining: -

- the design fire,
- the thermal analysis, and
- the structural analysis.

Pettersson used a lumped mass, step-by-step method and included 'shadow effects' in his paper, combining the emissivity and view factor in a single parameter, which he called the resultant emissivity.

Since 1976, the view factor has largely been overlooked, until in 2001 Wickstrom[44], suggested that the view factor should be used in steel beam analysis. He also used the term 'shadow-effect'. Franssen et al[20], in their book "Design of Steel Structures Subjected to Fire, Background and Design Guide to Eurocode 3", include a correction factor for the shadow effect, for the thermal analysis of steel beams exposed to fire.

Because the resultant emissivity is a combination of the emissivity and the view factor, the usual step-by-step method cannot be used in a case where the cross-section of a steel beam is partially protected. If a more general case is to be analysed using a step-by-step process, the view factor will need to be explicitly included in the formulation.

Introduction

The aim of this section is to develop a lumped-mass step-by-step analysis to analyse partially protected steelwork. To achieve this, radiative heat transfer between elements is incorporated into the analysis. The approach is kept as simple as possible, so that the analysis can be carried out on a spread-sheet.

Steel universal beams are modeled as three lumped masses – the top flange, the web and the bottom flange. The concrete slab, which the beam supports, is modeled using finite difference with constant material properties.

The analysis is applied to: -

1. a 200UB25 universal beam where the bottom of the bottom flange is protected with a block of timber, and
2. a 200UB25 universal beam enclosed in a light-gauge galvanized steel radiation shield.

Spread-Sheet Formulation

Radiation heat transfer between two surfaces is given by Incropera and DeWitt[23]

$$Q_{ij} = A_{ij} \cdot F_{ij} \cdot \sigma \cdot (T_i^4 - T_j^4)$$

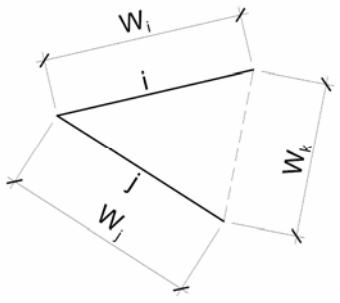

Where

Q_{ij} = Heat flow from surface i to surface j

$F_{ij} = (w_i + w_j - w_k)/(2 \cdot w_i)$

Figure 4.1 Radiant Heat Transfer Between Surfaces

This can be expressed in more general terms: -

$$F_{ij} = 1 - F_{ik} - F_{il}$$

$$= (w_m + w_n - w_k - w_l)/(2 \cdot w_i)$$

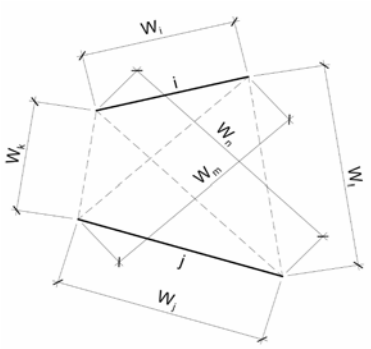

Figure 4.2 Radiant Heat Transfer Between Surfaces

This equation remains valid when any of the surface widths, except w_i, diminishes to zero. The above formula can be simply evaluated using a spread-sheet.

The step by step analysis proceeds as described in the text books (Buchanan[6]). The heat flow into each element is summed over the time interval and equated to the increase in enthalpy of the element (i.e. the increase in temperature * the specific heat * density). The different heat flows to be summed are shown in figure 4.3 below.

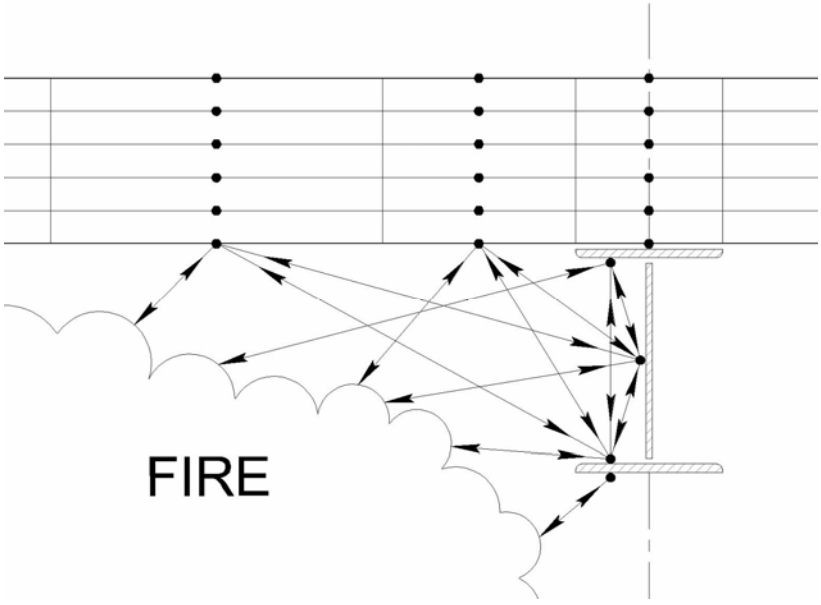

Figure 4.3 Radiant Heat Flows For General Steel Beam Design

For the above case there are thirteen heat flows to calculate. If additional elements are added the number of heat flows to be calculated at each time step increases rapidly.

The effect of flame depth can be incorporated into the analysis. Drysdale[14] relates flame emissivity to the depth of flame.

$$\varepsilon = 1 - e^{-k \cdot L}$$

Where: -

k is an effective emission coefficient, typically ranging between 0.43 for diesel oil to 0.7 for wood cribs to 1.5 for polystyrene, and

L is the depth of flame.

The view that one element has of another through the flames, is effectively

$$1 - \varepsilon = e^{-k \cdot L}$$

Figure 4.6 below shows the radiant heat transfers to be evaluated at each time step for analysing a steel beam enclosed in a light-gauge radiation shield.

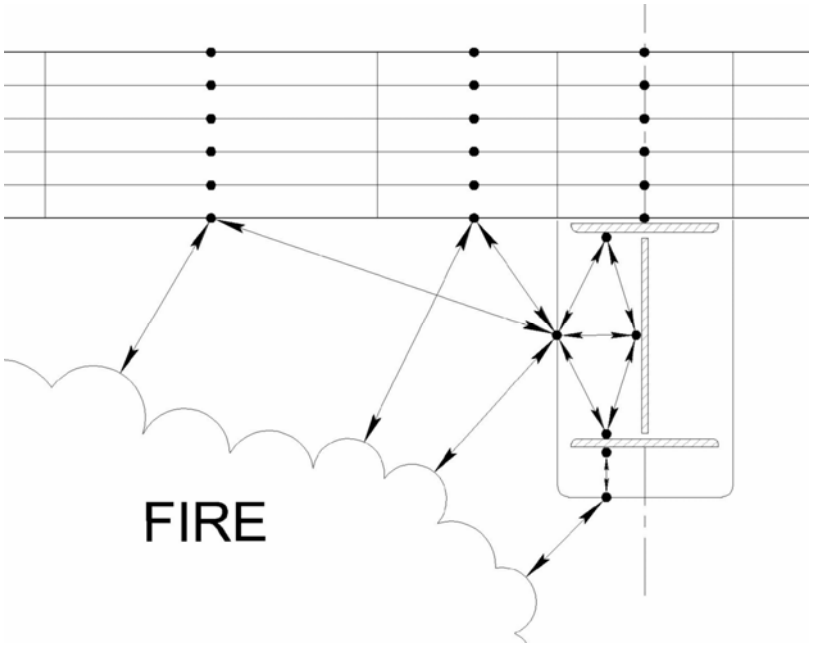

Figure 4.6 Radiant Heat Flows For Steel Beam Design With Radiation Shield

Steel Beam with Partial Protection Exposed to the ISO Fire

Figure 4.7 below shows the result of the analysis when applied to a 200UB25 steel beam exposed to the standard ISO fire. The steel beam is located below a gypsum plasterboard ceiling, which is known as 'three sided exposure'. The beam had no other protection.

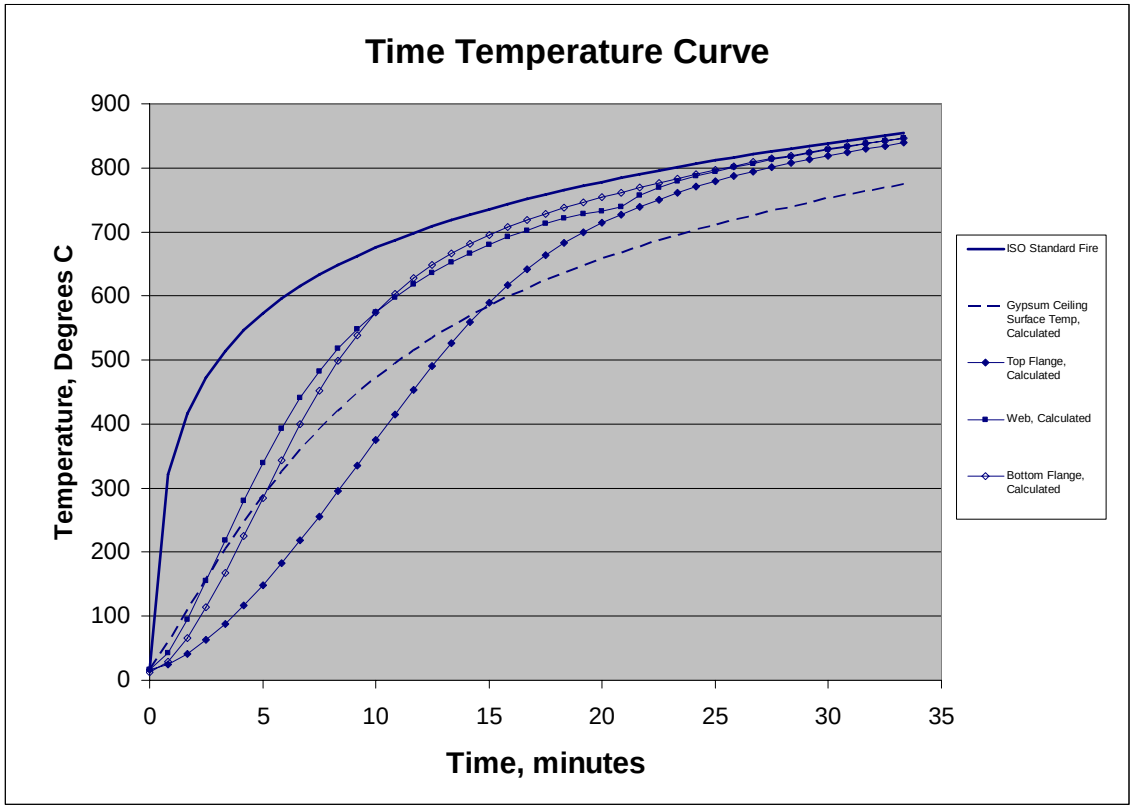

Figure 4.7 Steel Beam Below a Gypsum Plaster Ceiling – No Additional Protection

Figure 4.8 shows the result of the analysis when the bottom of the bottom flange is protected. The predominant difference is that the bottom flange temperature drops to approximately the same temperature as the top flange, rather than being approximately the same temperature of the web.

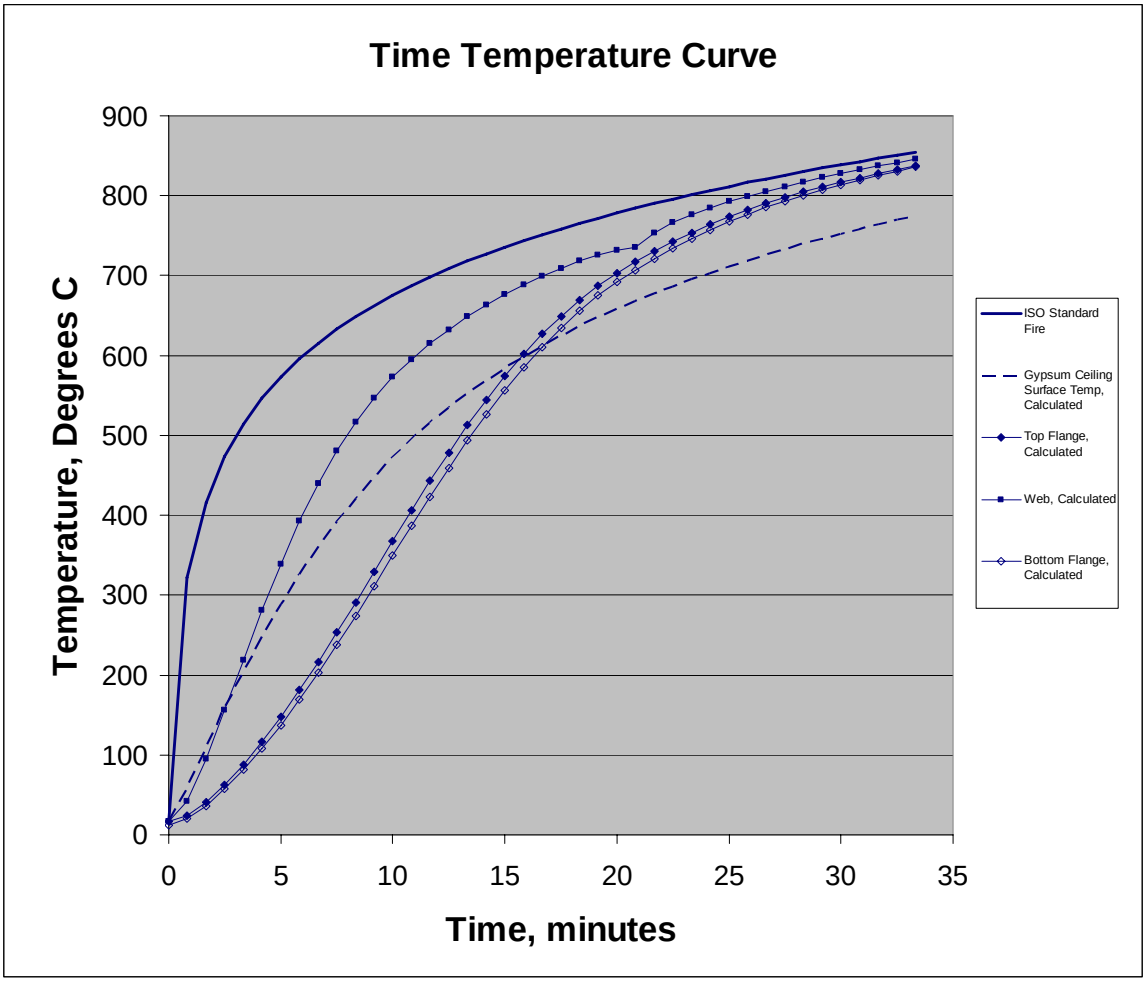

Figure 4.8 Steel Beam Below a Gypsum Plasterboard Ceiling
Bottom of Bottom Flange Protected With 50mm Thick Timber

Steel Beam with a Light Gauge Steel Radiation Shield Exposed to the ISO Fire

Figure 4.9 below shows the result of the analysis when applied to a 200UB25 steel beam, protected with a light gauge steel radiation shield, exposed to the standard ISO fire. The steel beam is located below a gypsum plasterboard ceiling. The radiation shield provides a similar level of protection as the partial protection of the bottom flange.

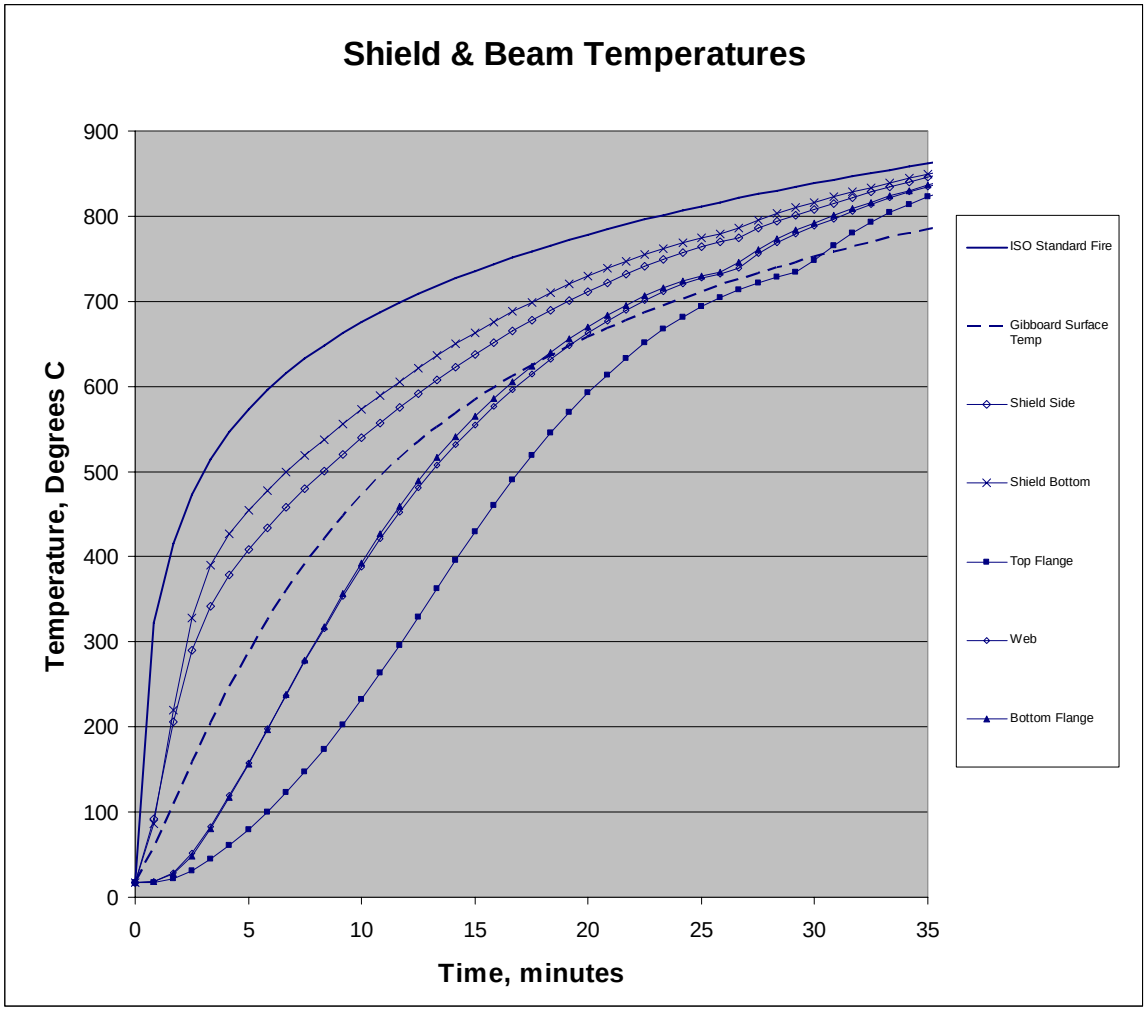

Figure 4.9 Steel Beam Protected With a Light-Gauge Steel Radiation Shield

Chapter 5 - Comparison of Calculated and Measured Temperatures for a Partially Protected Steel Beam

Introduction

Using the average compartment temperatures from the third experimental test and the following material values, the lumped-mass step-by-step method was used to calculate the steel beam temperatures. Conductive heat transfer through the timber was assumed to be nil. A comparison with only the third test is presented here because this was the only test where the ceiling remained intact for the duration of the test.

$\varepsilon_s = 0.88$ (emissivity of steel)

$\varepsilon_g = 0.40$ (emissivity of gypsum plasterboard)

$h_c = 25$ W/m^2/K (convective coefficient)

$k = 1.5$ m^{-1} (flame effective emission coefficient)

Steel beam = 200UB25 (203mm deep by 133mm wide)

$$Cp = 425 + 0.773 \cdot T - 0.00169 \cdot T^2 + 0.00000222 \cdot T^3 \qquad 20^oC \le T \le 600^oC$$

$$= 666 + 13002/(738 - T) \qquad 600^oC \le T \le 735^oC$$

$$= 545 + 17820/(T - 731) \qquad 735^oC \le T \le 900^oC$$

$$= 650 \text{ J/kg/K} \qquad 900^oC \le T \le 1200^oC$$

(Specific heat of steel)

Figure 5.1 compares the calculated temperatures with the measured temperatures.

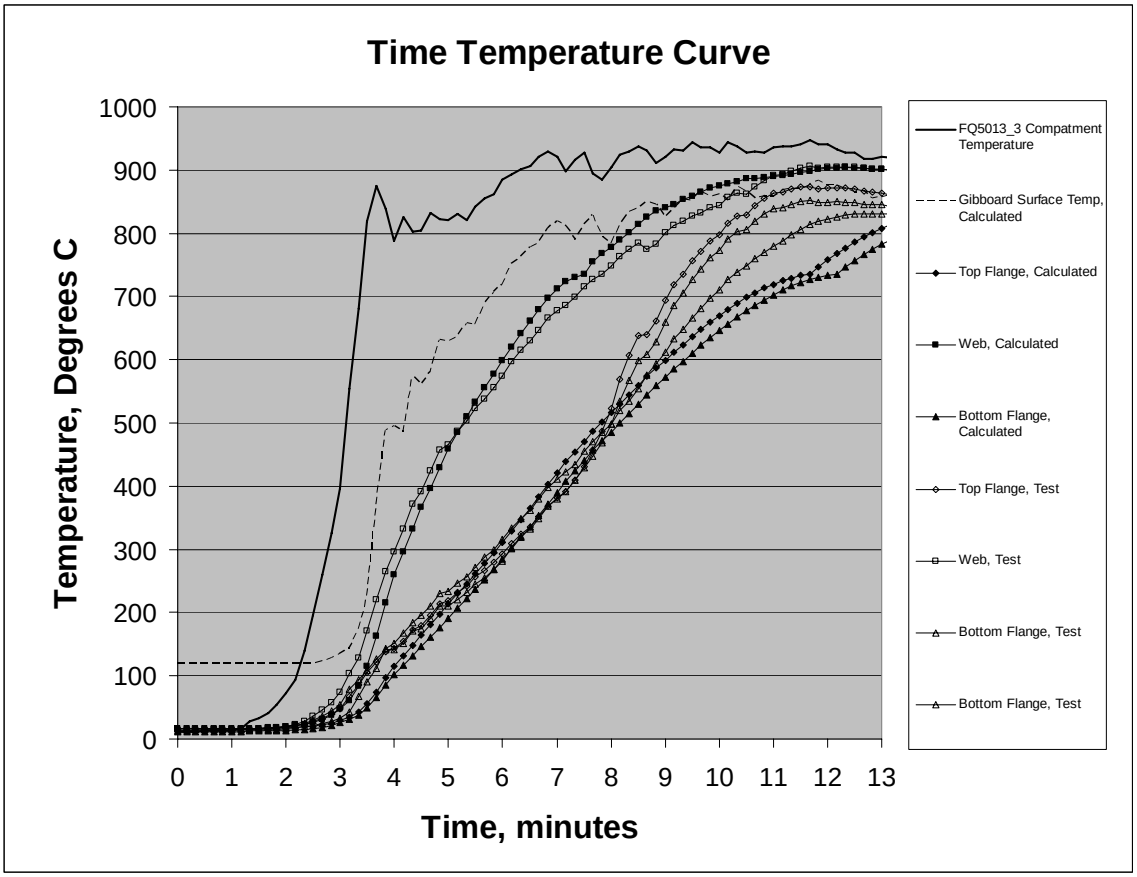

Figure 5.1 Comparison of Calculated and Measured Beam Temperatures

Discussion of Results

The timber bolted to the bottom of the bottom flange gives significant protection to the bottom flange. The temperature in the bottom flange is comparable to that of the top flange. The web is approximately 300 degrees higher over the period of rapid heating, from 5 minutes to 8 minutes.

The steel beam web temperature was measured at the mid height of the web. This is a maximum temperature of the web rather than the average temperature of the web. The calculated (average) temperature is therefore likely to be less than the measured web temperature in the experiments. For the flange, the temperature was measured half way between the flange extremity and the point where the flange and web intersects. Because

of the additional mass around the root radius, the measured temperature is again likely to be greater than the calculated (average) temperature.

There is a kink in the calculated temperature at approximately 12 minutes. This is due to the spike in the value of Cp at 735°C (refer to definition of Cp on page 50, or Buchanan[6]). In reality, the temperature of the steel will vary over the cross section by 100°C or more. This will have the effect of smoothing the temperature response in the flanges. To demonstrate the effect that this will have and analysis with a smoothing Cp function was carried out. Figure 5.2 compares the measured and calculated beam temperatures, when a constant specific heat of 600 J/kg/K is used in the analysis. Buchanan[6] suggests that this value can be used for simple analyses. All other material values remained unchanged.

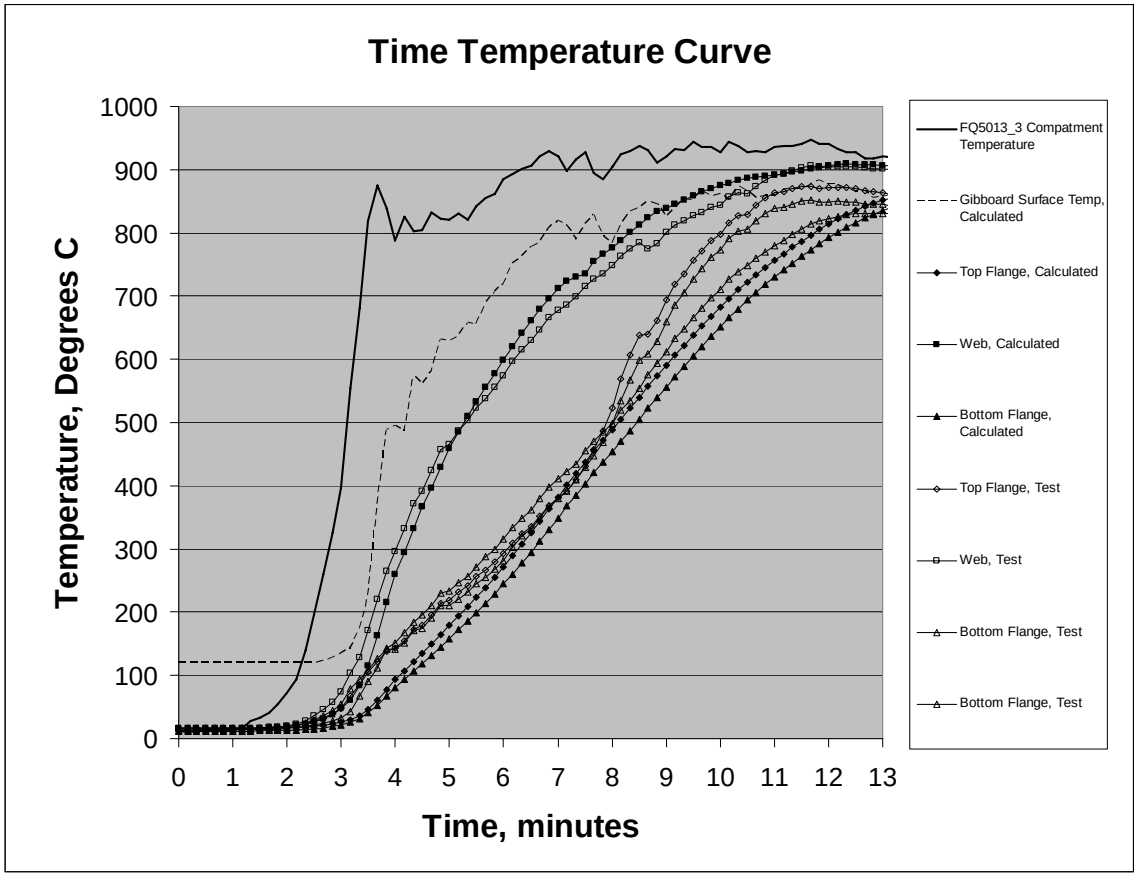

Figure 5.2 Comparison of Calculated and Measured Beam Temperatures

Conclusion

While the bottom flange of a steel beam can be kept significantly cooler during the early to middle stages of a fully-developed fire, by the addition of timber bolted to the bottom flange, eight to nine minutes of protection is of little use to the construction industry.

With radiative heat transfer proportional to the temperature to the fourth power, and gypsum plasterboard lined compartment fires being significantly hotter than the ISO fire in the early stages, unprotected portions of a steel beam absorb significant heat causing the temperature to rise rapidly above their limiting temperature (NZS 3404[32]). Partial protection of the bottom flange may be useful in less severe fires, such as in concrete carpark buildings.

It should be noted that the timber bolted to the steel section will burn when oxygen reaches the surface of the timber. This will occur at the start of the decay stage, or earlier if the timber is in the draught of an opening.

Chapter 6 - Comparison of Calculated and Measured Temperatures for a Steel Beam Protected with a Radiation Shield

Introduction

Using the average compartment temperatures from the third experimental test, the lumped-mass step-by-step method was used to calculate the radiation shield and the steel beam temperatures. The value of material constants used in the analysis are given in chapter 5.

Figure 6.1 compares the experimental data for the third test with the spread-sheet calculation using the average compartment temperature as the input for the steel beam analysis.

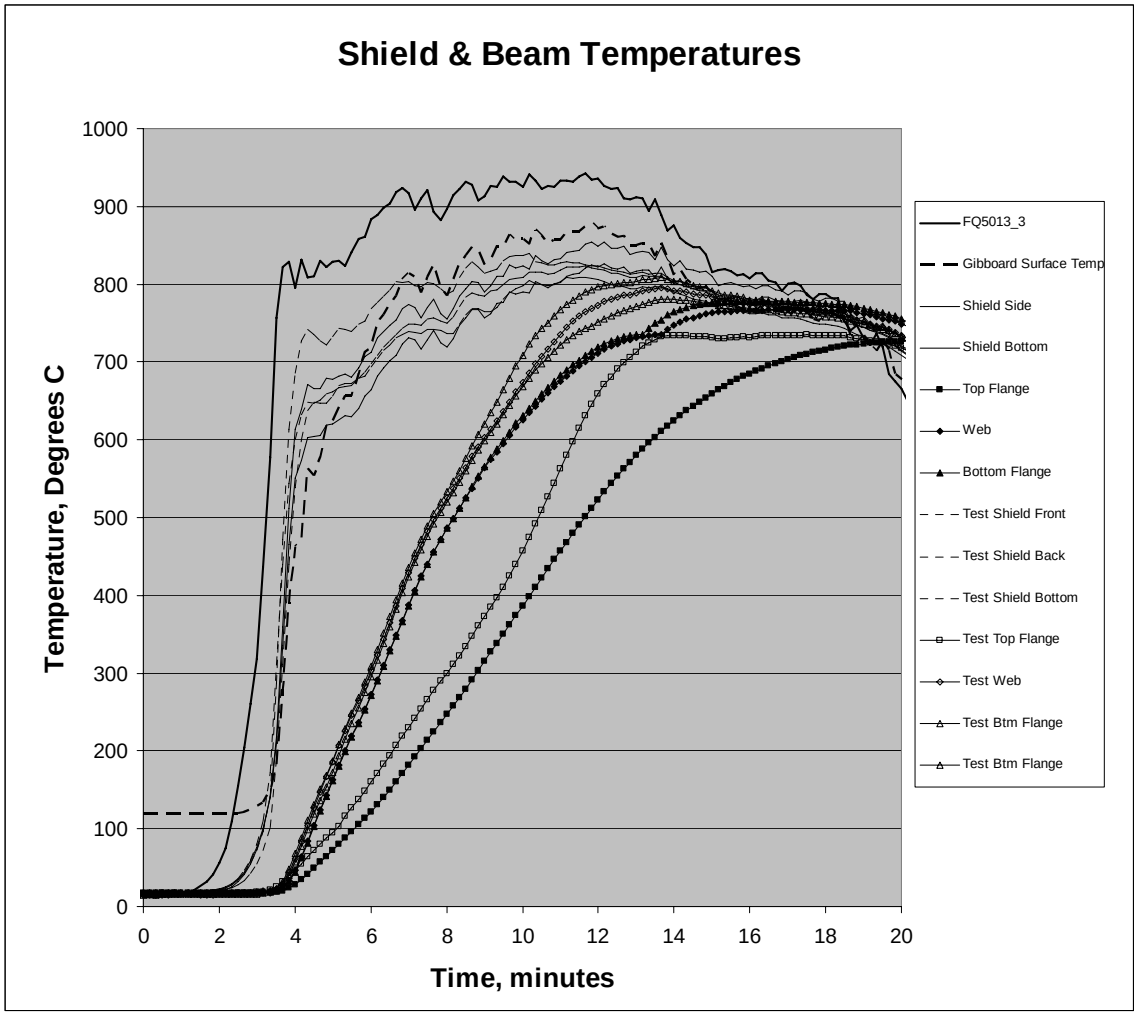

Figure 6.1 Calculated and Measured Beam and Shield Temperatures

Discussion of Results

The calculation tends to underestimate the shield temperature. The resulting calculated steel beam temperatures, the web, the bottom flange and the top flange, are reasonably estimated.

Fig 6.2 below illustrates the effect of changing the emissivity of the steel to 1.0.

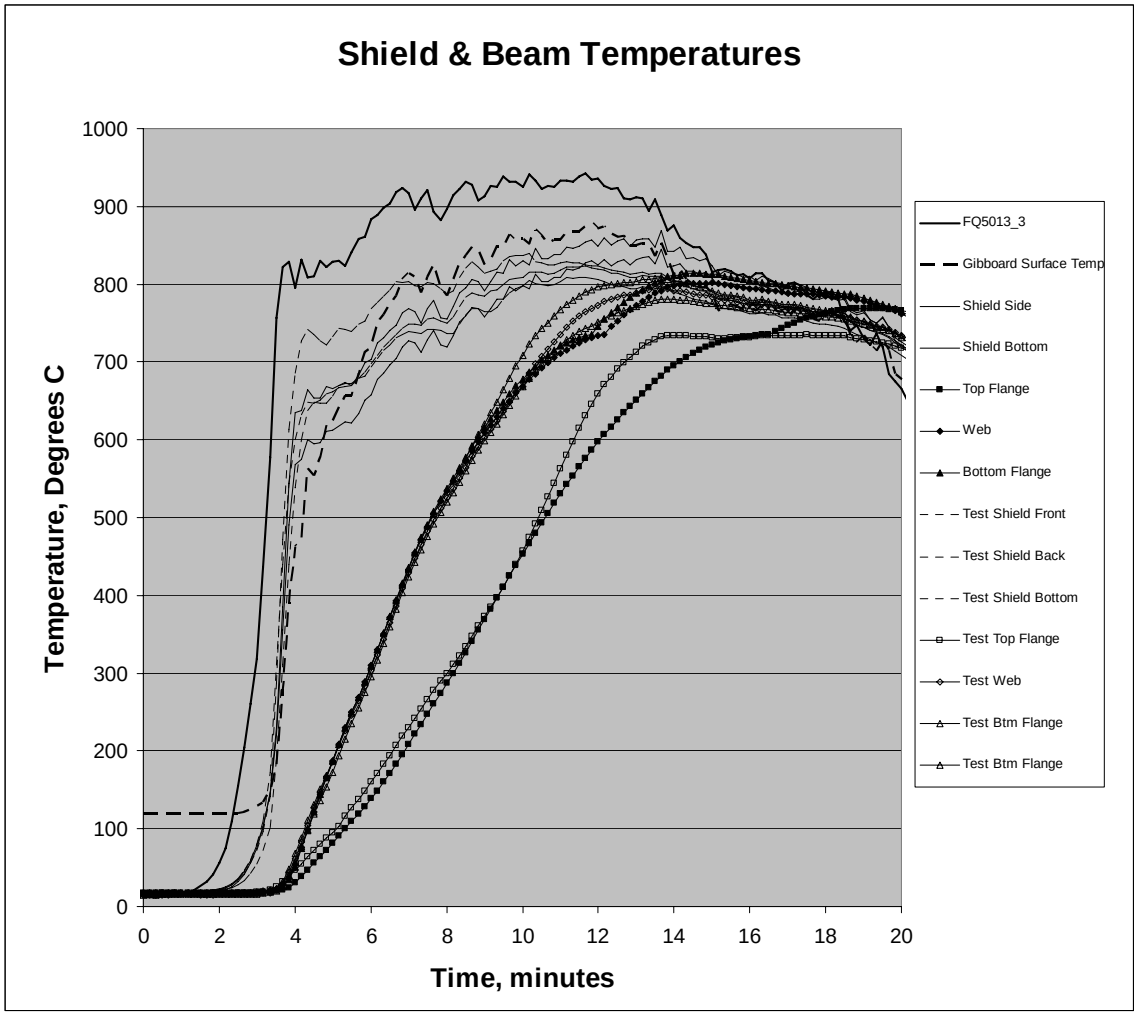

Figure 6.2 Calculated and Measured Beam and Shield Temperatures

Conclusion

As for the partial bottom flange protection, the radiation shield protection is insufficient to be useful in post-flashover fires in gypsum lined compartments. Light-gauge steel radiation shields may be useful in less severe compartment fires, such as in concrete carpark buildings.

The lumped mass analysis, with specific allowance for radiative heat transfer between surfaces, models the rise in steel beam temperatures adequately. The analysis could be used for other forms of construction where steelwork is partially protected.

Chapter 7 - Gypsum Plasterboard Model

Introduction

Heat transfer into and within gypsum plasterboard has usually been analysed by researchers using either a finite element analysis or a finite difference analysis.

Where an analysis focuses on the gypsum plasterboard itself, a relatively fine grid is used along with temperature dependent material properties. Such analyses have often used a purpose written computer program rather than a general purpose spread sheet. Where the gypsum plasterboard analysis is part of a larger study, such as for the calculation of energy losses through compartment walls, a coarse grid along with constant material properties keeps the analysis simple.

The aim of this section of this project is to derive a simple energy based analysis for gypsum plasterboard, which can be carried out using a spread-sheet. Ideally, the analysis would have sufficient detail to reflect the behaviour of gypsum plasterboard in an enclosure fire, and be able to give an estimate of when collapse of the gypsum plasterboard lining is likely to occur, but be simple enough so that it can be used to determine energy losses in an energy balance design-fire model.

Literature Review

Gypsum plasterboard has been well researched over the past decade.

- Jones[26] gives an excellent summary of gypsum plasterboard behaviour and material properties. He also carried out pilot furnace testing on both GIB® Standard and GIB Fyreline® (fire rated plasterboard), under both moderate and severe time-temperature curves.

- Nyman[31] carried out full scale tests of several fire rated gypsum plasterboard systems to study their behaviour during realistic compartment fires, which were significantly more severe than the standard ISO fire.
- Thomas[41] carried out a finite element analysis to study gypsum plasterboard systems under non-standard fires and compared the results with time equivalent formulae. Thomas also includes a very good summary of gypsum material properties.
- Collier[10,11,12] developed a finite difference model to predict the behaviour of gypsum plasterboard systems. The model allowed the effect of changes in construction and/or design fire to be studied. The model included the effect of temperature on load-bearing timber or steel framed systems. Sultan[39] also developed a finite difference analysis to model the thermal and structural performance of gypsum plasterboard systems.
- Axenenko & Thorpe[3] used finite element analysis to model the dehydration of gypsum plasterboard and to study the stresses within the plasterboard due to shrinkage. They used the concept of two dehydration fronts that progress from the heated side of the gypsum plasterboard to the unheated side.
- Gerlich[22] studied load-bearing light steel framed walls. Feng, Wang & Davies[18] also studied gypsum plasterboard lined light steel frame systems, as has Alfawakhiri, Sultan & MacKinnon[1].
- Clancy[8] carried out a parametric study to determine which aspects of light timber framed construction are the most important for fire rated construction. Sultan & Kodur[40] carried out a series of tests to study the importance of a variety of parameters in fire rated construction.
- Olsson[34] studied bench scale testing of light timber framed walls.

The scope of this report does not include an in-depth study of gypsum plasterboard. However a brief description is useful, particularly on the aspects which relate to the proposed analysis.

Gypsum Material Properties

Calcination/Dehydration:

When gypsum is exposed to heat, a chemical decomposition takes place releasing water vapour from the gypsum molecules. This occurs at between 100 ºC and 120 ºC. This chemical reaction accounts for the large peak in the specific heat at this temperature. The process is called calcination. Another chemical decomposition is stated by Axenenko & Thorpe[3] to take place between 600ºC and 700ºC when additional water molecules are driven off. Other researchers suggest that the second chemical decomposition occurs between 200ºC and 300ºC (Thomas[41]). The second reduction in plasterboard density occurs at approximately 600ºC (Thomas[41], Jones[26]), which supports the higher temperature for the second decomposition. The details of the decomposition are as follows: -

The chemical name for gypsum is Calcium Sulphate Dihydrate. It's chemical formulae is

$$CaSO_4.2(H_2O)$$

The atomic weight of the component parts are as follows: -

H	1
O	16
S	32
Ca	40

The atomic weight of Calcium Sulphate Dihydrate is 172. At approximately 120 ºC, 1 ½ molecules of H_2O are released yielding Calcium Sulphate Hemihydrate, $CaSO_4.{}^1/_2(H_2O)$, which has an atomic weight of 145. At approximately 600 ºC the remaining water molecules are driven off giving Calcium Sulphate Anhydrate, $CaSO_4$, which has an atomic weight of 136. If the free water within the gypsum, at ambient, is 3%, then approximately 18% of the gypsum plasterboard mass is lost at 120 ºC, and another 5% (of the original mass) is lost at approximately 600ºC.

When gypsum plasterboard is exposed to a fire, calcination begins on the exposed face and progressively works its way through the plasterboard. The temperature on the unexposed face of the gypsum plasterboard is effectively limited to 120ºC, until the calcination process reaches the unexposed face. Once this occurs, the temperature of the unexposed face climbs quickly. Axenenko[3] calls the progression of calcination through the gypsum plasterboard a dehydration front.

Ablation:

The term ablation relates to the progressive physical disintegration of the surface of the gypsum plasterboard, under furnace or fire conditions Jones[26], Collier[11].

Lining Collapse

The time to collapse of the exposed plasterboard lining is an important stage in the resistance of a light frame system, as after this event, the framing and the lining on the ambient side are exposed to the full severity of the fire. While the exposed lining remains in place, it provides a radiation shield to the framing and the unexposed lining.

Material Properties:

Jones[26] has summarised the results of several researchers. The following graphs, from his research, show how the relevant material properties vary with temperature – density, thermal conductivity and enthalpy in figures 7.1, 7.2, & 7.3 respectively.

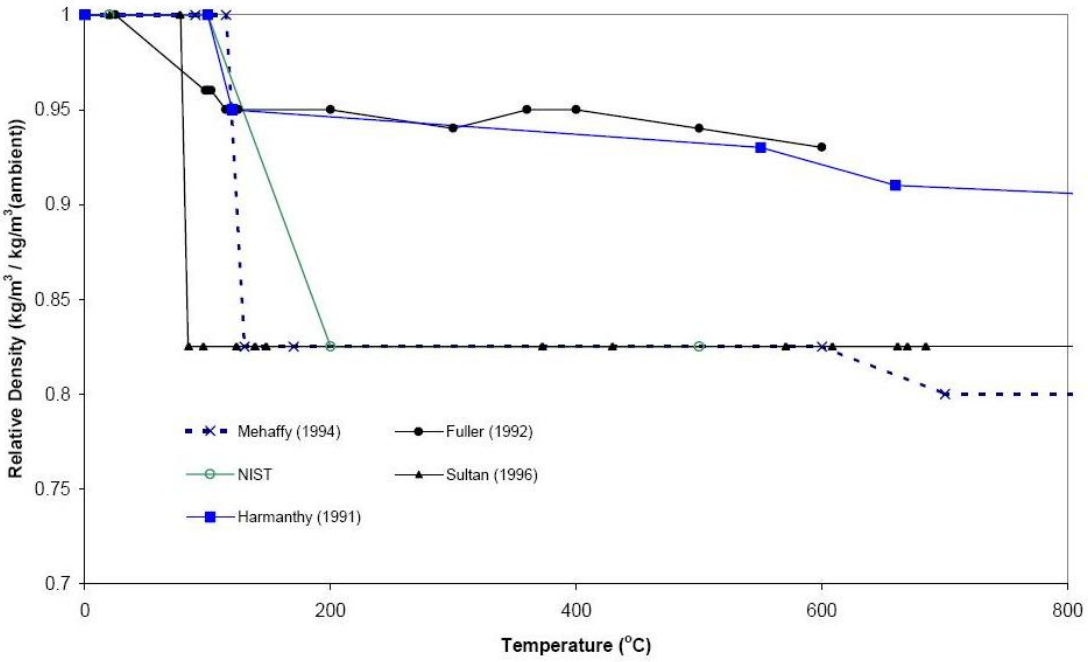

Figure 7.1 Relative Density Versus Temperature From Jones[26]

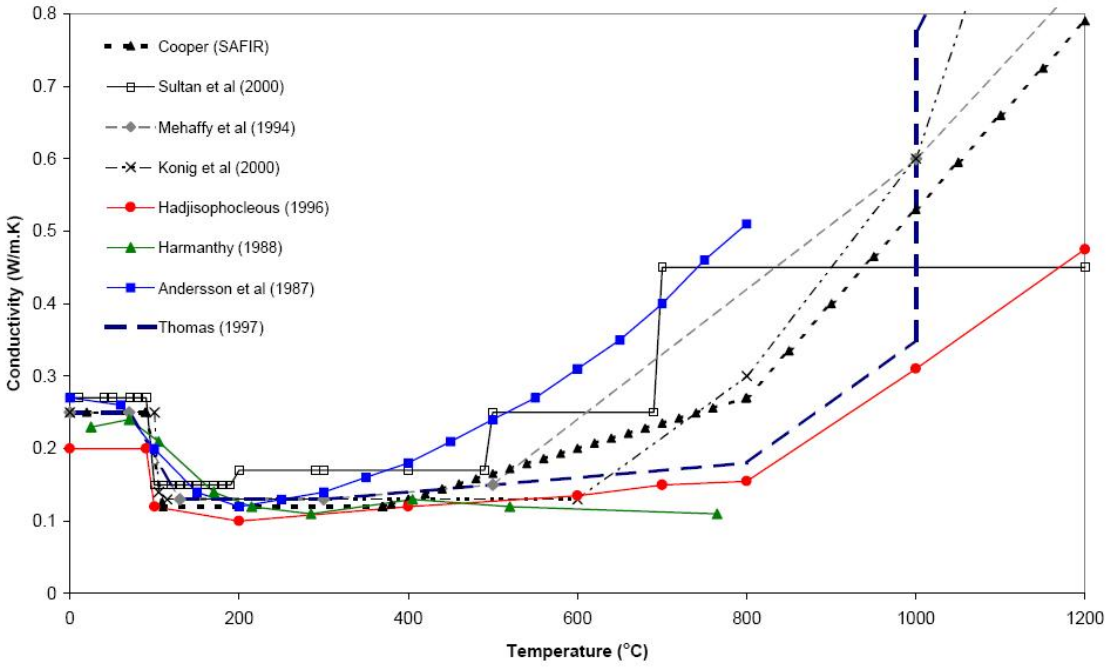

Figure 7.2 Thermal Conductivity Versus Temperature From Jones[26]

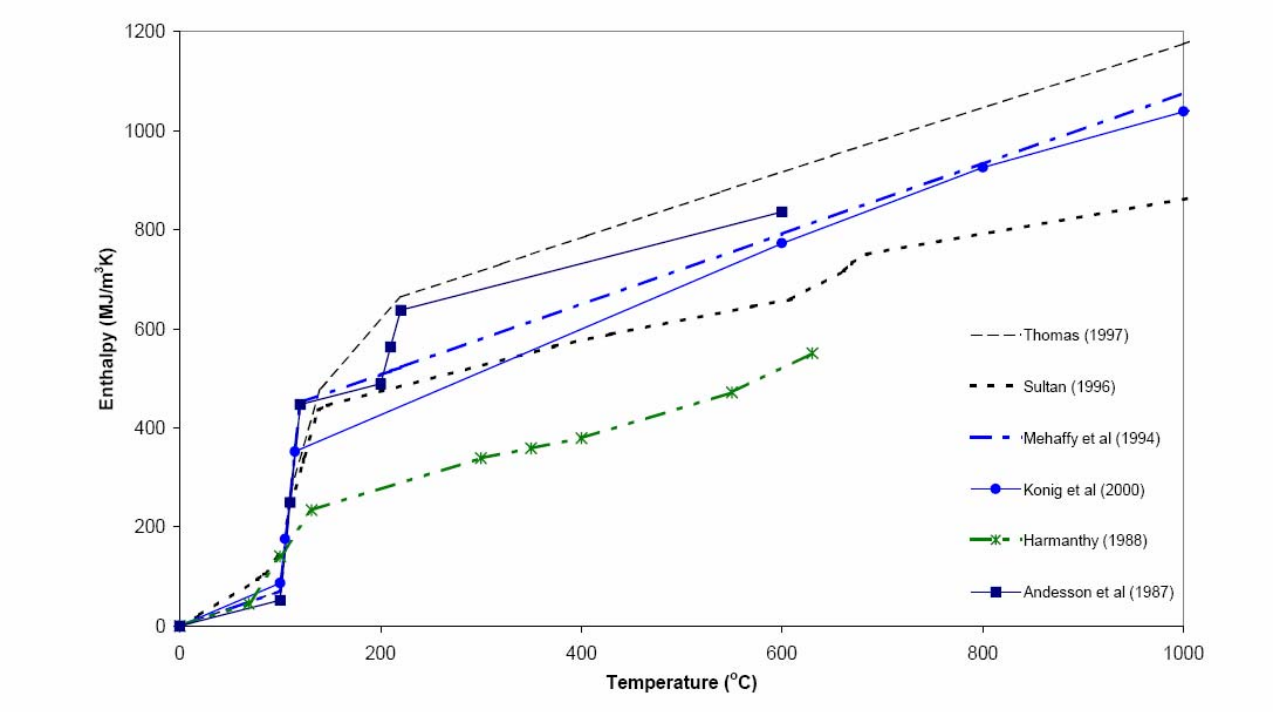

Figure 7.3 Enthalpy Versus Temperature From Jones[26]

Enthalpy (Specific Volumetric Enthalpy) is defined as

$$E(T) = \int_{Ta}^{T} (C_p \cdot \rho \cdot \tau) \partial \tau \qquad \text{Eqn 7.1}$$

Where

E = Enthalpy J/m^3

ρ = Density kg/m^3

C_p = Specific heat J/kg/K

T = Temperature, K

The Underlying Assumption of the Proposed Analysis

Figure 7.4 shows calculated temperature profiles through a layer of gypsum plasterboard lining, exposed to the standard ISO fire. The temperatures were calculated using a finite difference analysis with temperature dependent material properties.

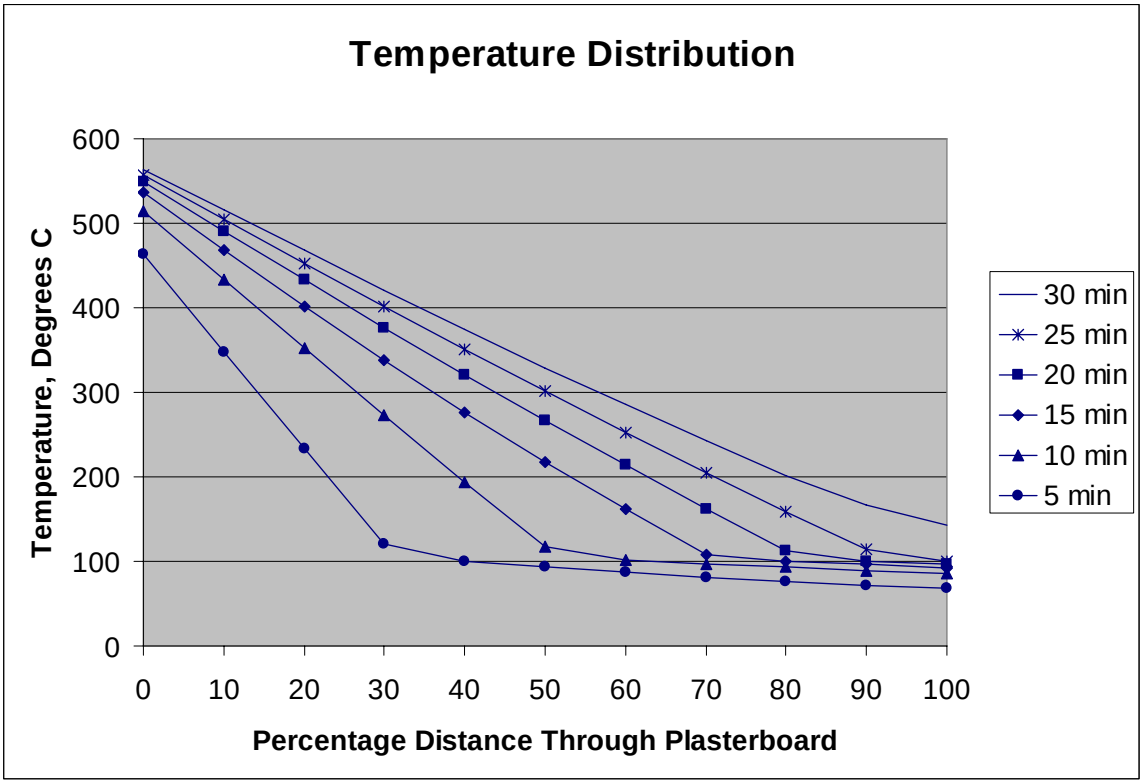

Figure 7.4 Calculated Temperature Profiles Through Gypsum Plasterboard

The change in the slope of the temperature profiles at 393 K (120ºC) is a result of the enthalpy associated with calcination. The progress of calcination (discontinuity of the temperature slope) can be clearly seen as it moves through the thickness of the gypsum plasterboard. The temperature on the unexposed surface does not rise above 120°C (393 K) until the calcination has worked its way through the plasterboard. The temperature profile, between the exposed surface of the gypsum plasterboard and the layer within the plasterboard where the calcination is taking place, is close to linear. The proposed analysis will assume that this temperature distribution is linear, or rather, that the heat flow through the gypsum plasterboard, from the exposed surface to the calcinating surface, is constant and can be expressed as: -

$$HF_e = k_{eq} \cdot (T_{sf} - T_c) / x \qquad \text{Eqn 7.2}$$

Where :-

HF_e = Heat flow through the gypsum plasterboard, W/m^2

k_{eq} = An equivalent thermal conductivity, W/m/K

T_{sf} = Temperature of the fire exposed surface

T_c = Calcination Temperature (393 K, or 120ºC)

x = The depth of the calcination layer, m.

Basic Formulation of the Analysis

The heat flow into the gypsum plasterboard can be equated to the rate of calcination.

$$E \cdot \partial x / \partial t = k_{eq} \cdot (T_{sf} - T_c) / x \qquad \text{Eqn 7.3}$$

Re-arranging and integrating

$$E \cdot x^2 / 2 = k_{eq} \cdot \int (T_{sf} - T_c) \partial t \qquad \text{Eqn 7.4}$$

Where

E = Enthalpy of the gypsum plasterboard, J/m^3

t = time, sec

Numerical Analysis

Equation 7.4 above can be solved numerically using a spread-sheet. The value of each term in the equation is discussed below.

Exposed Surface Temperature:

Equating the radiant heat flow from the fire to the conductive heat flow through the gypsum plasterboard allows a realistic estimate of the temperature of the exposed surface of the gypsum plasterboard, T_{sf}, to be established. The suggested numerical method of evaluating this temperature is the Newton-Raphson method.

The out-of-balance heat flow, HF_{oob}, at the exposed surface of the gypsum plasterboard is: -

HF_{oob} = radiant heat flow (from the fire) – conductive heat flow (through the plasterboard)

$$= \varepsilon_f \cdot \sigma \cdot (T_f^4 - T_{sf}^4) + h_{cf} \cdot (T_f - T_{sf}) - k_{eq} \cdot (T_{sf} - T_c) / x \qquad \text{Eqn 7.5}$$

where

ε_f = resultant emissivity of the fire to the exposed gypsum plasterboard

σ = Stephan Bolzmann Constant (5.67E-8)

h_{cf} = convective heat transfer coefficient between the fire and the exposed surface.

Differentiating:

$$\partial(HF_{oob}) / \partial(T_f) = -(\varepsilon_f \cdot \sigma \cdot 4 \cdot T_f^3 + h_{cf} + k_{eq} / x) \qquad \text{Eqn 7.6}$$

A revised estimate of the exposed surface temperature is:

$$T_{sf}' = T_{sf} - HF_{oob} / [\partial(HF_{oob}) / \partial(T_f)] \qquad \text{Eqn 7.7}$$

Usually the Newton-Raphson method is used to iterate to a closer solution within a time step. In this application, it was found that equation Eqn 7.7 could be used to estimate the gypsum plasterboard surface temperature at the next time step. Where the accuracy of the solution requires improvement, a shorter time step is as effective as iteration within the time step.

The method was found to be very stable and accurate over a wide range of temperatures.

Thermal Conductivity

The thermal conductivity of gypsum plasterboard increases with increasing temperature. Refer to figure 7.2 above from Jones[26]. The following empirical formula was used in the analysis.

$$k = 0.1 + (0.00055 \cdot Temperature)^3 \qquad \text{W/m/K} \qquad \text{Eqn 7.8}$$

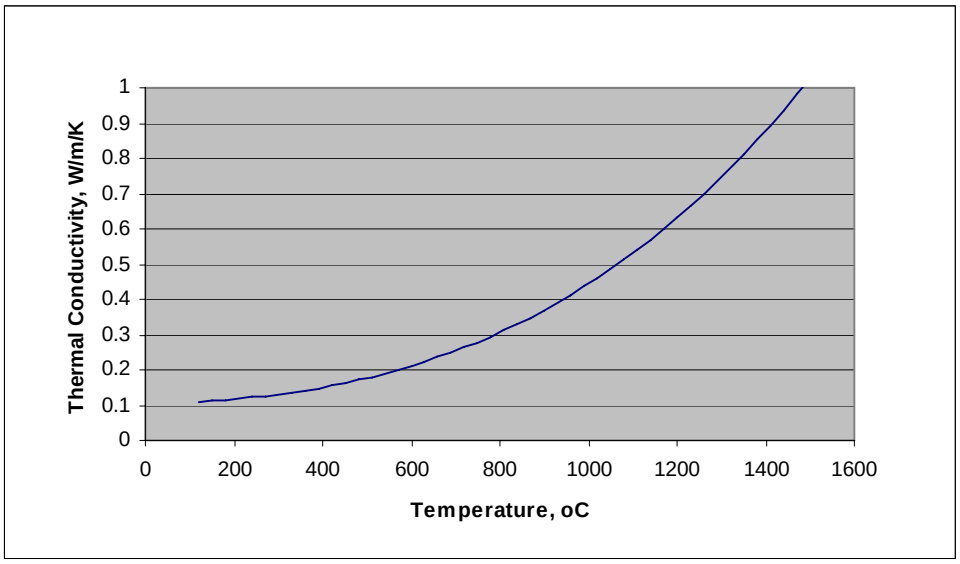

Figure 7.5 Thermal Conductivity Versus Temperature Used in the Analysis

As a spread sheet analysis will yield both the exposed surface temperature and the unexposed surface temperature, the thermal conductivity at both surfaces can be calculated. Using the underlying assumption that the heat flow through the gypsum plasterboard is constant, $\partial T/\partial x$ at both surfaces can therefore also be established.

$\partial T/\partial x$ = HF/k_{sf} at the exposed surface and

= HF/k_{ce} at the unexposed surface.

Where

k_{sf} = thermal conductivity at the surface fire side and

k_{ce} = thermal conductivity at the cavity, exposed lining.

Fitting a cubic equation to the temperature distribution, the following equivalent thermal conductivity can be derived.

$$k_{eq} = 3/(2/k_{ce} + 1/k_{sf})$$ Eqn 7.9

The assumed, or compatible, temperature distribution is

$$T(x) = T_{sf} - (T_{sf} - T_{ce}) \cdot (x/w) + 2 \cdot \alpha \cdot (x/w) - 3 \cdot \alpha \cdot (x/w)^2 + \alpha \cdot (x/w)^3$$ Eqn 7.10

Where

$$\alpha = (k_{eq}/k_{ce} - k_{eq}/k_{sf}) \cdot (T_{sf} - T_{ce})/3$$ Eqn 7.11

x = distance from the exposed face

T_{ce} = temperature, cavity side, exposed face

Enthalpy

The enthalpy, E, of gypsum plasterboard increases with increasing temperature. Refer to graph from Jones[26] above. The following empirical formula was used in the analysis for 13mm Gib Fyreline® (the enthalpy varies with different gypsum plasterboard composition).

$$E(T) = E_0 + Cpd \cdot (T - Tc)$$
$$= 480E6 + 480E3 \cdot (T - Tc) \quad J/m^3$$ Eqn 7.12

Where

Cpd = the specific heat * density

E_0 = Enthalpy associated with calcination

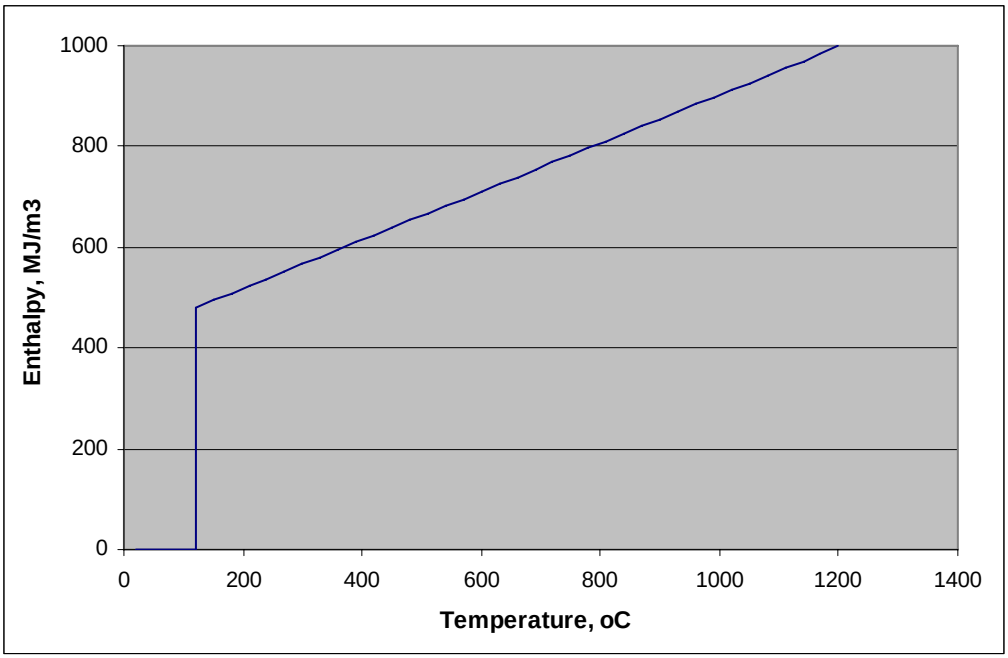

Figure 7.6 Enthalpy Versus Temperature Used in the Analysis

Flow of Water

Water is driven off in the process of calcination. On the basis that the calcinated board is more porous, it is assumed that most of the water vapour finds its way into the fire compartment. Water vapour leaving the exposed face will either be at the compartment temperature or, if cooler, will shield the gypsum plasterboard surface from the radiation of the fire. For simplicity it is assumed that the water vapour leaves the surface of the plasterboard at the fire temperature, and that the energy absorbed by the water vapour is consistent with this rise in temperature.

The energy absorbed by the water vapour as it leaves the plasterboard is potentially significant. To illustrate, a water content of 20%, a plasterboard density of 750 kg/m^3, a specific heat of 2000 J/kg/K, and a rise in temperature of 667 K, gives an enthalpy absorbed by the water vapour of 0.2 * 750 * 2000 *667 = 200 MJ/m^3. This is a significant proportion of the specific heat of the gypsum plasterboard.

Spread-Sheet Implementation of the Analysis

Figure 7.7 shows a single layer of gypsum plasterboard.

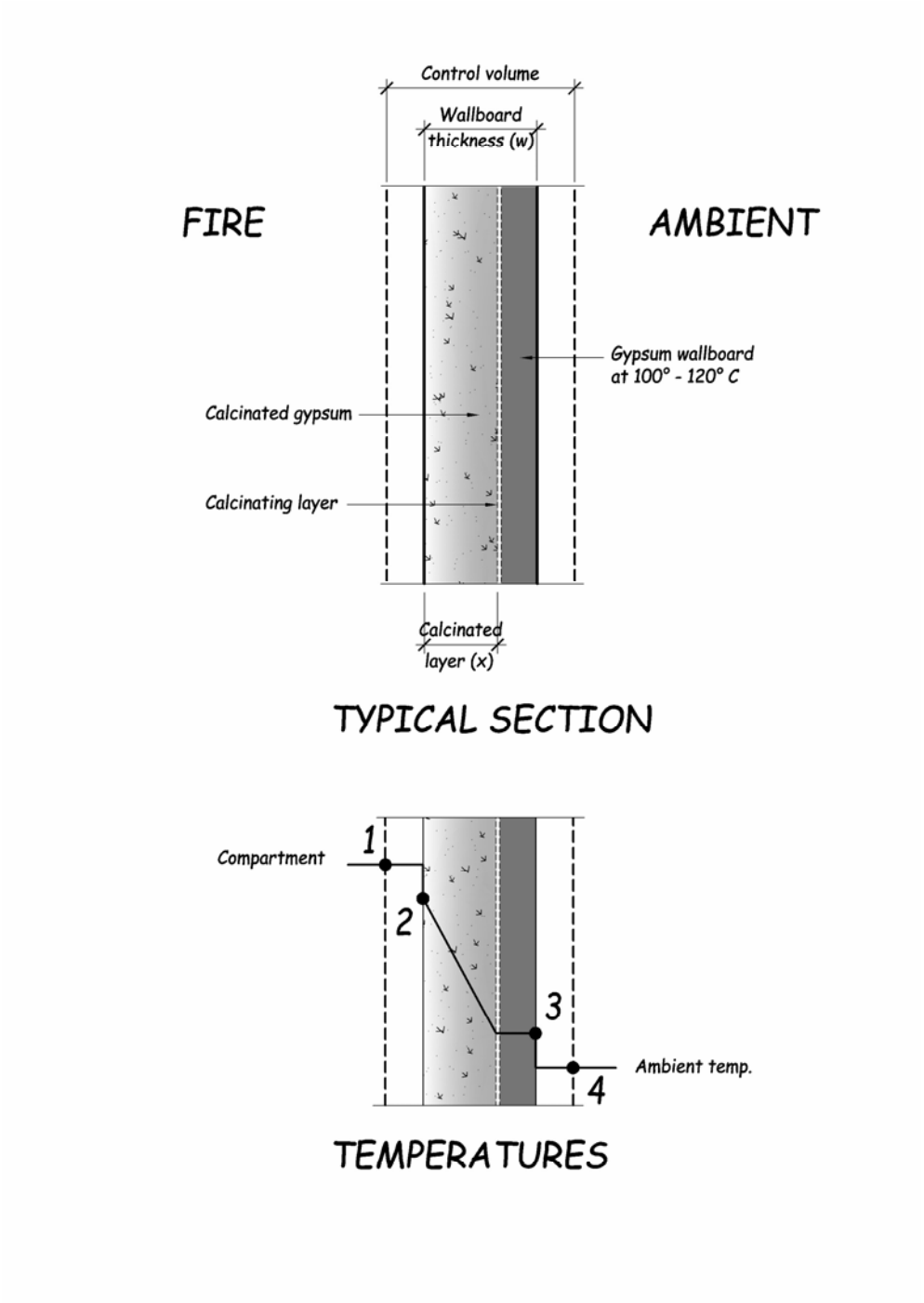

Figure 7.7 Single Layer of Gypsum Plasterboard

T_1 is the temperature of the fire or heat surface, K.

T_2 is the temperature of the exposed surface of the gypsum plasterboard, K.

T_3 is the temperature of the unexposed surface of the plasterboard, K, which is assumed to be not less than the calcination temperature, 393 K (120°C).

T_4 is the ambient temperature, K.

ε_{12} is the emissivity between surfaces 1 & 2.

σ is the Stephan Bolzmann constant (5.67E-8).

h_{c12} is the convective coefficient between surfaces 1 & 2.

wc is the water content of the gypsum (free and bonded) in kg/m^3.

Cpw is the specific heat of water vapour (approximately 2000 J/kg/K)

x is the depth of the calcination layer, m

The net heat flow into the plasterboard, at time increment i, is

$$HF^{(i)} = \varepsilon_{12} \cdot \sigma \cdot (T_1^{(i)4} - T_2^{(i)4}) + h_{c12} \cdot (T_1^{(i)} - T_2^{(i)}) \quad \{\text{radiant and convective heat flow in}\}$$

$$- \varepsilon_{34} \cdot \sigma \cdot (T_3^{(i)4} - T_4^{(i)4}) - h_{c34} \cdot (T_3^{(i)} - T_4^{(i)}) \quad \{\text{radiant and convective heat flow out}\}$$

$$- wc \cdot Cpw \cdot (x^{(i)} - x^{(i-1)}) \cdot (T_1^{(i)} - T_3^{(i)}) \quad \{\text{energy lost to rise in water vapour temperature}\}$$

Eqn 7.13

The total heat flow absorbed by the gypsum plasterboard is the integral of the heat flow above, over time

$$E^{(i)} = \sum_j (HF^{(i)} \cdot dt), \text{ from j = 1 to i} \qquad \text{Eqn 7.14}$$

Equating the total heat absorbed with the increase in gypsum plasterboard enthalpy, E_{gib}

$$E_{gib} = E_0 \cdot x^{(i+1)} + Cpd \cdot (T_2^{(i)} + T_3^{(i)}) \cdot x^{(i+1)} / 2 \qquad \text{Eqn 7.15}$$

Solving for $x^{(i+1)}$

$$x^{(i+1)} = E^{(i)} / (E_0 + Cpd \cdot (T_2^{(i)} + T_3^{(i)}) / 2), \quad x^{(i+1)} <= w \qquad \text{Eqn 7.16}$$

If $x^{(i)}$=w then

$$T_3^{(i+1)} = 2 \cdot (E^{(i)} / w - E_0) / Cpd - T_2^{(i)} \qquad \text{Eqn 7.17}$$

$T_2^{(i+1)}$ is established by calculating the out of balance of heat flow at node 2 and minimising using the Newton-Raphson method.

$$T_2^{(i+1)} = [\varepsilon_{12} \cdot \sigma \cdot (T_1^{(i)4} - T_2^{(i)4}) + h_{c12} \cdot (T_1^{(i)} - T_2^{(i)}) - k_{eq} \cdot (T_2^{(i)} - T_3^{(i)}) / x^{(i)}]$$

$$/[\varepsilon_{12} \cdot \sigma \cdot 4 \cdot T_2^{(i)3} + h_{c12} + k_{eq} / x^{(i)}] \qquad \text{Eqn 7.18}$$

Applications

Stud Wall

The above analysis can be doubled up, in series, to analyse gypsum plasterboard on both sides of a stud wall. The heat input into the unexposed lining will be the radiant and convective heat crossing the cavity. This enables the analysis to be calibrated against test data.

Suspended Gypsum Plasterboard Ceiling

The above analysis can be combined with a finite difference analysis of a concrete slab to analyse a suspended ceiling below a concrete slab.

Calibration and Verification

Jones[26] test FP 2882 (moderate fire, 13 GIB Fyreline® on steel studs) was used to calibrate the analysis. The constants (thermal conductivity, etc) were adjusted so that the calculated temperatures were consistent with the experimental results. The comparison between the analysis and the test data is shown in Figure 7.8.

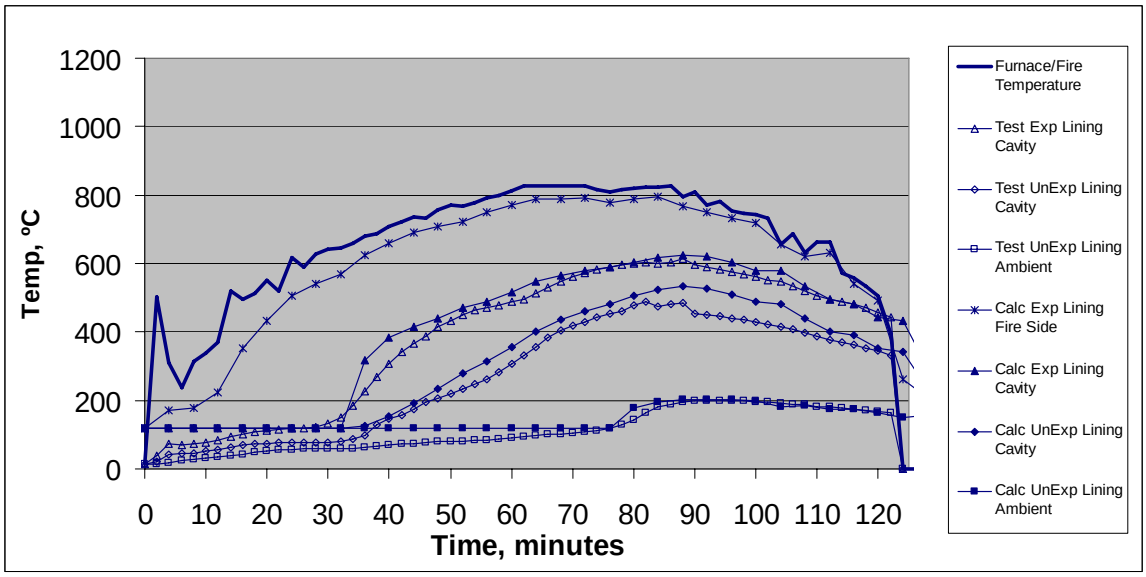

Figure 7.8 Comparison Between Test Data and Calculated Temperatures

Constants used in the analysis are those presented earlier in this chapter and the following: -

- A water content of 100 kg/m^3 was used in the analysis, which allows for water vapour losses, other than to the compartment.
- A gypsum plasterboard emissivity of 0.4 was used in the analysis. The value of emissivity is insensitive with respect to the surface temperature of the fire exposed lining, and also to the surface temperature of the ambient surface, however it has a significant effect on the temperature difference across the cavity. The low value of emissivity may be due to the presence of carbon dioxide and water vapour within the cavity (Thomas[41]).
- Convective coefficients were taken from Thomas[41].

For verification the spread-sheet analysis was compared with available test data. Refer to Figure 7.9 and Appendix A. The following observations were noted from the comparison: -

- When the cavity temperature of the exposed lining rises rapidly to match the furnace temperature, this is an indication that the exposed lining has collapsed. Comparisons after this event are invalid, as the spread-sheet analysis did not incorporate failure of the exposed lining.
- When the cavity temperature of the exposed lining rises above 120ºC, the calcination has penetrated the exposed lining. Similarly for the unexposed lining.
- The temperature comparison up until the exposed lining collapse is generally fair to good.
- The analysis predicts the time to when calcination has penetrated the plasterboard consistently and reasonably accurately.

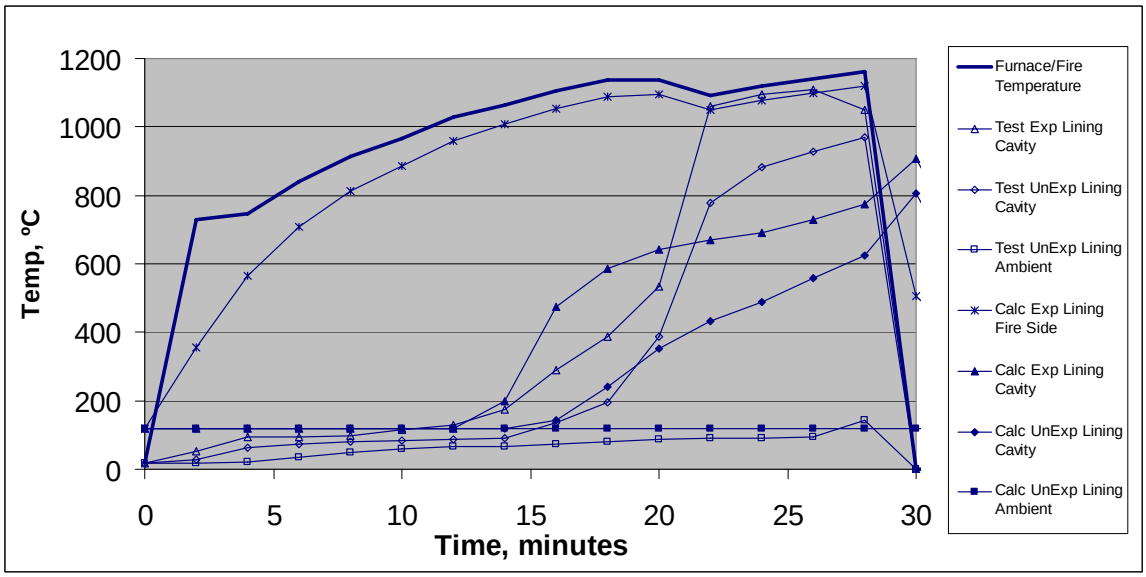

Figure 7.9 Jones[26] Test FP 2881
(Severe Fire, 13 GIB Fyreline® on Steel Studs)

Collapse of the Exposed Lining

Generally the proposed analysis gives reasonable results up until when the exposed lining collapses. Once the exposed lining falls away, the framing and unexposed linings face the full effects of the fire and the deterioration of the supporting frame and unexposed lining

accelerates. The ability to predict when the exposed lining collapses is very important if the structural &/or thermal impact on the building elements behind the exposed layer are to be analysed with any degree of accuracy.

Collier[11],in his drywall model, changed the mathematical modeling of the exposed lining, when the average temperature of the plasterboard exceeded (approximately) 750ºC. Collier called this temperature the Ablation Temperature. Above the Ablation Temperature, Collier modeled the plasterboard as thermally thin (uniform temperature through the thickness of the plasterboard). After reaching the Ablation Temperature, the temperature of the exposed lining, in Collier's model, tends to quickly rise to that of the fire. This corresponds with the failure of the exposed lining, as the cavity and unexposed lining are then subjected to the full intensity of the fire. Collier[11] adjusts the Ablation Temperature to calibrate his model to test data. The Ablation Temperature marks the onset of collapse of the exposed lining.

Sultan[39] proposes a collapse criterion, for type X fire-rated gypsum plasterboard, of when the average temperature of the exposed lining exceeds 600ºC.

Axenenko & Thorpe[3] showed that, for type X fire-rated plasterboard, the structural capacity of the dehydrated lining could not resist the stresses consistent with the shrinkage associated with dehydration. Thus the proportion of plasterboard on the ambient side of the dehydration front provides the structural capacity to resist the dehydration shrinkage stresses in the plasterboard on the fire side of the dehydration front. When the dehydration front passes some point in the plasterboard, the shrinkage stresses overcome the structural capacity of the remaining plasterboard and the plasterboard collapses.

When gypsum plasterboard is used as a ceiling lining, the gypsum plasterboard is also required to support it's own weight between supports. The additional stress from gravity results in an earlier collapse time for ceilings.

Factors which affect the failure time of the exposed lining are: -

- plasterboard composition, (density, fibre reinforcing, etc)
- plasterboard position - wall or ceiling,
- the rate of heating, and
- thermal expansion or shrinkage of the supporting framing.

The ends of plasterboard sheets, where the gypsum plasterboard is not continuous over the supporting stud/joist/batten, will be more susceptible to structural collapse. Short pieces of plasterboard around penetrations, and the like, will be particularly susceptible to early failure. Ceilings can also fail during the cooling down phase, when there is a reversal of the thermal expansion. In the third test, FQ5013_3, portions of the ceiling collapsed when the compartment temperatures had dropped to 400ºC.

For standard gypsum plasterboard ceilings, it is suggested that the plasterboard will collapse at, or very shortly after, the calcination front reaches the unexposed face of the plasterboard, i.e. when the temperature of the unexposed face rises above 120ºC. In the first compartment test, FQ5013_1, the ceiling failed immediately the temperature of the unexposed lining rose above 120ºC. The paper facing on the unexposed side of the plasterboard is still in place at this time. Certainly a standard gypsum plasterboard ceiling will not be able to remain intact once the unexposed paper facing ignites and disintegrates at approximately 300ºC.

For fire rated gypsum plasterboard, the glass reinforcing within the plasterboard provides additional structural strength. As a consequence the plasterboard remains intact even after the paper facing on the unexposed side of the plasterboard disintegrates. It is suggested that after the second dehydration (at approximately 700ºC), the gypsum/glass-fibre bond has little or no strength. Thus, when the thickness of the plasterboard, which has not yet reached a temperature of, say, 700ºC (973K), diminishes below some critical thickness, the plasterboard fails structurally and collapses.

This critical thickness will be dependent on several factors, including: -

- whether the plasterboard is a ceiling or a wall lining,
- the weight, thickness and composition of the plasterboard,
- the construction details (batten spacing, fixing centres, edge fixing, etc) and,
- thermal expansion/shrinkage properties of the supporting structure.

In the furnace tests of wall constructions, collapse of the plasterboard is associated with a very rapid rise of temperature of the unexposed face of the exposed lining (i.e. when the thermocouple measuring this temperature is exposed to the full severity of the fire or furnace). From the test time-temperature graphs, an estimate of the temperature of both the exposed surface and the unexposed surface of the plasterboard lining at failure can be estimated. Figure 7.10 shows the temperature profile through the plasterboard at failure, assuming a linear temperature profile through the plasterboard.

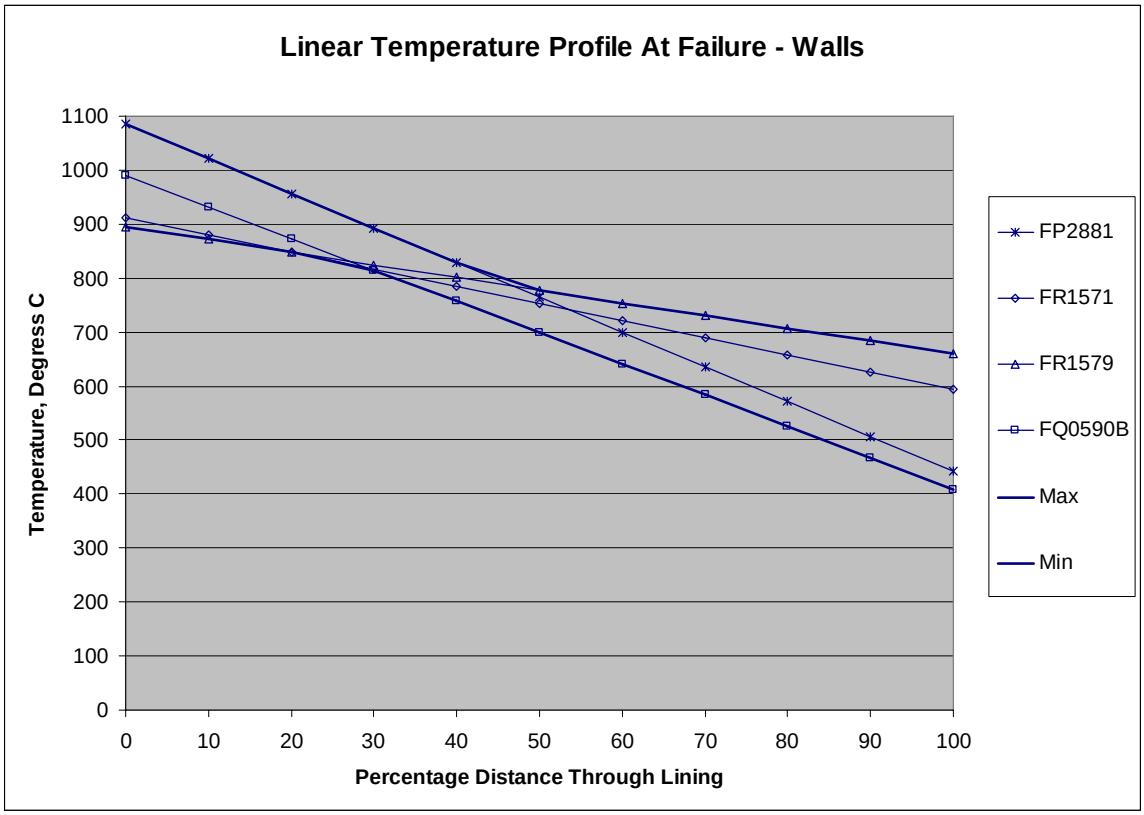

Figure 7.10 Calculated Temperature Profiles Through 13mm GIB Fyreline® Plasterboard at Collapse

This graph suggests that, on average, collapse occurs when a temperature of 800 ºC is reached at a location 40% into the plasterboard thickness. This is approximately the same as Collier's Ablation Temperature concept, where the onset of collapse occurs at an average plasterboard temperature of approximately 750ºC (1023K). Sultan's[39] collapse criteria of 600ºC was proposed for type X fire-rated gypsum plasterboard and would be conservative if it was applied to GIB Fyreline®.

Another way of interpreting the graph above is: -

- collapse of the plasterboard will not occur until the second dehydration front passes through at least 40% of the thickness of 13mm GIB Fyreline® plasterboard, **BUT**
- collapse will occur before the second dehydration front passes through 75% of the thickness of the plasterboard.

Equation 7.10 above is the equation of a cubic temperature profile through the gypsum plasterboard, compatible with the higher thermal conductivity on the fire side of the plasterboard. The temperature profile is based on the assumption that the heat flow through the gypsum plasterboard is constant. Fig 7.11 shows the compatible cubic temperature profile through the plasterboard at failure, based on the surface temperatures on each face.

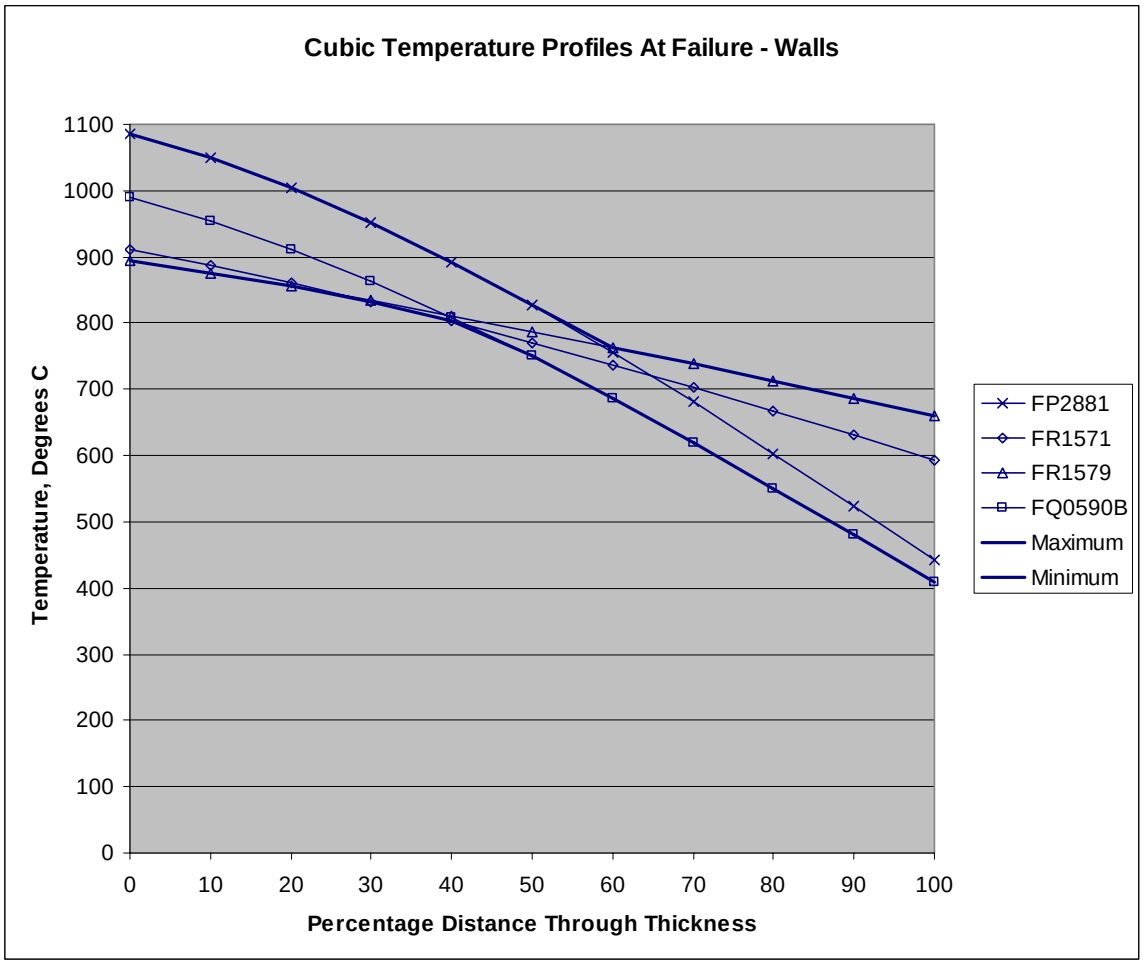

Figure 7.11 Calculated Temperature Profiles Through 13mm GIB Fyreline® Plasterboard at Collapse

The same conclusions can be drawn from this graph, although here collapse of the gypsum plasterboard does not occur until the second dehydration front passes through at least half the lining.

Figures 7.12 & 7.13 give temperature profiles at collapse for ceilings.

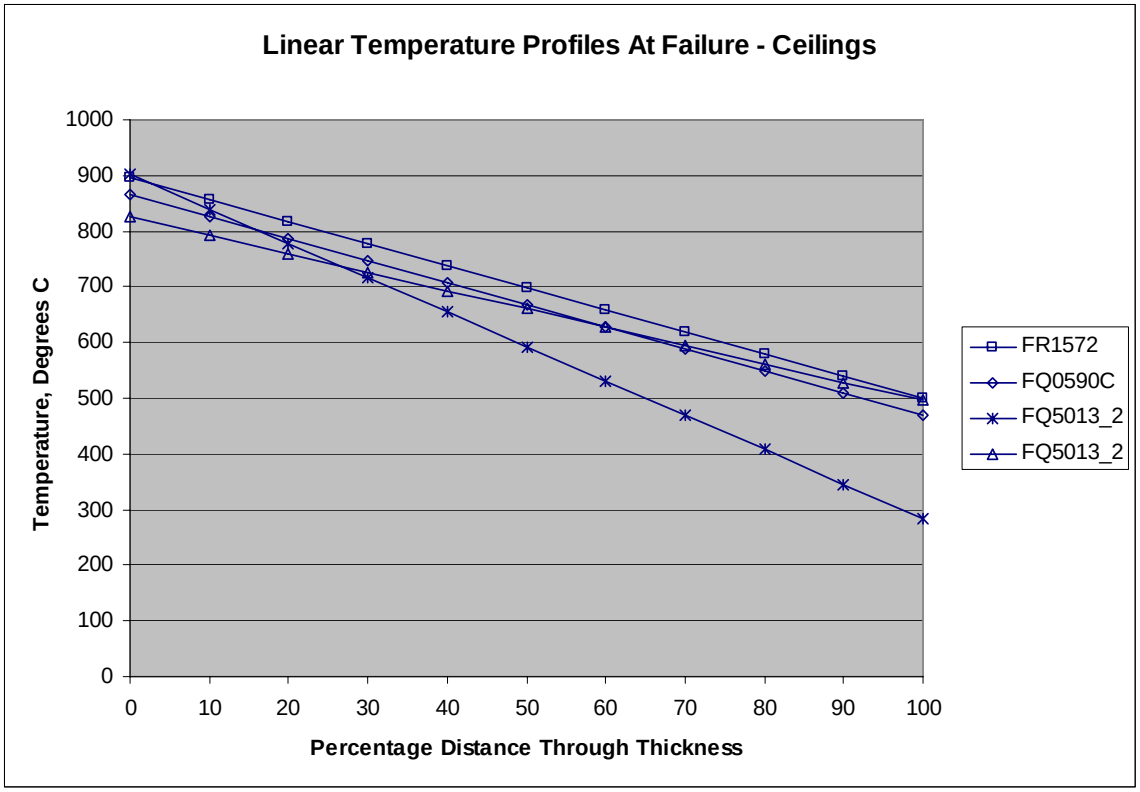

Figure 7.12 Calculated Temperature Profiles Through 13mm GIB Fyreline® Ceilings at Collapse

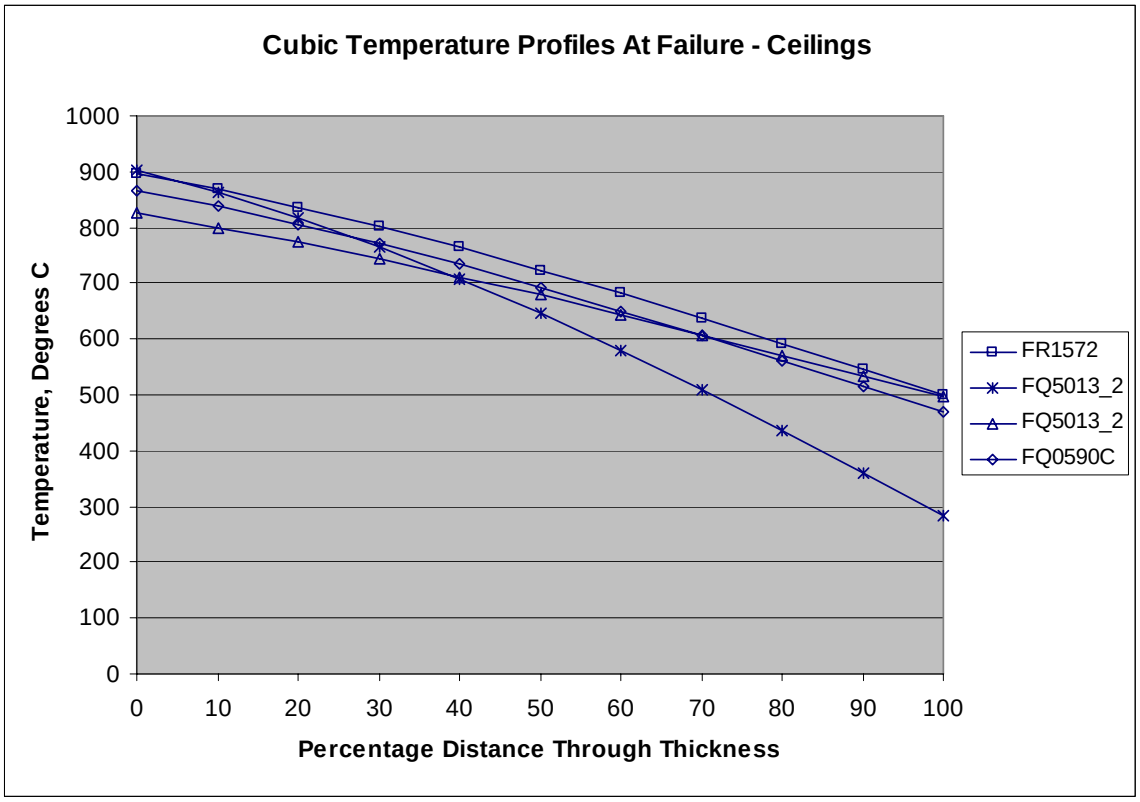

Figure 7.13 Calculated Temperature Profiles Through 13mm GIB Fyreline® Ceilings at Collapse

As there is a scarcity of data, few conclusions can be drawn. It is noted that ceiling collapse occurs when less of the plasterboard thickness is affected by the second dehydration front. It should be noted that in the FQ5013_2 test, the 13mm GIB Fyreline® was not installed in accordance with the requirements for a fire-rated ceiling. Specifically: -

- the edges were not back-blocked, and
- the ends of the plasterboard sheets were not joined on a ceiling batten (but they were back-blocked).

For the purposes of this study, collapse criteria for 13mm GIB Fyreline® is as follows: -

- When assuming a cubic temperature profile through the plasterboard
    - For walls: when the portion of plasterboard, which is at less than 750°C, is less than 50% (6.5mm) of plasterboard thickness.
    - For ceilings: when the portion of plasterboard, which is less than 750°C, is less than 65% (8.5mm) of plasterboard thickness.

- When assuming a linear temperature profile through the plasterboard
    - For walls: when the portion of plasterboard, which is at less than 750°C, is less than 60% (7.8mm) of plasterboard thickness.
    - For ceilings: when the portion of plasterboard, which is less than 750°C, is less than 75% (9.8mm) of plasterboard thickness.

Figure 7.14 is a graph of the standard ISO fire test of 13mm GIB Fyreline® on Steel Studs, showing when the calculated collapse of the exposed lining occurs, based on the above criteria. The lining collapsed during the test at 61 minutes.

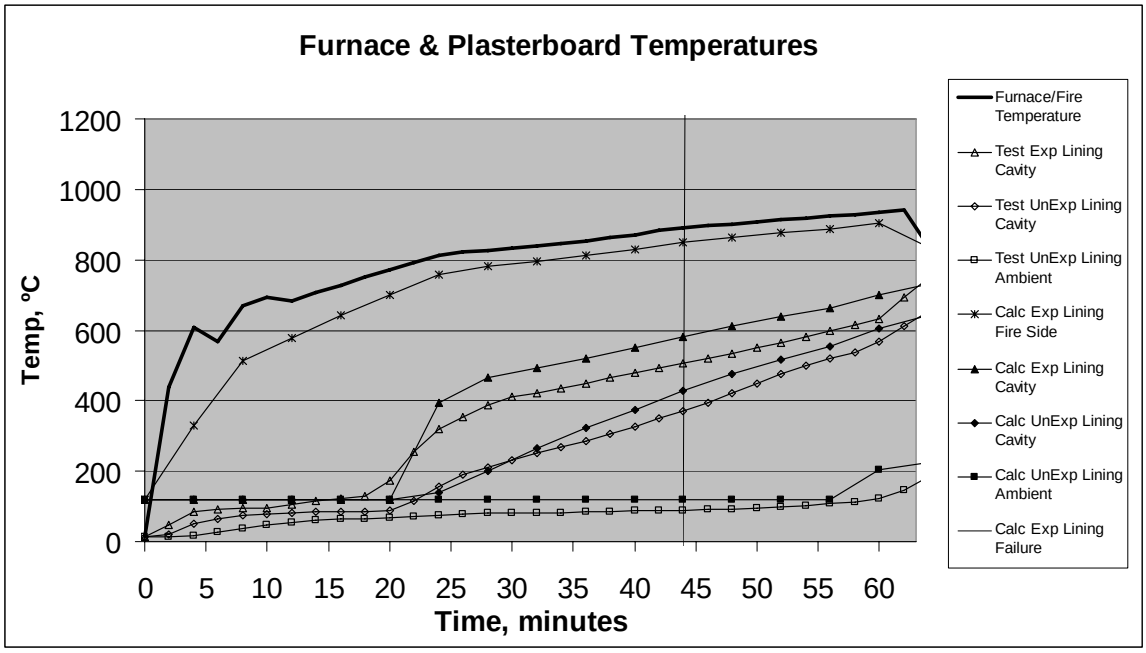

Figure 7.14 FR1579 ISO Furnace Test - 13mm GIB Fyreline® on Steel Studs

The predicted time to failure of the lining, 44 minutes, is conservative for two reasons: -

1. The calculated temperature of the unexposed surface of the exposed lining is overestimated, and
2. A lower bound (conservative) collapse criteria has been set.

The time to collapse is very sensitive to the calculated gypsum plasterboard temperatures. Because the plasterboard is increasing in temperature slowly, a small overestimation in the calculated temperature leads to a large reduction in the time to failure. The result shows some sensitivity to the specified critical thickness. A sensitivity analysis was carried out varying both the critical plasterboard thickness and the critical temperature. Results are in table 7.1 below.

Collapse Time Minutes	**Critical Temperature 1000 K**	**Critical Temperature 1023 K**	**Critical Temperature 1050 K**
Critical Thickness 60%	34.7	53.3	57.7
Critical Thickness 55%	34.2	50.8	55.8
Critical Thickness 50%	33.7	48.5	53.3
Critical Thickness 45%	33.3	46.0	50.8
Critical Thickness 40%	32.8	43.7	48.3

Table 7.1 Sensitivity Analysis: for Plasterboard Collapse Times in minutes for different values of Critical Temperature and Critical Thickness

The failure mechanism of fire-rated gypsum plasterboard requires further research. Until more in known, there is little choice but to adopt a conservative approach. Fig 7.15 is another graph illustrating the analysis and prediction of the exposed lining collapse.

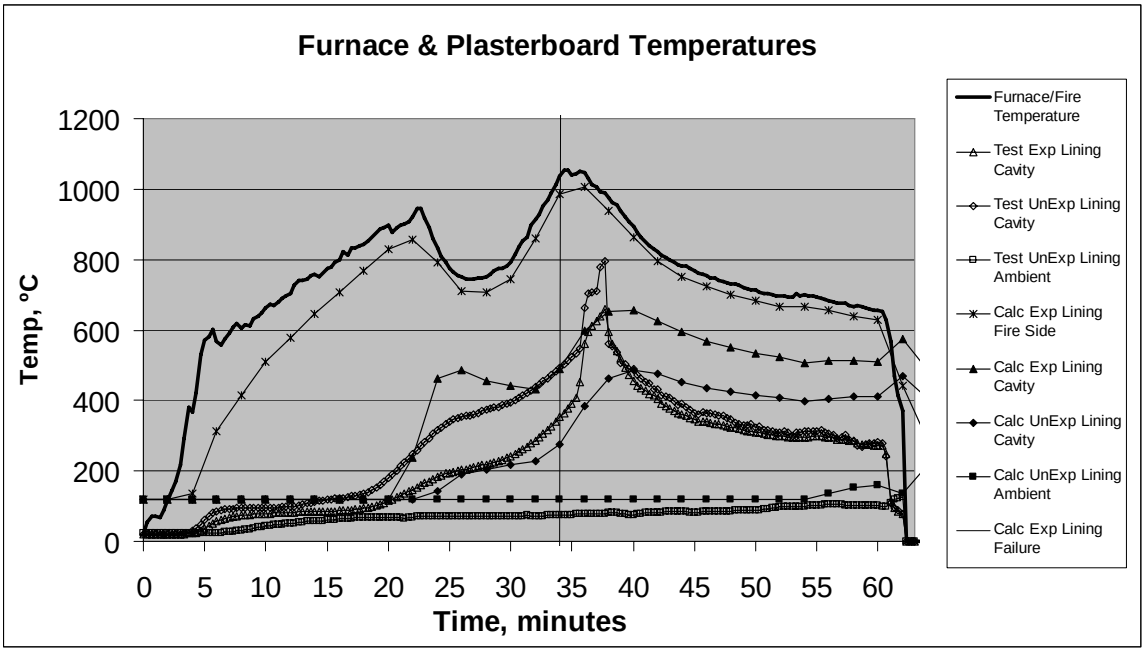

Figure 7.15 FQ0590B, Nyman's Compartment Fire, 13mm GIB Fyreline® on Steel Studs

In this case the prediction is conservative, but not unduly so (35 minutes compared to the actual collapse time of approximately 38 minutes).

[If a thermal analysis, other than the one presented above, is carried out, which requires a failure criteria in terms of the temperature of the unexposed face of the plasterboard, then the following failure criteria are suggested: -

- Standard gypsum plasterboard wall linings collapse when the unexposed face reaches a temperature of 200°C.
- Standard gypsum plasterboard ceiling linings collapse when the unexposed face reaches a temperature of 120°C.
- GIB Fyreline® wall linings collapse when the unexposed face reaches a temperature of 400°C.
- GIB Fyreline® ceiling linings collapse when the unexposed face reaches a temperature of 300°C.

This failure criteria for GIB Fyreline® will be very conservative in some situations, particularly for less intense fires.]

Approximate Analysis

Equation 7.4, derived above, is the underlying formulae behind the above analysis.

$$E \cdot x^2 / 2 = k_{eq} \cdot \int (T_{sf} - T_c) \partial t \qquad \text{Eqn 7.4}$$

The integral on the right hand side is an "area under a time-temperature curve". With simplifying assumptions this formula reduces to the "Equal Area Concept".

Equal Area Concept

The equal area concept states that different time-temperature curves have equivalent fire severity if the areas under the time temperature curve are equal. The simplifying assumptions are discussed below.

1. ***That T_{sf} is approximately the same as the compartment gas temperature, T_f.***
   This is a valid assumption when the compartment gas temperature is high. Because radiant heat flow is proportional to the fourth power of the absolute temperature, a very small temperature difference will give rise to significant heat flow, when the temperatures are high. At modest temperatures, the difference between the compartment gas temperature and the exposed gypsum plasterboard surface temperature can be significant.

2. ***That the thermal conductivity is constant.***
   In reality, the thermal conductivity of gypsum plasterboard is greater at higher temperatures.

3. ***That the plasterboard volumetric enthalpy is constant.***
   In reality the total enthalpy change from ambient, of the gypsum plasterboard, increases with increasing temperature.

4. ***That the base temperature, when calculating the area under the time temperature curve, is the calcination temperature, Tc (approx.120ºC), (i.e. the temperature associated with the dehydration front).***
   If the baseline is taken as ambient temperature (or absolute zero) rather than the calcination temperature, 120ºC, then areas under the time-temperature can not be directly compared.

5. ***That the wall lining remains intact throughout the fire.***
   For fire-rated gypsum plasterboard, the above equation is valid only while the (exposed) gypsum plasterboard remains intact. The lining is more likely to fall away from its support in a higher temperature fire. Thus the fire severity of higher temperature fires will tend to be underestimated by the equal area concept. 'Equal Area' remains valid for standard gypsum plasterboard because the collapse of the exposed lining coincides with the penetration of the calcination front through, and collapse of, the plasterboard. Therefore the heat transfer through more than one layer of standard gypsum plasterboard can be analysed independently and simply added.

Assumptions 1, 2 & 3 above, compensate each other to some extent (i.e. while E and k_{eq} increase with temperature, the ratio E/k_{eq} is relatively constant). The temperature associated with the dehydration front must be used as the baseline when calculating and comparing areas under the time-temperature curves. The "Equal Area Concept" can not be used beyond the point at which fire-rated gypsum plasterboard linings collapse.

The following illustrates the equal area concept for 13mm plasterboard on each side of steel stud framing. Figure 7.16 plots Jones's[26] test data for 13mm GIB® standard plasterboard. Figure 7.17 plots Jones's[26] test data for 13mm GIB Fyreline® plasterboard. The areas under the time-temperature curve are given in table 7.2 below.

Fire Test Number	Gypsum Board Type	Fire Description	Failure Type	Failure Time	Area Celsius-Minutes
FP2879	GIB® standard	Severe	Integrity	34	20200
FP2880	GIB® standard	Moderate	Integrity*	50	21310
FP2922	GIB® standard	ISO	Integrity*	38	23057
FP2881	GIB Fyreline®	Severe	Integrity*	28	24034
FP2882	GIB Fyreline®	Moderate	Insulation	82	44656
FR1579	GIB Fyreline®	ISO	Insulation	63	42649

* Insulation following quickly afterwards

Table 7.2 Comparison of Areas Under the Time-Temperature Curves

For standard plasterboard, the 'areas', at failure, are within a plus/minus 6.5% range of the average. The 'ISO' and 'moderate' fire tests compare favorably for the fire rated plasterboard. In the 'severe fire', fire-rated plasterboard test, the exposed lining collapsed at a relatively earlier stage during the fire, resulting in an earlier failure time for the wall system. The early failure of the fire-rated plasterboard exposed lining invalidates the 'Equal Area' concept as a method of comparing Test FP2881 with the other tests.

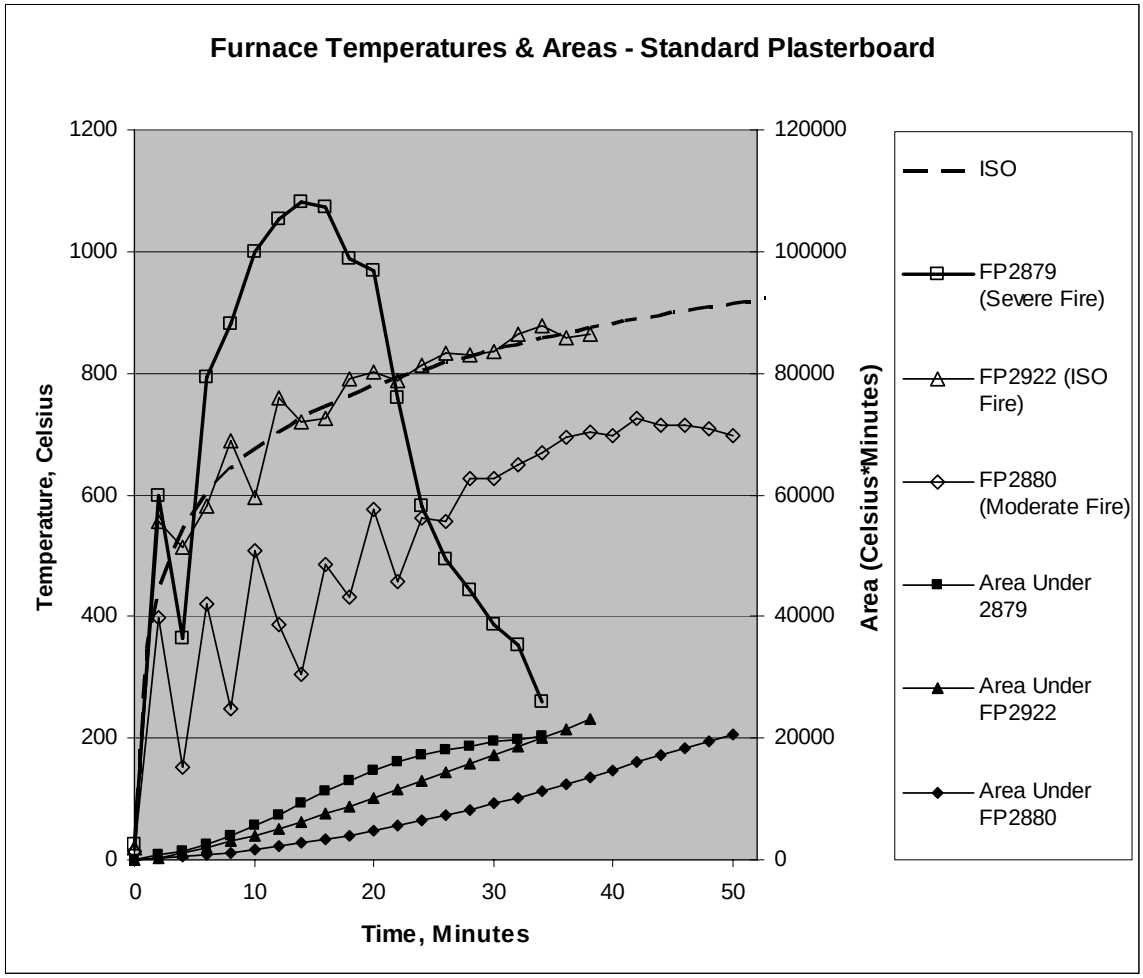

Figure 7.16 Areas Under the Time-Temperature Curve – Standard Plasterboard

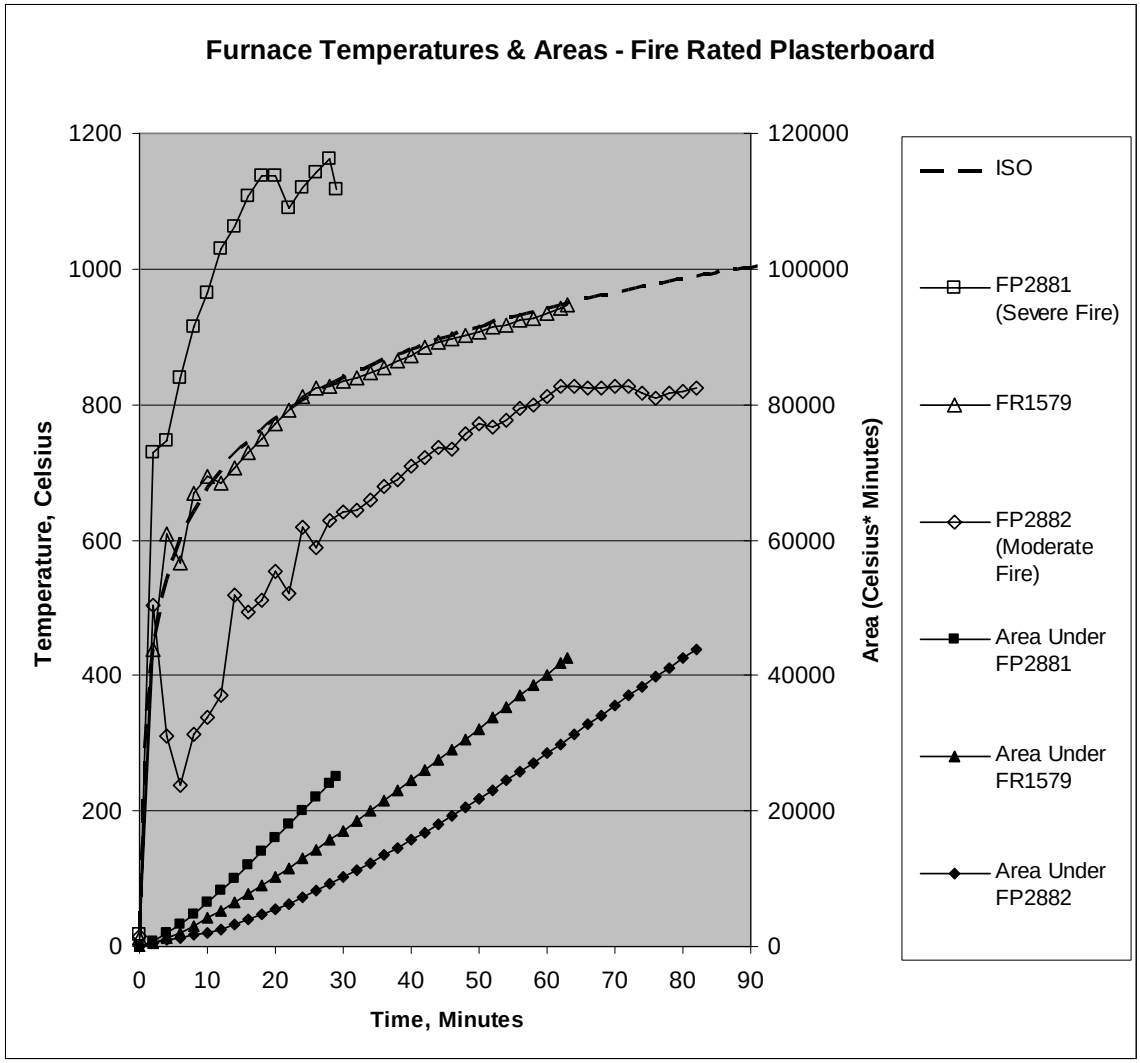

Fig 7.17 Areas Under the Time Temperature Curve – Fire Rated Plasterboard

Standard Gypsum Plasterboard

For standard gypsum plasterboard, when the dehydration front reaches the unexposed face of the plasterboard, both the rapid rise in temperature of the unexposed face, and structural collapse of the plasterboard is imminent. The 'Equal Area' concept can be used to predict both insulation and integrity failure, which will occur at approximately the same time.

Collapse of Fire-Rated Gypsum Plasterboard

The physics behind equation 7.4 is: -

1. The dehydration front progresses through the gypsum plasterboard when the compartment fire temperature is greater than the temperature associated with the dehydration, and
2. The progression of the dehydration front through the gypsum plasterboard, squared, is proportional to the area under the time-temperature curve (the temperature being the compartment temperature over and above the dehydration temperature).

This can be applied to fire-rated gypsum plasterboards. The area under the time–temperature curve can be used to estimate the depth of penetration of the second dehydration front into the plasterboard. Table 7.3 compares the area under the time-temperature curve for different tests at the time of lining collapse of the exposed plasterboard lining. 800°C was used as the dehydration temperature, as this yielded the most meaningful results. This temperature is close to 750°C, which was used in the earlier analysis. Figures 7.10 and 7.11 indicate that 750°C is a good lower-bound lining collapse temperature but that 800°C is a good average lining collapse temperature.

Fire Test Number	Gypsum Board Type And Construction	Failure Time	Area Celsius-Minutes
FQ5013_2	13 GIB Fyreline® Ceiling	17	2219
FQ0590B	13 GIB Fyreline® Ceiling	25	2431
FQ0590B	13 GIB Fyreline® on timber studs	52	4013
FR 1571	13 GIB Fyreline® on timber studs	68	4077
FP2882	13 GIB Fyreline® on steel studs	20	3219
FR1579	13 GIB Fyreline® on steel studs	62	3079

Table 7.3 Comparison of Areas Under the Time-Temperature Curve for Various 13 GIB Fyreline® Tests.

It is noted that the areas under the time-temperature curves for different fires are comparable, provided the construction is the same.

Where the construction is different, the penetration distance of the second dehydration front, at collapse of the plasterboard, is not the same and thus the area under the time-temperature curve will be different. Ceilings collapse at a smaller penetration distance of the second dehydration front due to the additional structural strength required to support the dead weight of the plasterboard lining. Steel studs expand during a fire test, placing the exposed plasterboard lining under tension. This exacerbates the effects of shrinkage of the plasterboard, which occurs during heating. Timber studs however shrink, reducing the effect of plasterboard shrinkage. Fire-rated plasterboard linings supported on timber framing can therefore sustain a deeper penetration of the second dehydration front than fire-rated plasterboard linings supported on steel framing, and thus the increase in the corresponding area under the time-temperature curve at collapse of the exposed lining.

Conclusions and Summary

- The basic formulation for the proposed gypsum plasterboard analysis, equations 7.13 to 7.18 above, can be simply solved using a spread-sheet. The results adequately predict the end of the calcination period of the gypsum plasterboard for any given time-temperature design fire.

- The temperature of the exposed lining after the end of the calcination period shows the correct trend but is usually overestimated.

- Collapse of a standard gypsum plasterboard ceiling is imminent once the calcination front reaches the unexposed face.

- Collapse of glass reinforced fire-rated gypsum plasterboards may be related to the second dehydration front, which occurs at approximately 750ºC. It is suggested that collapse of the plasterboard will occur when the portion of the plasterboard, which has yet to reach a temperature of 750ºC, is less than some critical thickness. This critical thickness being related to: -

- Plasterboard composition, particularly thickness, weight, and reinforcement
- Position of the plasterboard - ceiling or wall,
- Details of the construction – batten centres, fixing centres, etc
- Thermal expansion/shrinkage properties of the supporting structure

- The predicted time to the exposed lining collapse is very sensitive to the calculated plasterboard temperatures. A small error in the calculated temperature results in a significant error in the time of collapse.

- The proposed analysis allows the time to collapse of the exposed lining to be estimated, although the estimate maybe conservative.

- The equal area concept can be used to compare the effect of different time-temperatures curves (i.e. different fires) on a given plasterboard construction. The equal area concept will give good estimates of when the exposed plasterboard lining collapses. For standard gypsum plasterboard, this also closely coincides with the insulation failure criteria.

- Further study to improve the above analysis should concentrate on the following items: -
    - Refinement of the spread-sheet analysis to better predict the plasterboard temperature after the calcination front has reached the unexposed surface. Axenenko's concept of a double front should be included in the analysis. The second front would be particularly useful as a collapse criterion for fire-rated gypsum plasterboard.
    - A better understanding and collection of data to indicate how the critical failure thickness relates to the composition of the gypsum plasterboard and the details of construction.

Chapter 8 - Comparison of Calculated and Measured Temperatures for a Steel Beam Protected with a Gypsum Plasterboard Ceiling

Introduction

When a steel beam is in the ceiling space above a suspended gypsum plasterboard ceiling, the steel beam is protected from the full intensity and duration of the fire. The temperatures within the ceiling space are effectively limited to 120ºC, until the calcination front has penetrated the full thickness of the gypsum plasterboard ceiling. If the ceiling is a fibre-glass-reinforced, fire-rated plasterboard, then the ceiling will remain intact for a further period of time, whereas standard gypsum plasterboard will collapse almost immediately the calcination front has reached the unexposed face. (Refer to section 7 above.)

This section will compare calculated and measured temperatures in the steel beams within the ceiling space.

Standard Gypsum Plasterboard Ceiling

Figures 8.1 and 8.2 compares the calculated and measured temperatures for the steel beams within the ceiling space for the first test, which had a standard gypsum plasterboard ceiling. Material constants used in the analysis were: -

- Emissivity of steel 0.9
- Emissivity of concrete 0.8
- Emissivity of gypsum 0.4
- Convective heat transfer constant, hc, 20 $W/m^2/K$

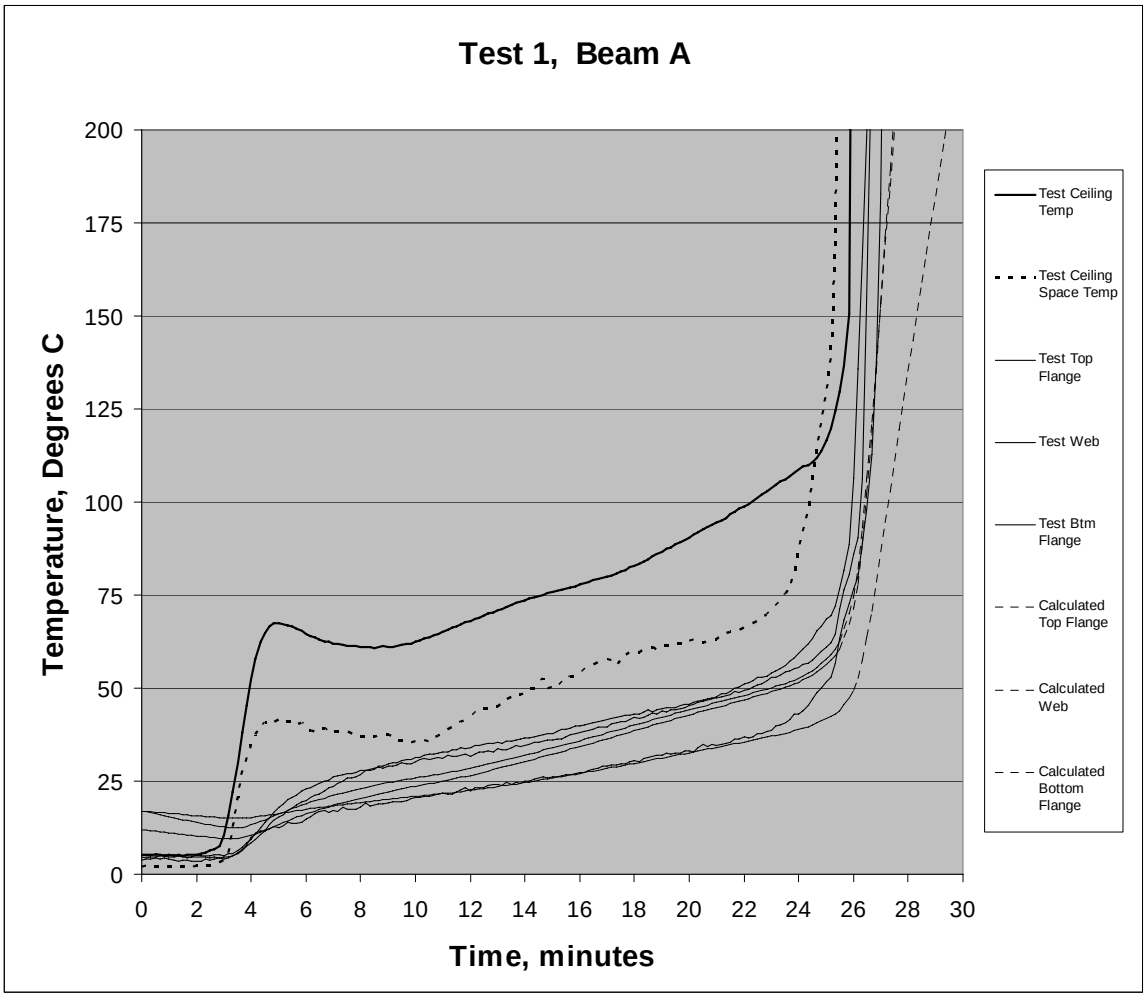

Figure 8.1, Calculated and Measured Beam Temperatures, Test 1, Beam A

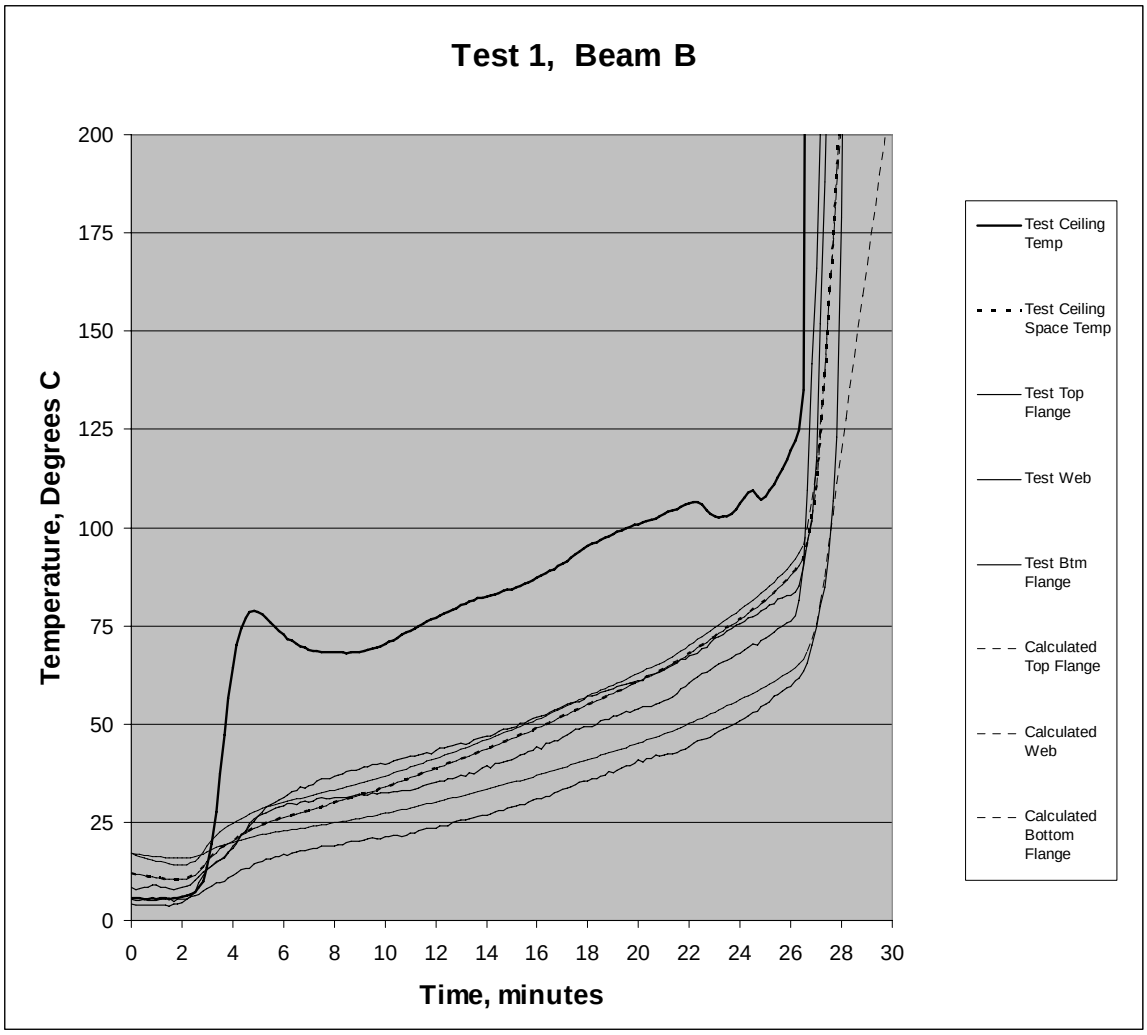

Figure 8.2, Calculated and Measured Beam Temperatures, Test 1, Beam B

Fire-Rated Gypsum Plasterboard Ceiling

Figures 8.3 to 8.5 compares the calculated and measured temperatures for the steel beams within the ceiling space for the second and third tests, which had a GIB Fyreline® plasterboard ceiling.

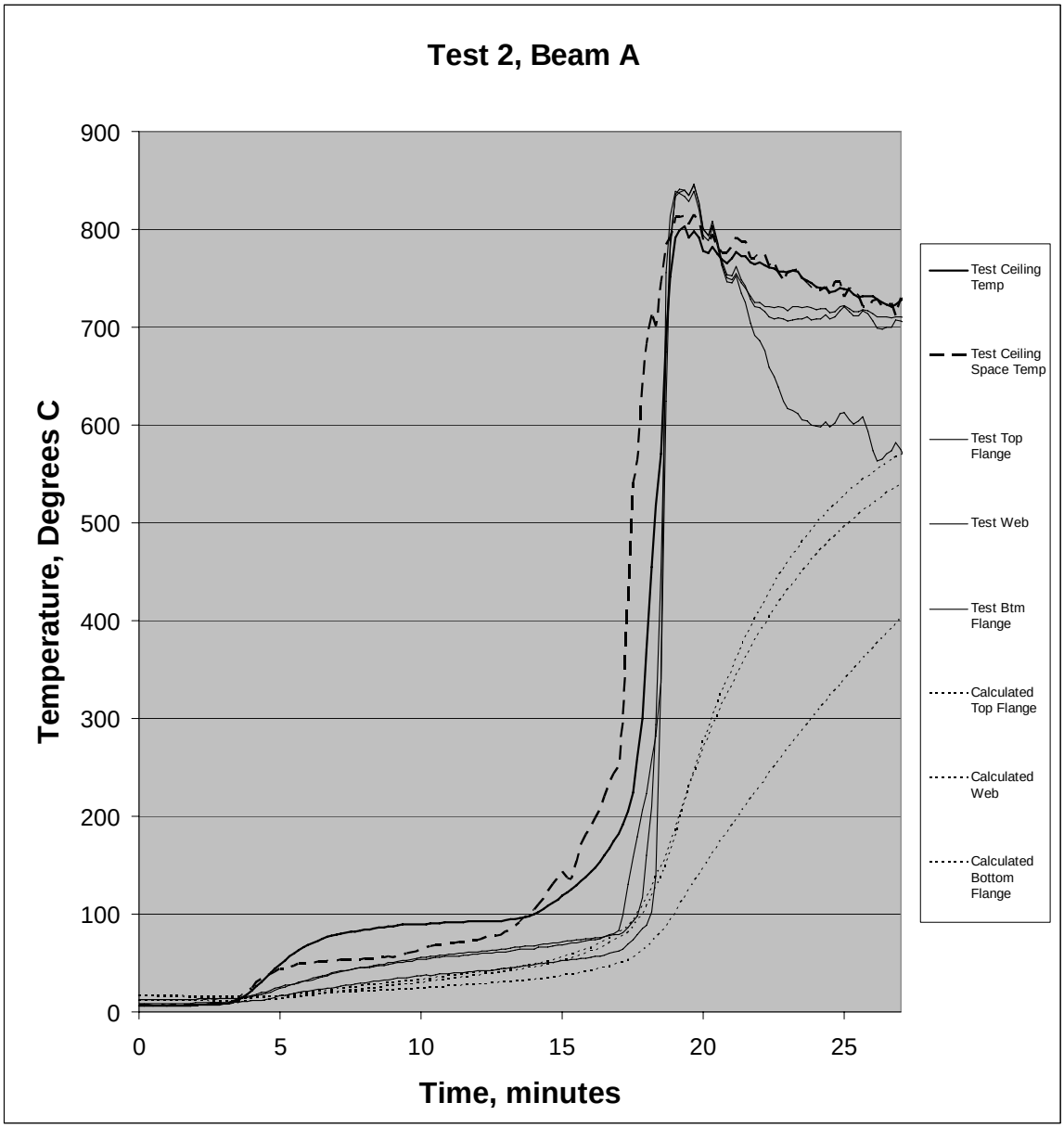

Figure 8.3, Calculated and Measured Beam Temperatures, Test 2, Beam A

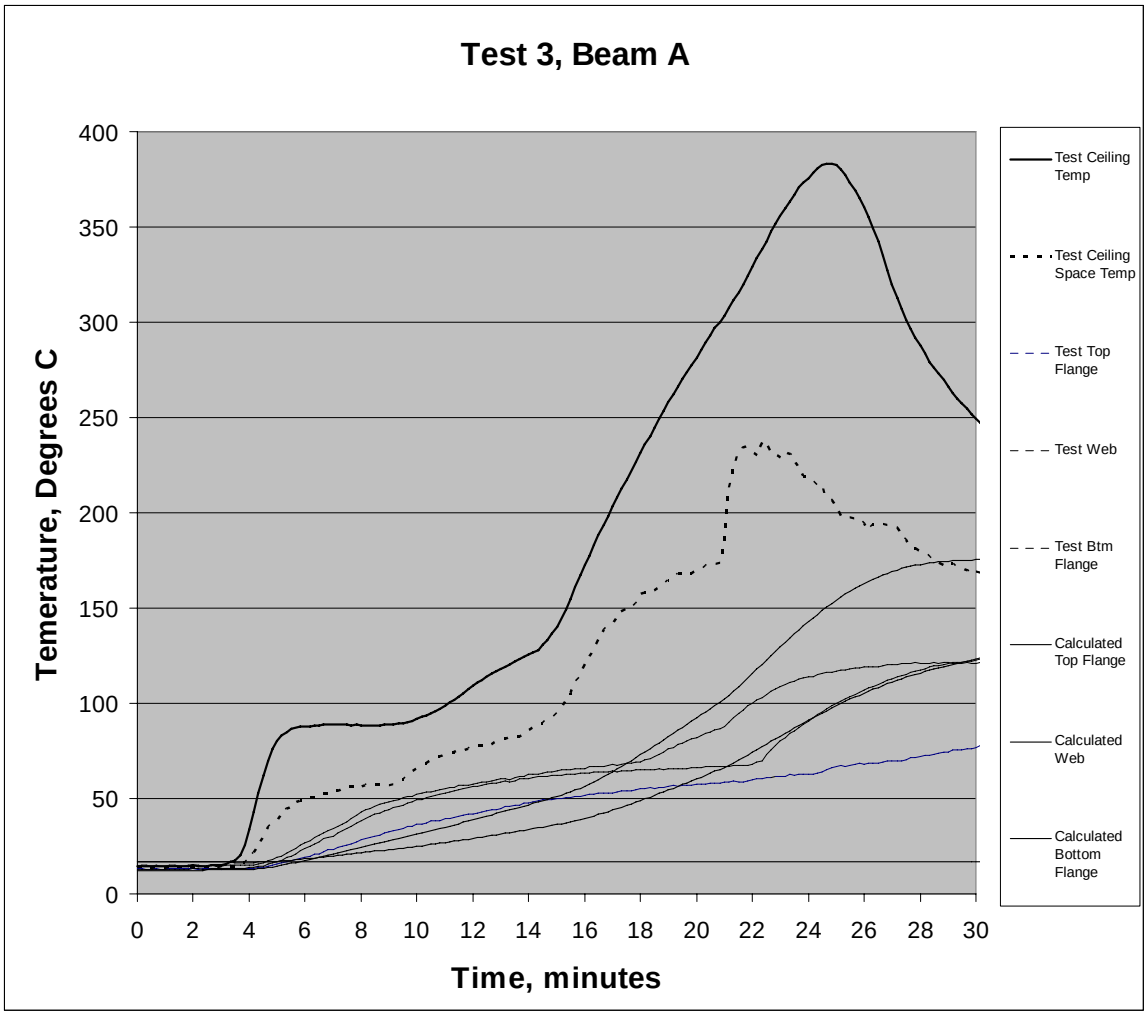

Figure 8.4, Calculated and Measured Beam Temperatures, Test 3, Beam A

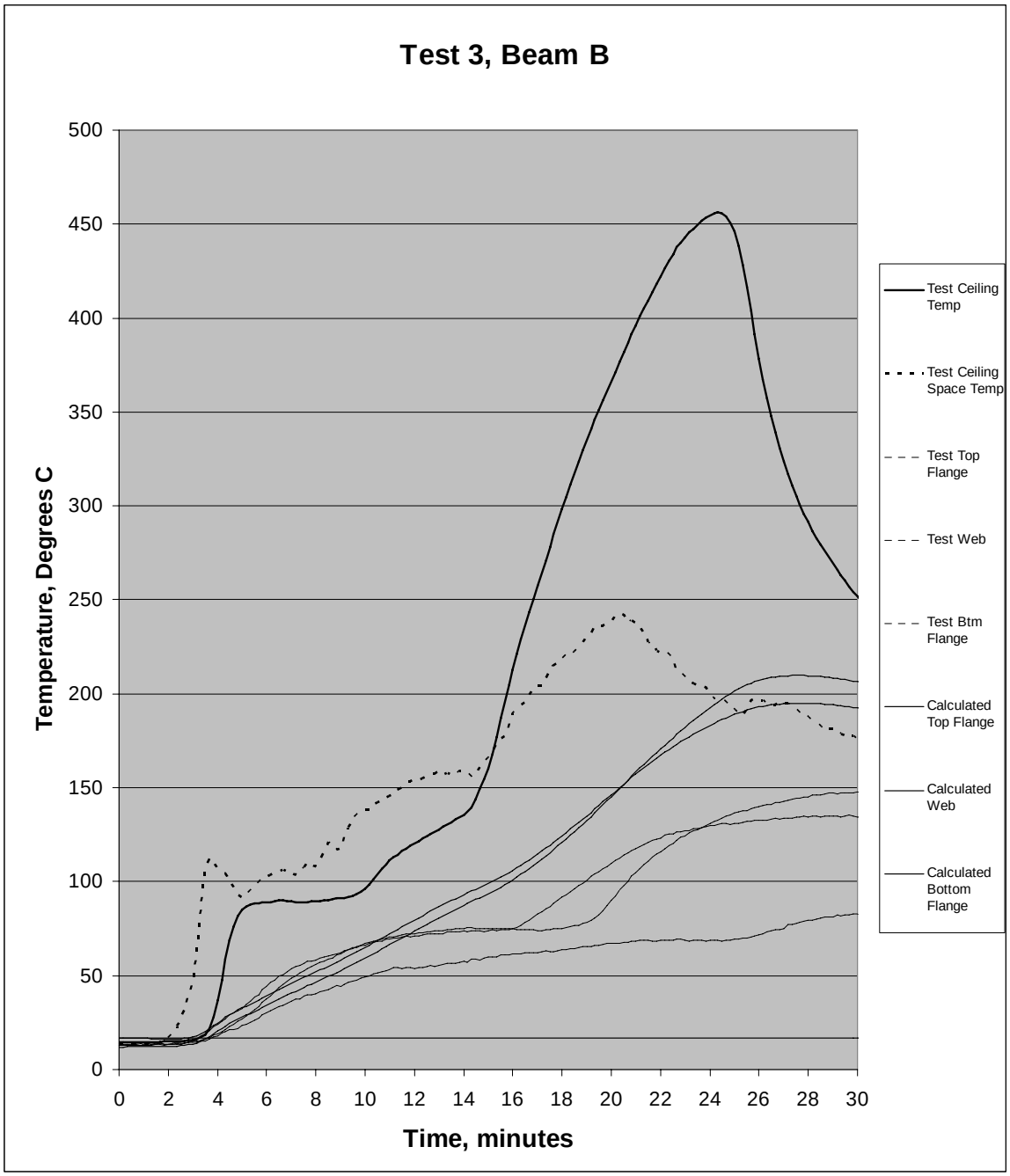

Figure 8.5, Calculated and Measured Beam Temperatures, Test 3, Beam B

The analysis did not take into account the collapse of the ceiling by changing the emissivity to that appropriate for flame. Accordingly, the calculated temperatures are invalid in figure 8.3, after approximately 18 minutes.

It is noted that after the collapse of the ceiling, the beam temperatures very rapidly climb to the compartment temperature, which is well above any useful limiting temperature. Continuing the analysis after the collapse of the ceiling, would only be useful, if the fire temperatures were much lower, such as during the decay stage of the fire.

The correlations between the measured and calculated temperatures are mixed, but they do show the correct trend. The reasons for inaccurate calculated temperatures may be related to water vapour or humidity within the ceiling space. This is likely to affect the emissivity and convective heat transfer constants. The accuracy of calculations at temperatures below 400°C have little relevance, as at these temperatures, steel beams will always be able to carry the required fire emergency load.

Conclusion

- Generally, if the ceiling remains in place then the temperatures within the steel beams will not exceed their limiting temperature (NZS 3404[32]). This is because the second dehydration front moving through the gypsum plasterboard ceiling occurs at approximately 700ºC, which is approximately the same as, or slightly higher than, the limiting temperature for steelwork.

- A step-by-step analysis could be used to analyse the beam temperatures after the ceiling collapse. Care is required as the calculated steel temperatures may be quite sensitive to some of the key parameters, particularly the fire load, the ventilation and the fire growth rate. A small increase in the fire load may delay the start of the decay period, possibly exposing the steel beam to the higher temperatures for a longer period. A sensitivity analysis with respect to the total fire load, the ventilation, and the fire growth rate is recommended for design.

Chapter 9 – Design Fires

Scope

The aim of this section is: -

- To compare the experimental compartment temperatures with the Eurocode parametric fires.
- To discuss two of the key observations of the test fires: -
    - burning of char during the decay stage, and
    - the exposure of the cooler concrete surfaces when the plasterboard ceiling collapses,

  and the impact that these have on the compartment time-temperature curve.
- To identify an appropriate design fire for an analysis of unprotected steelwork in the ceiling space, which incorporates collapse of the plasterboard ceiling.

Introduction

A design fire is required if a detailed thermal analysis is to be carried out. For the calculation of a structural endurance rating, or the fire resistance rating of a steel member, the required design fire is a time-temperature curve that represents the temperature within the fire compartment. The options are: -

1. The standard ISO fire using the equivalent severity concept (this has been discussed in the earlier chapters and accordingly will not be discussed further in this chapter).
2. A Parametric Design Fire, which is an empirical relationship between temperature and time and other critical and relevant parameters (namely the fire load, the ventilation and the compartment wall lining properties), or
3. A calculated time temperature curve based on first principles of the conservation of mass, and the conservation of energy.

Eurocode Parametric Design Fires

Background

The Eurocode Parametric Fires[13] were first published in 1994. HERA[9] introduced a modification to the Eurocode Fire in 1996 (called the modified Eurocode Fire), which raised the temperatures during the heating phase and slowed the decay phase of the fire. These changes were based on comparisons between predicted and experimental results, particularly those from a series of natural compartment tests undertaken by BHP. In 2001, the 1994 Eurocode Parametric Fire was amended[37]. Details of the parametric fires are available in the literature and accordingly are not presented or discussed in this project report. The three versions of the Eurocode Parametric Design Fires are compared with the experimental compartment test data below.

Comparison With The Third Test

Figure 9.1 below compares the time temperature curve of test #3 with the Eurocode parametric fires. A compartment wall lining thermal inertia, b, factor of 700 was used, as is appropriate for gypsum plasterboard.

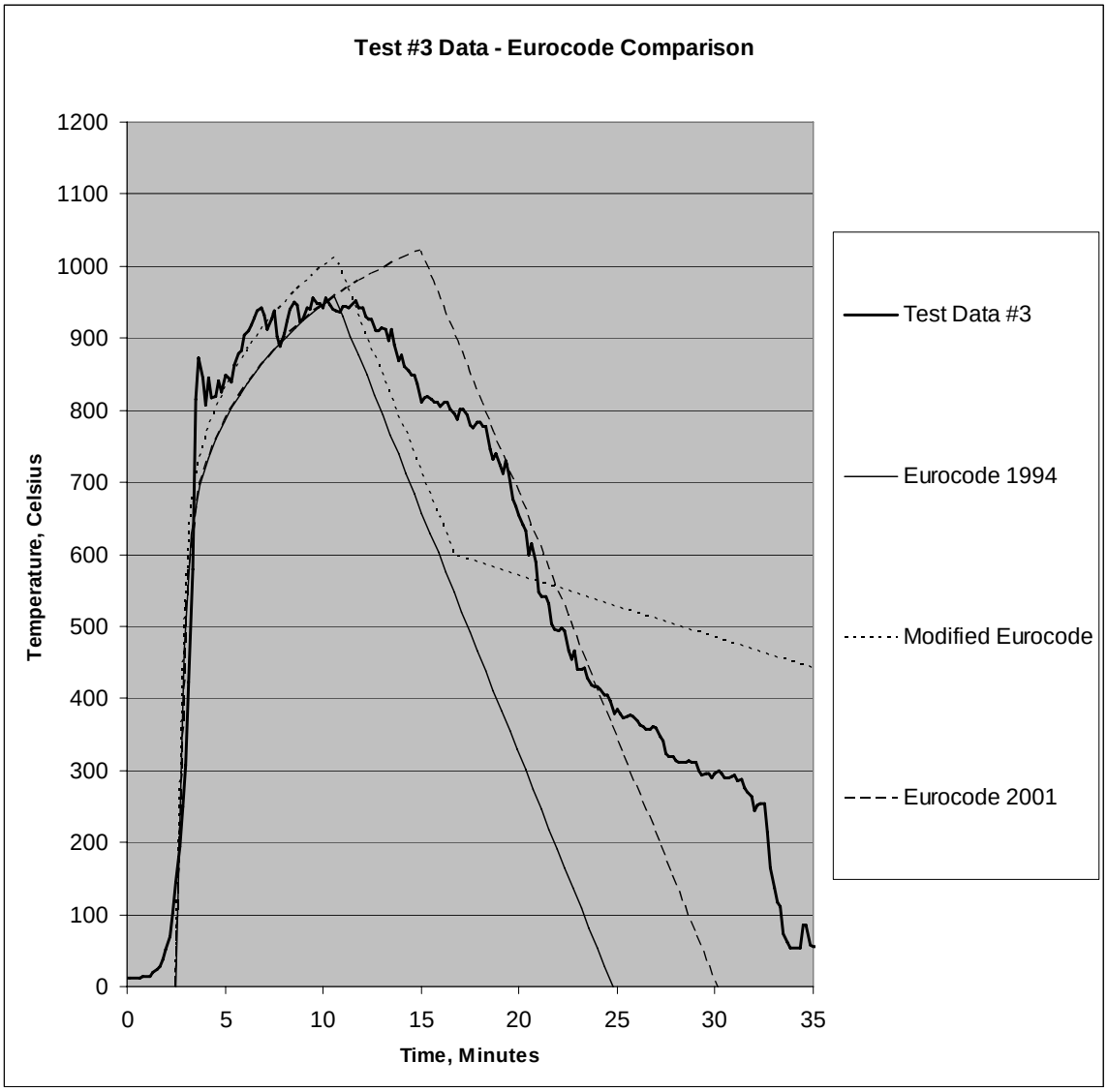

Figure 9.1 – Eurocode Parametric Fire Comparison with Test #3

The Eurocode 1994 Design Fire is non-conservative. The Modified Eurocode and the Eurocode 2001 design fires, both represent the experimental results reasonably well.

Comparison With The Second Test

Figure 9.2 below compares the compartment time temperature curve of test #2 with the Eurocode Parametric fires.

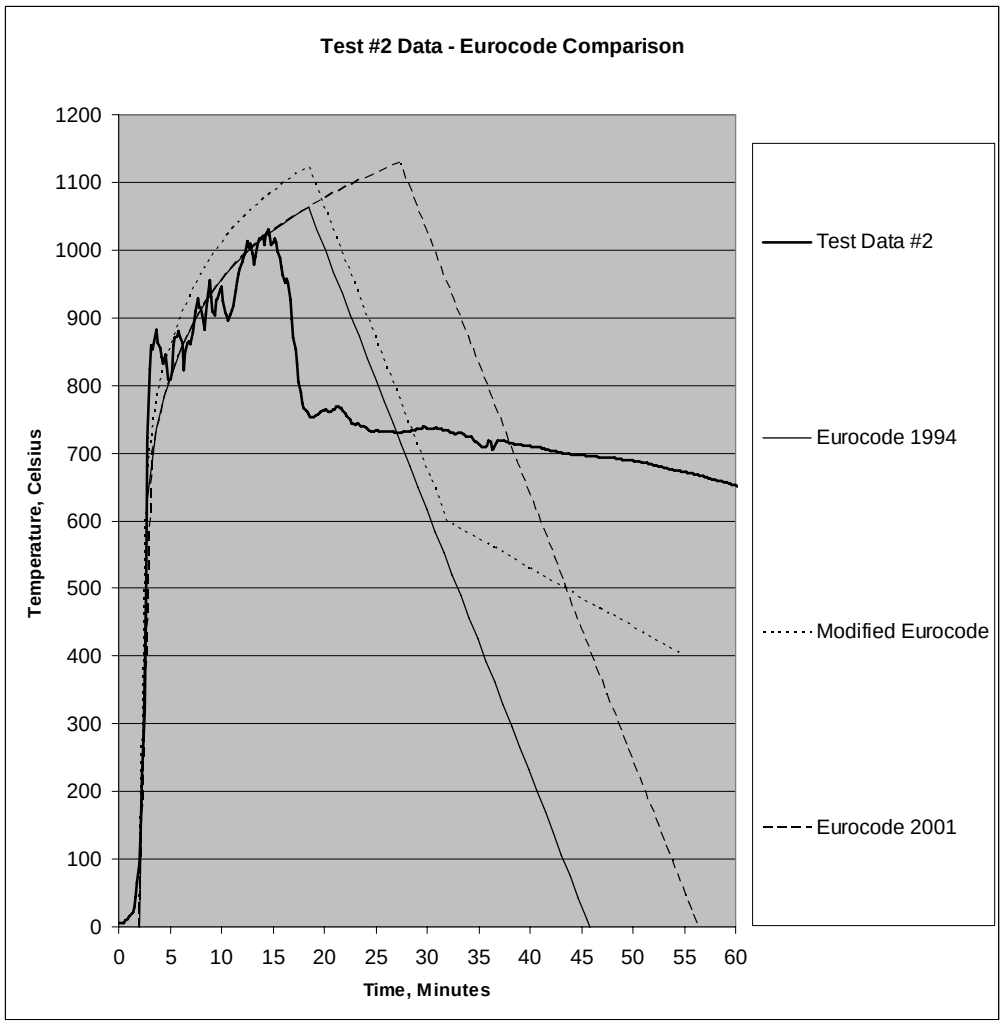

Figure 9.2 - Eurocode Parametric Fire Comparison with Test #2

The comparison is reasonable, up until when the gypsum ceiling collapses at approximately 16 minutes. At this time the fire is exposed to cooler concrete surfaces, which has a significant effect on compartment temperatures.

Figure 9.3 below is the Eurocode Parametric Fires using a wall lining thermal inertia factor, b, of 1450, as is appropriate for concrete.

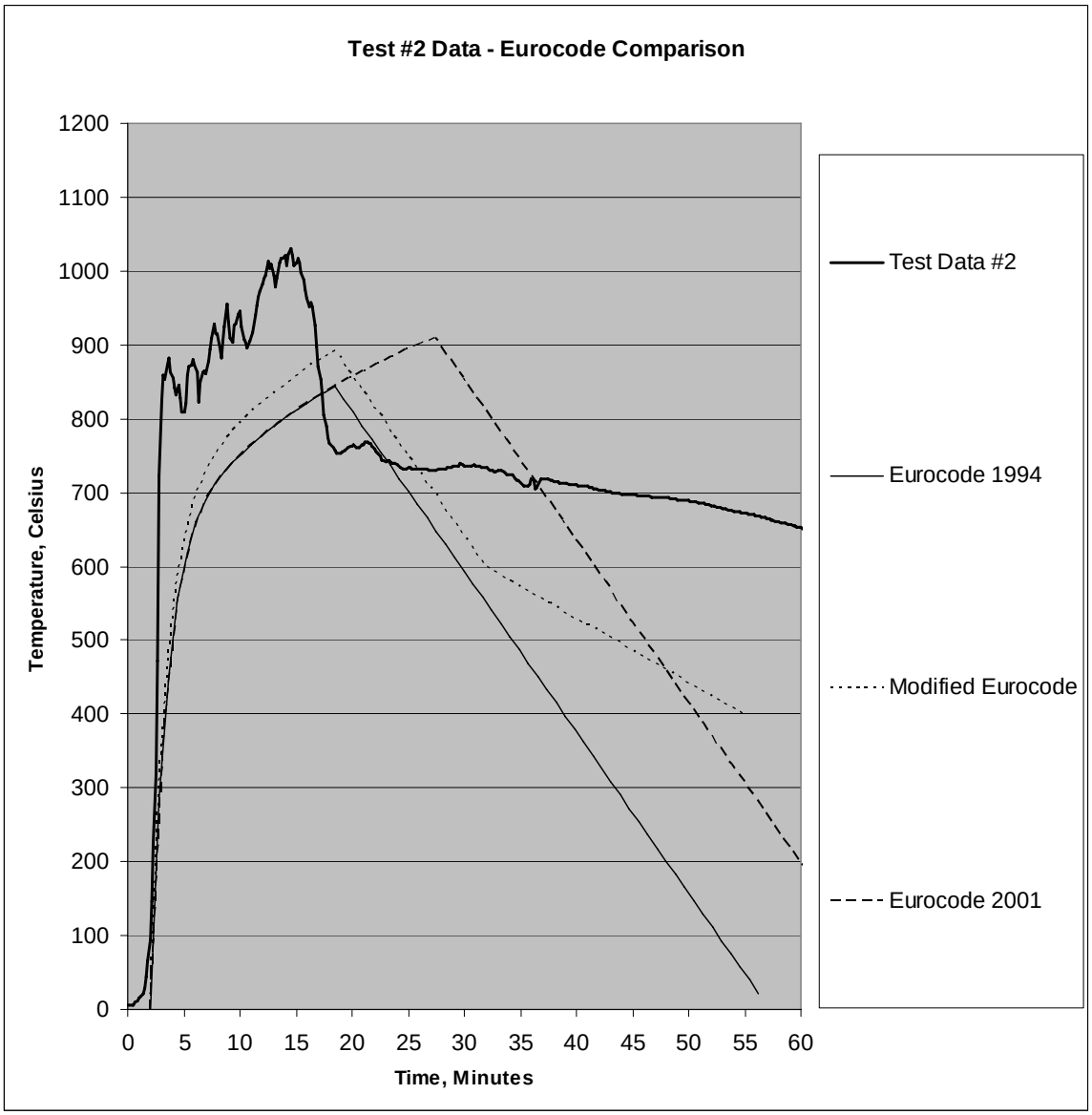

Figure 9.3 – Eurocode Parametric Fire Comparison with Test #2

This figure is included only to illustrate the effect of the cooler concrete surface. It is not suggested that the later half of this time-temperature curve could be used as the part of a design fire.

The figure shows that a change in material properties is required, if the compartment temperatures after the collapse of the ceiling are to be modeled accurately. Currently the Eurocode Parametric fires cannot handle this degree of detail.

Comparison With The First Test

Figure 9.4 below compares the Eurocode Parametric Fires with test #1.

The failure of the gypsum plasterboard ceiling has less effect than in test #2, as the decay period is short and it starts at approximately the same time as the ceiling collapse. The Modified Eurocode Fire and the 2001 Eurocode Fire both adequately represent the later half of the fire. There is however significant heating during the first 18 minutes, which the parametric fires do not model. A slow growth rate fire followed by a ventilation controlled phase is more severe on the compartments linings and structural members, than a fire which quickly grows from ignition to flashover.

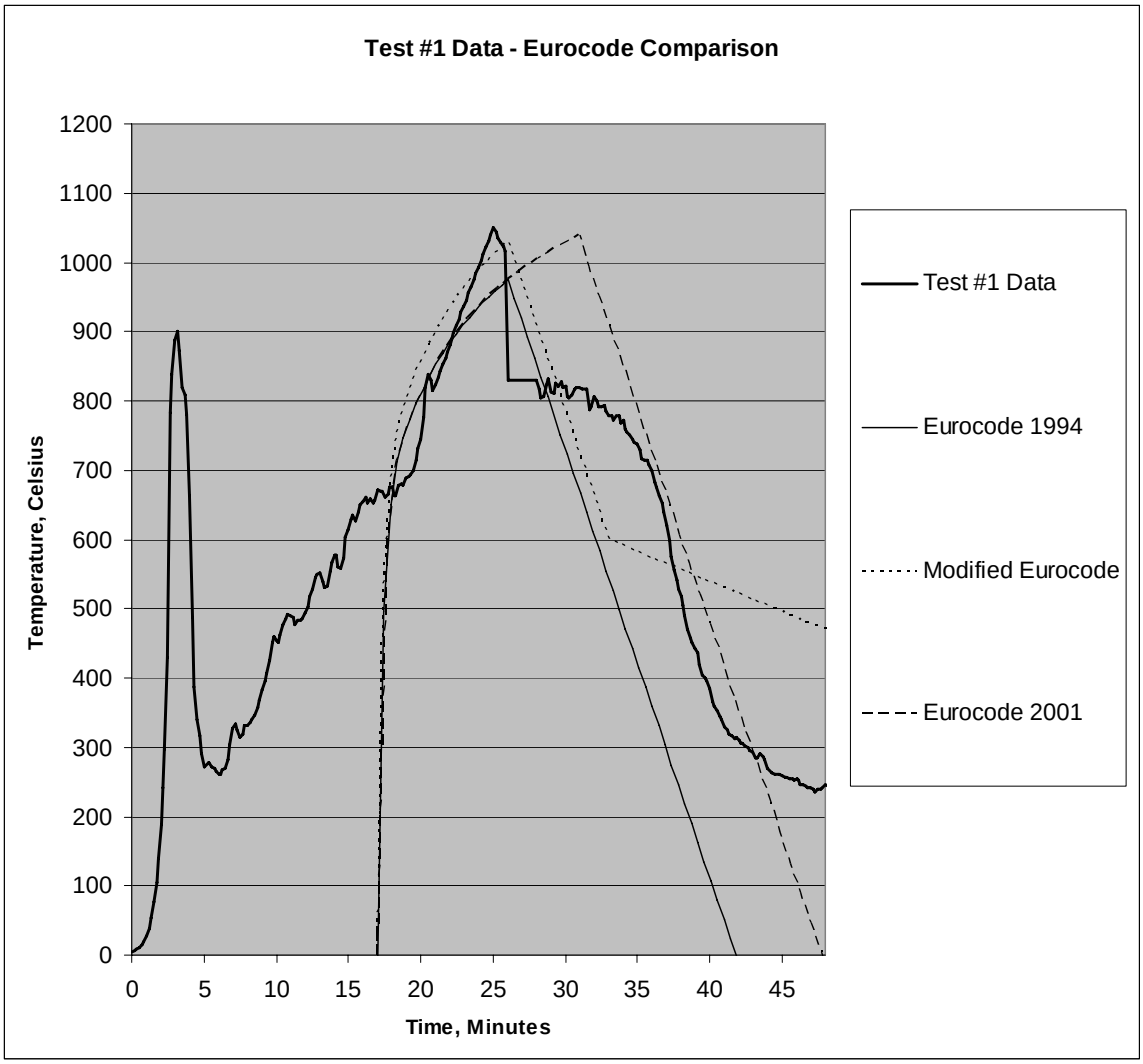

Figure 9.4 – Eurocode Parametric Fire Comparison with Test #1

Comparison of Tests #2 & #3

Figure 9.5 below compares the time-temperature curves of tests #2 & #3.

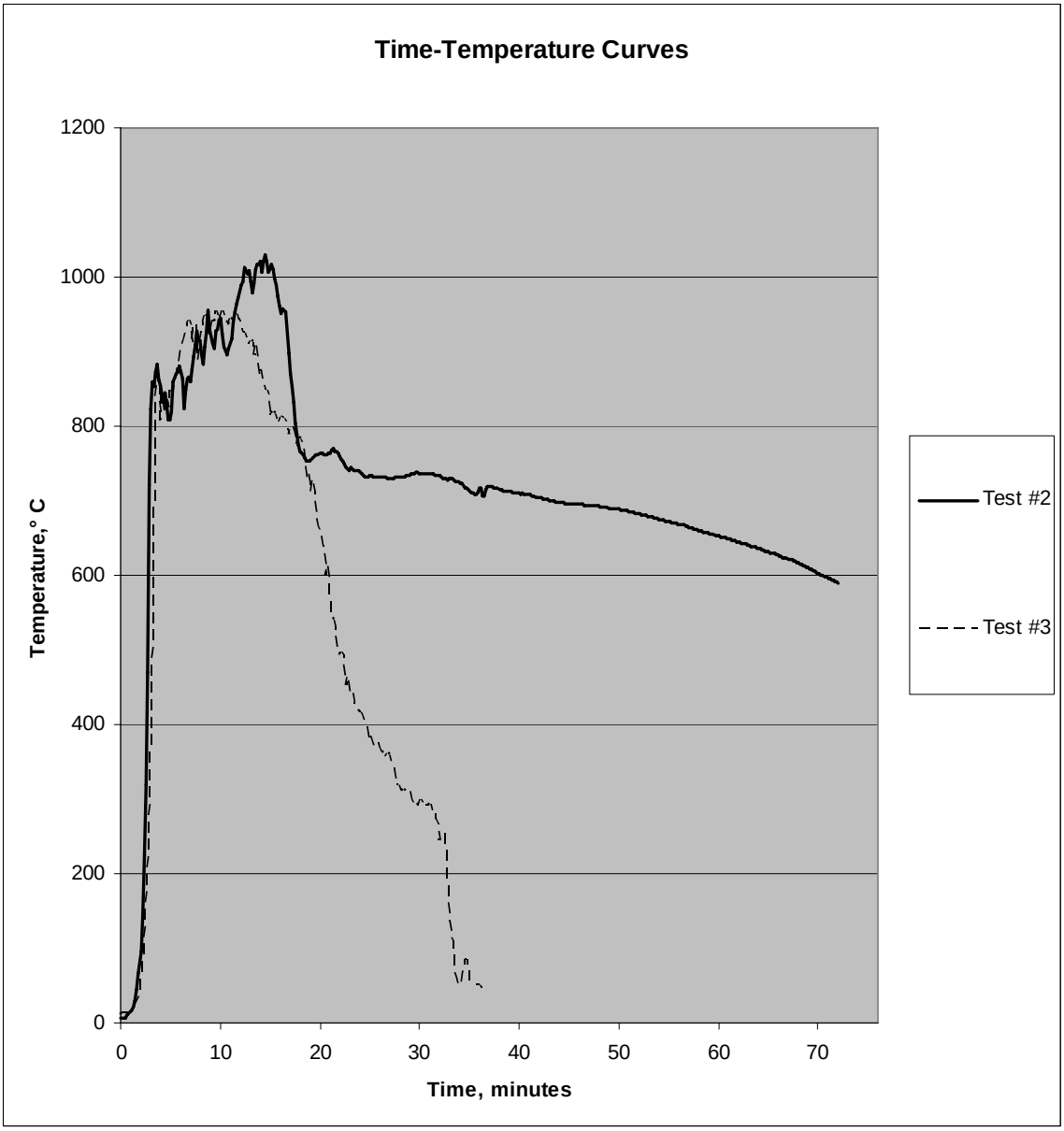

Figure 9.5 – Time-Temperature Curves for Tests #2 & #3

Tests #2 & #3 were identical except that test #2 had twice the fuel load, with the additional fuel being in the form of blocks of 250x50 Pinus Radiata timber representing book cases. Points to note in the above comparison are: -

1. The decay period in test #3 started at 12.0 minutes. Test #2 decay period started at 15.0 minutes.

2. Test #2 shows a marked drop in temperature at 16.0minutes when the ceiling collapsed. The ceiling in test #3 did not fail until the very end of the test.
3. Test #3 has a very short steep decay phase, whereas test #2 has a quite long protracted decay stage.

The reason for the marked difference in the decay stages is due to the quantity of char within the fuel. As observed in the tests, the char does not burn unless oxygen reaches the surface of the char. This is consistent with Janssens[22] statement that "Under certain conditions, oxygen may diffuse to the surface (of the timber) and lead to char oxidation". Char within the draught of a compartment opening, burns freely during the ventilation controlled phase, but char remote from the opening cannot burn until the equivalence ratio drops below unity, i.e. until oxygen can diffuse to the surface of the char. The equivalence ratio drops below unity in the decay stage. In test #3 there is relatively little fuel (char) remaining at the start of the decay stage. In test #2 there is a lot of char present in the compartment at the start of the decay stage. This char burns throughout the decay stage making this stage long and protracted. [To further illustrate, consider a hydrocarbon pool fire, which is an extreme case of a short rapid decay phase. In hydrocarbon pool fires there is virtually no fuel consumed during the decay stage.]

Summary

Both the Modified Eurocode Parametric Design Fire[9] and the 2001 Eurocode Parametric Design Fire[37] adequately model the experimental test results when: -

- flashover and the ventilation controlled phase occurs quickly after ignition, and when
- the ceiling remains intact for most of the duration of the fire.

The Eurocode Parametric Fires do not model the following: -

- the fire growth rate before flashover,

- variations in fuel (proportions of volatiles and char), which affects the duration of the fully-developed stage and the behaviour during the decay period, and
- changes in compartment conditions during the fire (collapse of a ceiling).

Energy Based Design Fires

Energy based design fires calculate compartment temperatures from first principles based on the conservation of mass and the conservation of energy. The numerical calculation process allows: -

- a growth phase to be added before flashover
- the fuel properties and surface areas to be specified, and
- changes to the compartments wall linings during the fire.

Computer programs which provide energy based design fires have been developed by a variety of researchers. Various parameters can be specified by the user, depending on the specific development. The author knows of no energy derived design fire that: -

- models a drop in compartment temperature at ceiling collapse stage when concrete in the ceiling space becomes exposed to the fire, or
- models a decay stage based on the char component of the fuel.

A purpose written program may need to be developed if the relevant features identified in this chapter are to be included in a design fire. Development of such an energy based design fire is outside the scope of this report.

References of energy based design fires are: -

- Wade (Branzfire) [42]
- Babrauskas (COMPF2) [4]
- Poon[36]
- Yii (CFIRE) [15]

Chapter 10 – Conclusions And Recommendations

Partially Protected Steelwork

The insulation protection of only a portion of the surface perimeter of a steel beam slows the rate of temperature increase in the steel beam.

An analysis for calculating the flange and web temperatures for a beam with partial protection, for any given time-temperature design fire, has been formulated. The analysis includes view factors and the radiant heat transfer to and from the beam's surfaces. The analysis can be carried out using a spread-sheet. The analysis gives reasonable correlation with test data.

While the partial insulation slows the rate of temperature increase, the protection is not useful to the fire protection industry in gypsum plasterboard lined compartments, where compartment temperatures are high, resulting in high radiant heat flux levels, which in turn leads to the rapid rise in temperature of any unprotected steel surface. Partial protection may possibly be useful in compartments lined with other materials such as concrete, where temperatures similar to, or below, the standard ISO fire are expected.

Steelwork Protected With A Radiation Shield

The conclusions for steelwork protected with a thin galvanised steel radiation shield are identical to those above, for partially protected steelwork.

Steelwork Protected With A Gypsum Plasterboard Ceiling

A gypsum plasterboard ceiling will protect steel beams within the ceiling space from a fire below the ceiling, for as long as the ceiling remains intact. Minor unprotected penetrations in the ceiling have no significant effect on the steel beam temperatures, provided the ceiling space is effectively sealed, preventing the buoyancy-driven movement of hot gases through the ceiling space.

A standard gypsum plasterboard ceiling will collapse shortly after the calcination front travels through the plasterboard to the unexposed side.

For a fire-rated (glass-reinforced) plasterboard ceiling, collapse can be expected when the proportion of plasterboard, yet to be exposed to the second dehydration front, reduces below a critical thickness. The critical thickness depends on the plasterboard composition (thickness, density, reinforcement, etc), and details of the construction (batten centres, fixing centres, etc).

A single dehydration-front model analysis for calculating the progression of a single dehydration front through the gypsum plasterboard ceiling, for any given time-temperature design fire, has been formulated. The analysis can be carried out using a spread-sheet. The analysis gives good correlation with test data with respect to progression of the calcination front. The single dehydration front model is generally conservative with respect to predicting the location of the second dehydration front. The analysis could be improved by extending the model to a double dehydration front model.

The equal area concept gives a good method of comparing different fires for a given gypsum plasterboard construction. The method allows the time at which a gypsum plasterboard ceiling will collapse to be established, under a variety of fire conditions.

If a designer chooses to carry out a simply analysis, it is recommended that a ceiling construction be chosen so that the ceiling will remain in place for the duration of the fire, in which case the temperatures within a steel beam above the ceiling will not exceed 550ºC. Design of the steelwork can be carried out accordingly. The gypsum plasterboard model given in chapter 7 can be used to verify that the ceiling remains in place for the duration of a fire.

If a designer chooses to carry out a more sophisticated analysis, then a ceiling construction should be chosen so that the ceiling remains in place until the fire is well into the decay stage. A compartment time-temperature design fire should be selected that takes into account the drop in compartment temperature, which occurs at ceiling collapse when the fire becomes exposed to the cooler compartment surfaces above the ceiling. The fire growth rate and the decay phase should also be realistically modeled. The design fire for the beam analysis would be: -

- the unexposed ceiling lining temperature for the period of time up until the collapse of the ceiling, and
- the compartment temperature for the period of time after the collapse of the ceiling.

A thermal analysis of the steelwork can be carried out using the standard step-by-step, lumped-mass method. Once the beam temperatures have been established a structural analysis will confirm whether or not the fire emergency loads can be supported.

Further Study

The following areas require further study: -

- The development of the single dehydration front model into the double dehydration front model.
- Research into how the composition, position (ceiling or wall) and support details of fire rated gypsum plasterboard affects it's structural strength and thus the collapse criteria for the plasterboard lining.

- Energy based design fire formulations that take into account:-
    - A (slow) fire growth rate,
    - The exposure of cooler compartment surfaces when the ceiling collapses, and
    - The effect that the fuel composition (proportion of char) has on the decay phase of the fire.

Nomenclature

A_{ij}	Area of surface i for heat transfer to surface j
Ah	Area of horizontal openings
Av	Area of vertical openings
b	Thermal inertia property of wall lining
C_p	Specific heat
Cpd	Product of specific heat and density
Cpw	Specific heat of water
E	Enthalpy
E_0	Enthalpy associated with calcination
E(T)	Enthalpy as a function of temperature
F_{ij}	View factor of surface j to surface i
h_c	Convective coefficient
h_{ca}	Convective coefficient, ambient side
h_{cf}	Convective coefficient, fire side
h_{c12}	Convective coefficient, between surfaces 1 & 2
HF	Heat flow
HF_e	Effective heat flow through gypsum plasterboard
HF_{oob}	Out of balance heat flow
k	effective emission coefficient
k_{eq}	equivalent thermal conductivity
L	Depth of flame
Q_{ij}	Heat Flow from surface i to surface j
r_f	Ration of Design Actions
SF	Section Factor
t	Time
T	Temperature
T_c	Calcination temperature
T_{ce}	Temperature, cavity, exposed lining side
T_f	Fire temperature

T_i Temperature of surface i

T_j Temperature of surface j

T_l Limiting temperature

T_{sf} Surface temperature of the fire exposed surface

T_{sf}' Revised estimate of surface temperature of the fire exposed surface

T_1 Temperature of the fire

T_2 Temperature of the exposed lining, fire side

T_3 Temperature of the exposed lining, cavity side

T_4 Ambient temperature

w Thickness of plasterboard lining

wc Water content

w_i Width of surface i

w_j Width of surface j

w_k Width of surface k

x Depth of calcination layer, or depth variable (into face of plasterboard)

α Coefficient

ε Emissivity

ε_f Emissivity of the fire (or resultant emissivity)

ε_s Emissivity of steel

ε_g Emissivity of gypsum plasterboard

ε_{12} Emissivity between surfaces 1 & 2

ρ Density

σ Stefan-Boltzmann Constant 5.67E-8

$^{(i)}$ superscripts indicate time step i

List of Figures

List of Tables

References

1. Alfawakhiri, F., Sultan A.M., & MacKinnon, D.H. ‘Fire Resistance Of Loadbearing Steel Stud Walls Protected With Gypsum Board: A Review’, Fire Technology, Vol 35, Nov 1999, Pages 308-335.

2. Approved Document C/AS1, Acceptable Solution for the C (Fire) Clauses of the New Zealand Building Code, (including amendments 1 to 5), October 2005, Department of Building and Housing, NZ Government.

3. Axenenko, O. & Thorpe, G. ‘The Modeling of Dehydration and Stress Analysis of Gypsum Plasterboards Exposed to Fire’, Computational Materials Science, Vol 6, 1996, pages 281-294.

4. Babrauskas and Williamson, ‘Post-flashover Compartment Fires: Basis of a Theoretical Model’, Fire and Materials, Vol 2, No 2, 1978.

5. BIA ‘Proposed Changes to The Approved Documents for the Fire Safety Clauses of the Building Code’. November 2004, Building Industry Authority.

6. Buchanan A.H. ‘Structural Design For Fire Safety’, Wiley, 2001, pages 35-37.

7. Chang, J.,’2-D Analysis Of The Performance Of Connections With Unprotected Steel Structural Members Exposed To Parametric Fire’, Fire Engineering Research Report 03/7, University of Canterbury, Christchurch.

8. Clancy, P. ‘A Parametric Study On The Time-To-Failure Of Wood Framed Walls In Fire’, Fire Technology, Vol 38, July 2002, Pages 243-270.

9. Clifton, ‘Fire Models For Large Firecells, HERA Report R4-83, with an update in HERA Steel Design and Construction Bulletin, Issue No 154, page 22.

10. Collier, P. ‘A Model For Predicting The Fire Resistance performance Of Small-Scale Cavity Walls In Realistic Fires’, Fire Technology, Vol 32, Apr 1996, Pages 120-136.

11. Collier, P.C.R., Fire Barrier Technical Reference Guide, BRANZ Study Report No 127, 2004.

12. Collier, P. ‘Fire Resistance Of Lightweight Framed Construction’, Fire Engineering Research Report 00/2, March 2000, University of Canterbury, Christchurch, NZ.

13. DD ENV 1992-2:1996, Eurocode 3: Design of Steel Structures Part 1.2 General Rules – Structural Fire Design; BSI Standards, London, England

14. Drysdale, D.,’An Introduction to Fire Dynamics’, John Wiley & Sons, 1985.

15. Ee Hieng Yii, ‘Modelling the Effects of Fuel Types and Ventilation Openings on Post-Flashover Compartment Fires’, Fire Engineering Research Report 03/1, March 2003.

16. European Convention for Constructional Steelwork, Committee T3 – Fire Safety of Steel Structures, Technical Note No 1.7, ‘Partial Protection of Steel Members by Horizontal or Vertical Screens’.

17. Feeney, M.J. ‘Design Of Steel Framed Apartment And Hotel Buildings For Fire’, Australasian Structural Engineering Conference, Auckland, Oct 1998.

18. Feng, M., Wang Y.C. & Davies J.M. ‘Thermal Performance Of Cold-Formed Thin-Walled Steel Panel Systems In Fire’, Fire Safety Journal, Vol 38, 2003, Pages 365-394.

19. Fire Engineering Design Guide, Ed A H Buchanan, Centre for Advanced Engineering, Christchurch, New Zealand, Second Edition, April 2002.

20. Franssen J.M. & Zaharia, R. ‘Design of Steel Structures Subjected to Fire’, Background and Design Guide to Eurocode 3’, Les Editions de l’Universite de Liege, 2005.

21. Gerlich, Barnett, McLellan and Buchanan, ‘Predicting The Performance OF Drywall Construction Exposed To Design Fires’.

22. Gerlich, J.T.(Hans) ‘Design of Loadbearing Light Steel Frame Walls For Fire Resistance’, Fire Engineering Research Report 95/3, August 1995, University of Canterbury, Christchurch, NZ.

23. Incropera, F.P. & De Witt, D.P., ‘Fundamentals of Heat and Mass Transfer’, John Wiley & Sons, 2002.

24. ISO 834.1:1999, Fire Resistance Tests – Elements of Building Construction Part 1 General Requirements; ISO Geneva Switzerland.

25. Janssens, Marc L. ‘Modelling of the Thermal Degradation of Structural Wood Members Exposed to Fire’, Second International Workshop “Structures in Fire” Christchurch, March 2002.

26. Jones, B.H. ‘Performance of Gypsum Plasterboard Assemblies Exposed to Real Building Fires’, Fire Engineering Research Report, University of Canterbury, Christchurch, NZ.

27. Lamont S., Lane B., Flint G. & Usmani A., ‘Behaviour of Structures an Fire and Real Design – A Case Study’, Journal of Fire Protection Engineering, Vol 16, Feb 2006.

28. Lewis, K.R., ‘Fire Design Of Steel Members’, Fire Engineering Research Report 2000/07, University of Canterbury, Christchurch.

29. Mason, J.E. ,‘Heat Transfer Programs For The Design Of Structures Exposed To Fire’, Fire Engineering Research Report 00/9, University of Canterbury, Christchurch.

30. Moss P., Buchanan A., Seputro J., Wastney C. & Welsh, ‘Effect Of Support Conditions On The Fire Behaviour Of Steel And Composite Beams’, Second International Workshop “Structures in Fire” – Christchurch, Mar 2002.

31. Nyman, J.F. ‘Equivalent Fire Resistance Ratings Of Construction Elements Exposed To Realistic Fires’, Fire Engineering Research Report, May 2002, University of Canterbury, Christchurch, NZ.

32. NZS 3404: Part 1: 1997 Steel Structures Standard

33. NZS 4203:1999 Code of Practice for General Structural Design and Design Loadings for Buildings.

34. Olsson, P.A. ‘Bench Scale Testing of Light Timber Frame Walls’, Fire Engineering Research Report 98/6, June 1998, University of Canterbury, Christchurch, NZ.

35. Pettersson, O., Magnusson, S-E., & Thor, J. ‘Fire Engineering Design Of Steel Structures’, Swedish Institute of Steel Construction, Stockholm, Sweden, Publication 50, 1976.

36. Poon, ‘A Design Fire For Use In predicting The Performance of Exposed Structural Steel Members’, BHP Research – Melbourne Laboratories.

37. prEN 1991-1-2:2001, Eurocode 1 – Actions on Structures Exposed to Fire, Third Edition; European Committee for Standardisation, Brussels, Belgium

38. Proe, D.J. & Bennetts, I.D. ‘Timber Crib Fire Test For Comparison of Ceiling Tiles’, The Broken Hill Proprietary Company Limited, Oct 1994.

39. Sultan, A. M ‘A Model For Predicting Heat Transfer Through Noninsulated Unloaded Steel-Stud Gypsum Board Wall Assemblies Exposed To Fire’, Fire Technology, Vol 32, August 1996, Pages 239-259.

40. Sultan, A.M. & Kodur, V.R. ‘Light-weight Frame Wall Assemblies: Parameters For Consideration In Fire Resistance Performance-Based Design’, Fire Technology, Vol 36, May 2000, Pages 75-88.

41. Thomas, G.C. ‘Fire Resistance Of Light Timber Frames Walls and Floors’, Fire Engineering Research Report 97/7, May 1997, University of Canterbury, Christchurch, NZ.

42. Wade, ‘BRANZFIRE Technical Reference Guide’, Branz Study Report No 92 (2002).

43. Wastney C., ‘Performance Of Unprotected Steel And Composite Steel Frames Exposed To Fire’, Fire Engineering Research Report, 2002, University of Canterbury, Christchurch.

44. Wickstrom, U. ‘Calculation Of Heat Transfer To Structures Exposed To Fire – Shadow Effects’, Interflam, 2001, pages 451-459.

45. Winstones Wallboards Ltd, GIB® Fire Rated Systems’, January 2006

Appendix 1: Thermocouple Locations

Thermocouple Number	Plan Location	Height Above Floor	Description
17	1	2400	Thermocouple Tree
18	1	2300	Thermocouple Tree
19	1	2100	Thermocouple Tree
20	1	1800	Thermocouple Tree
21	1	1200	Thermocouple Tree
22	1	300	Thermocouple Tree
23	1	100	Thermocouple Tree
24	2	2300	Under Ceiling Front
25	2	2300	Under Ceiling Rear
26	3	2800	Underside of Concrete Slab Between A&C
27	3	2800	Underside of Concrete Slab Between B&C
28	3	2800	Underside of Concrete Slab Between B&D
29	3	2800	Underside of Concrete Slab Between D&A
30	3	2600	Centre of Ceiling Space Between A&C
31	3	2600	Centre of Ceiling Space Between B&C
32	3	2600	Centre of Ceiling Space Between B&D
33	3	2600	Centre of Ceiling Space Between D&A
34	3	2400	Top of Ceiling Lining Between A&C
35	3	2400	Top of Ceiling Lining Between B&C
36	3	2400	Top of Ceiling Lining Between B&D
37	3	2400	Top of Ceiling Lining Between D&A
38		2400	Top of Ceiling Lining Under Beam A
39		2400	Top of Ceiling Lining Under Beam B
40		2400	Top Flange of Beam A
41		2400	Top Flange of Beam B
42		2400	Top Flange of Beam C
43		2400	Top Flange of Beam B
44		2200	Web of Beam A
45		2200	Web of Beam B
46		2200	Web of Beam C
47		2200	Web of Beam D
48		2000	Bottom Flange of Beam A

49	2000	Bottom Flange of Beam B
50	2000	Bottom Flange of Beam C
51	2000	Bottom Flange of Beam B
52	2000	Bottom Flange of Beam A (backup)
53	2000	Bottom Flange of Beam B (backup)
54	2000	Bottom Flange of Beam C (backup)
55	2000	Bottom Flange of Beam B (backup)
56	2200	Beam C Front Side of Shield
57	2200	Beam C Front Side of Shield
58	2000	Beam C Bottom of Shield

Table A1.1 Thermocouple Locations

Appendix 2: Observations Test #1

- From ignition the fire grew quickly over the sofa.
- 1’40” Flames are illuminating the whole compartment. The smoke layer is clearly defined at approx 1.300m above floor level.
- 2’30” All the polyurethane is now alight. Hot smoke layer dropping to approximately 1.0m.
- 2’45” Flashover occurs. Smoke layer down to 850mm. Hot smoke is flaming as it exits the opening. The whole of the couch is alight and melted drops of flaming polyurethane are falling to the floor.
- 2’50” A huge amount of flaming is occurring outside the door of the compartment. The top of the cribs have caught alight.
- 3’40” The couch fuel is nearly expended. The front crib is well alight, although only on the top. The black hot smoke is still flaming outside the compartment.
- 4’20” Fire on the rear cribs is dying out. The top 200mm of the front crib is alight and burning strongly. Couch is almost out.
- 7’00” The front crib fire is growing slowly – now the top 300mm alight. The front crib continues to grow slowly, burning down from the top for the next ten minutes.
- 13’00” In an effort to ignite all the fuel, methylated spirits on tissue paper was positioned under the front crib using a 200x20mm timber board approximately 3.0m long. It had little effect. Methylated spirits on tissue paper was positioned under the right hand side rear crib using a 100x50 timber stud approximately 3.000m long. This appeared to ignite the rear cribs, although the growth rate was very slow, and overall is considered to have had little effect.
- 17’45” The whole of the front crib (800mm) is now alight and burning strongly. The rear cribs are not yet burning strongly.
- 19’00” The 200x20 timber board beside the front crib ignites (from the front crib’s radiant heat).

- 19’45” Loud cracking sounds are heard, as the floor cover concrete starts to spall.
- 20’00” Flames are reaching the ceiling. The right hand rear crib is burning strongly. The top of the left hand rear crib has re-ignited.
- 20’30” The compartment is full of flame. The burning is very clean and the smoke is not black or thick. The thermocouple tree is visible above the front crib, between the turbulent waves of the flames.
- 21’00” Occasional flames are now exiting the top of the opening. Compartment flashes over again at 21’30”.
- 22’10” The smoke is starting to get darker and the line of neutral pressure at the door is dropping. The rear cribs are burning strongly. Volatiles are being released from the rear timber cribs. First small pieces of ceiling are falling to the floor.
- 22’30” Front crib is showing signs of disintegration, and starts to collapse at 23’00”.
- 24’00” Smoke exiting the compartment is blacker. The neutral pressure plane has also lowered at the door opening.
- 25’45” Half of the front crib collapses. Also the line of the neutral pressure plane rises at the door opening. Period of strongest burning has finished.
- 26’00” The ceiling on the right hand side starts to collapse.
- 27’30” Fire is now fuel controlled. The decay period has started.
- 27’45” The timber bolted to the bottom flange of Beam D starts to burn and continues to burn until falls off the beam at 33’15”.
- 28’10” The fire is burning very cleanly again. The rear cribs have become charcoal. The fire becomes localized to the three cribs by 28’30”.
- 32’00” Fire is visible in the timber studs behind the joint in the gibboard on the rear wall. Smoke leaking out the joint between the blockwork and the concrete lid indicates that other wall framing is also burning.

Appendix 3: Observations Test #2

- From ignition the fire grew quickly over the sofa, as in the first test.
- 2’30” Flashover occurs. Smoke layer down to 850mm. Hot smoke is flaming as it exits the opening. The whole of the couch is alight and melted drops of flaming polyurethane are falling to the floor. Edges of the polyurethane slabs within the timber cribs are also alight.
- 6’00” polyurethane largely completely burnt.
- 15’00” Cribs collapsing.
- 17’00” Ceiling on the right hand side collapses.
- 18’00” Ceiling on the right hand side collapses.
- 17’00” - 18’00” Decay stage starts. Fire becoming fuel controlled.
- 19’00” Cribs collapsed. Both ‘book cases’ well ablaze.
- 26’00” The front ‘book case’ collapses on the floor.
- 43’00” The front ‘book case’ is just a few embers on the floor, while the rear ‘book case’ is still fixed to the rear wall.

Appendix 4: Observations Test #3

- From ignition the fire grew quickly over the sofa, as in the first two test.
- 3’00” Flashover occurs. Smoke layer down to 850mm. Hot smoke is flaming as it exits the opening. The whole of the couch is alight and melted drops of flaming polyurethane are falling to the floor. The polyurethane slabs within the timber cribs are also well alight.
- 7’00”Polyurethane is largely completely burnt.
- 10’00” Fewer flames protruding from the opening. Fire becoming fuel controlled. Start of the decay period.
- 11’10” The timber on the bottom of Beam D is burning.
- 18’30” Cribs collapsing.
- 19’30” Timber on bottom of Beam D falls off, still burning. Fire is just embers of the cribs as a heap on the floor.

24’00” and 30’00” Small make-up end pieces of the Gib® Fyreline ceiling fall from the ceiling, on both sides of the compartment. The full sheets stay in place.

Appendix 5: Comparison of Calculated Gypsum Plasterboard Temperatures with Test Data

The following graphs compare the analysis with 13mm GIB Fyreline® experimental data.

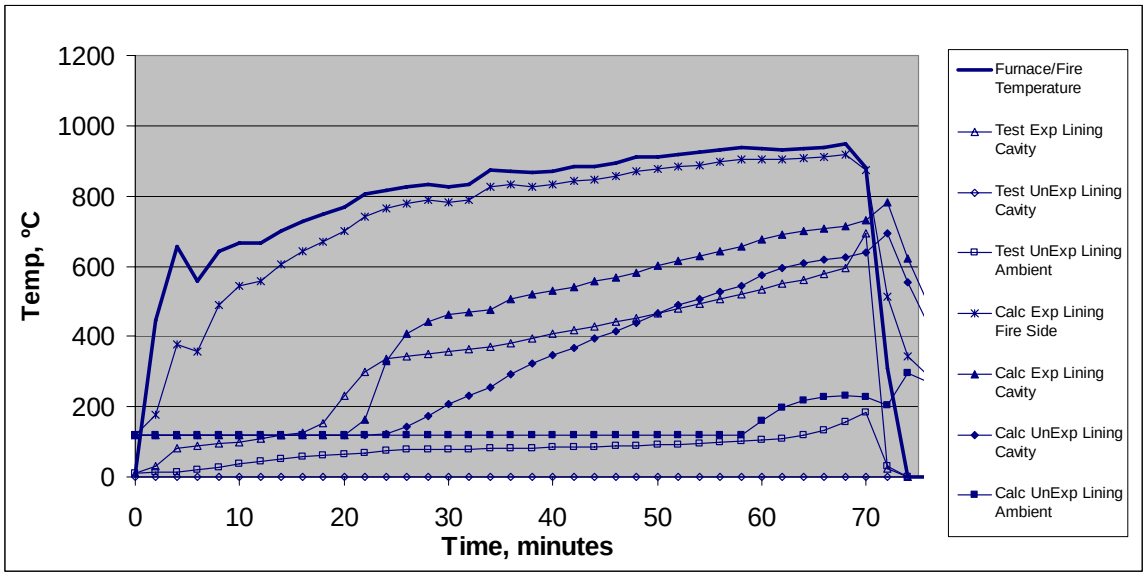

Figure A5.1 BRANZ Test FR1571 (ISO Fire, 13 GIB Fyreline® on timber studs)

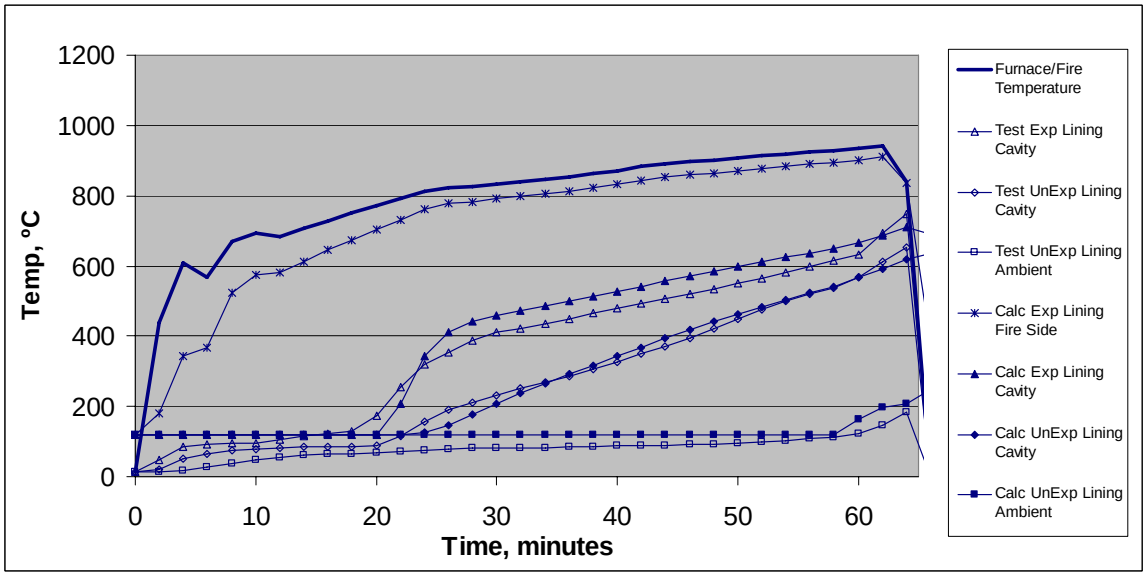

Figure A5.2 BRANZ Test FR1579 (ISO Fire, 13 GIB Fyreline® on steel studs)

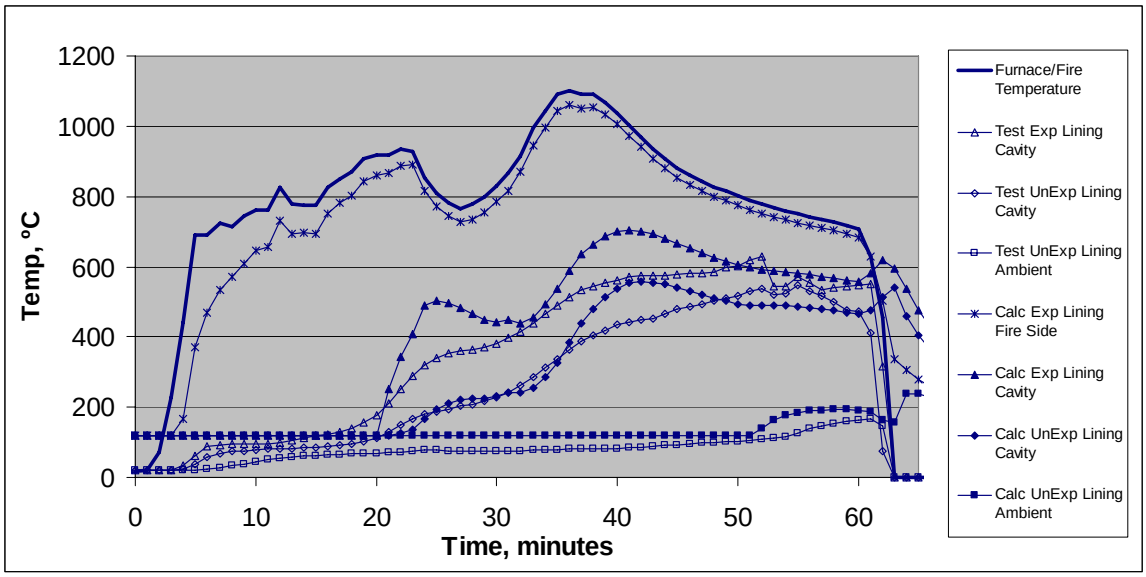

Figure A5.3 Nyman Test FQ0590B

(Compartment Fire, 13 GIB Fyreline® on timber studs)

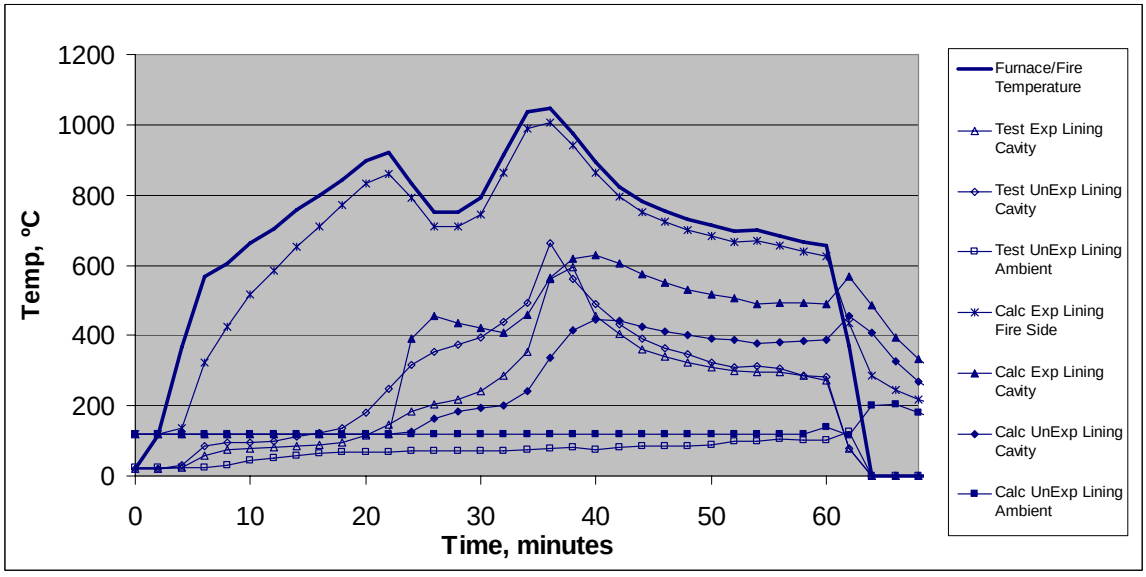

Figure A5.4 Nyman Test FQ0590B

(Compartment Fire, 13 GIB Fyreline® on steel studs)

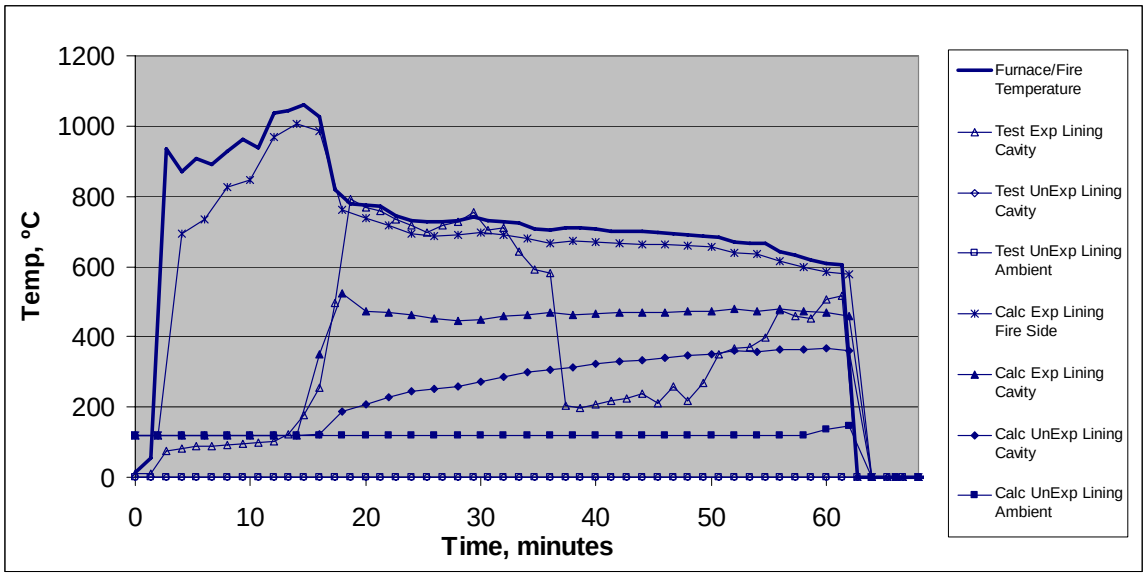

Figure A5.5 Brown Test FQ5013_2

(Compartment Fire, 13 GIB Fyreline® on steel ceiling battens)

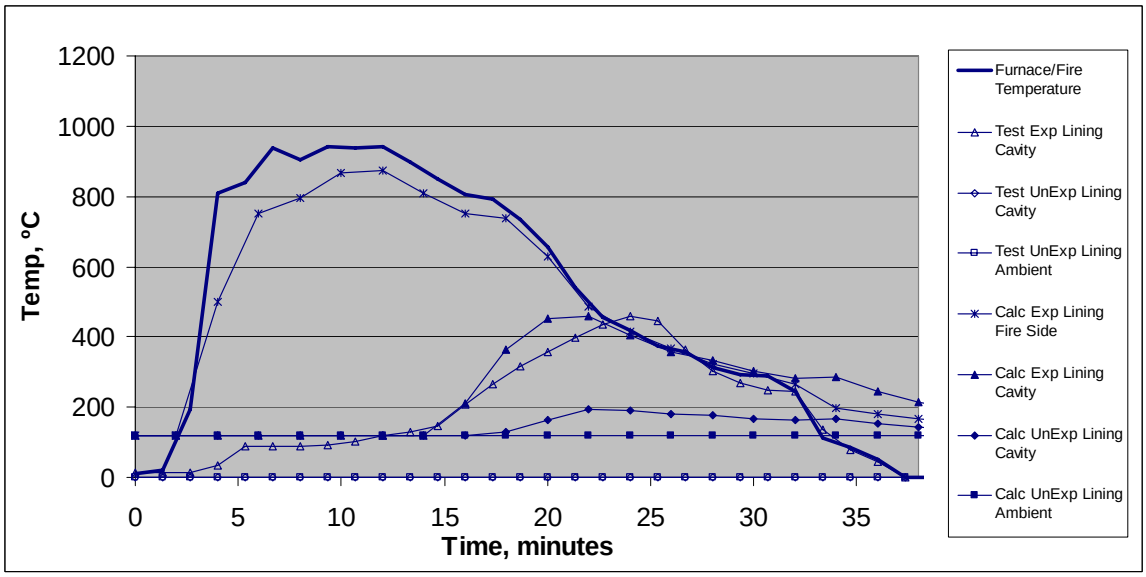

Figure A5.6 Brown Test FQ5013_3

(Compartment Fire, 13 GIB Fyreline® on steel ceiling battens)

The following graphs compare the analysis with 13mm GIB® Standard experimental data. 13mm GIB® Standard was used in the first test, FQ5013_1.

13mm GIB® Standard weighs 8.7 kg/m^2 compared with 9.8 kg/m^2 for the 13mm GIB Fyreline®. This is approximately 90% of the GIB Fyreline® density. For the following GIB® Standard comparisons, the constants in the analysis were changed as follows:-

- The enthalpy was reduced by 10%,
- The water content was reduced by 10%, and
- The thermal conductivity was increased by 10%.

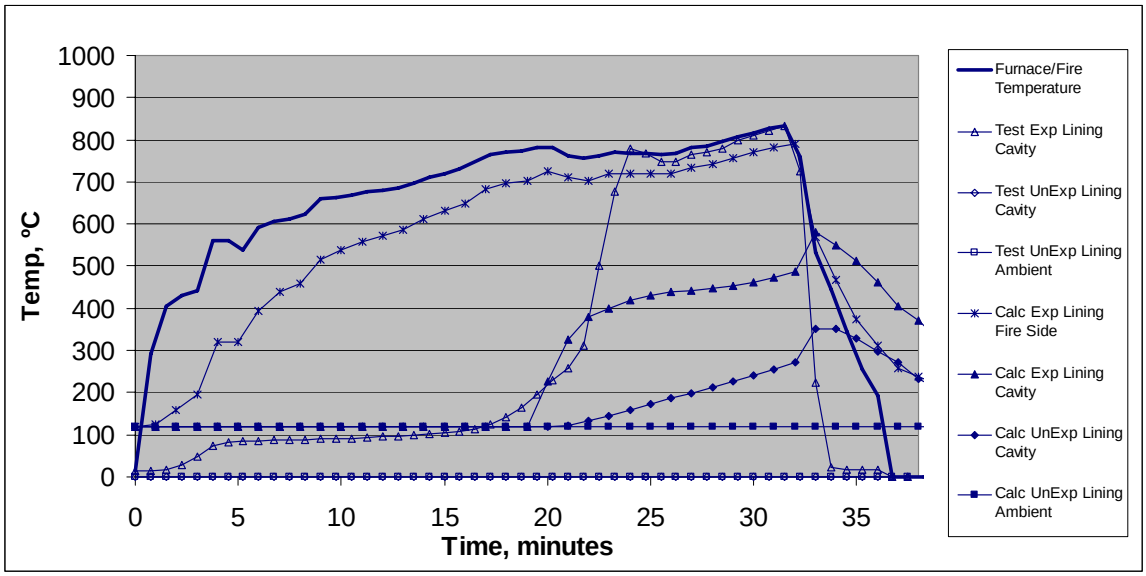

Figure A5.7 BRANZ Test FR1281

(ISO Furnace Test, 13 GIB® Standard on Steel studs)

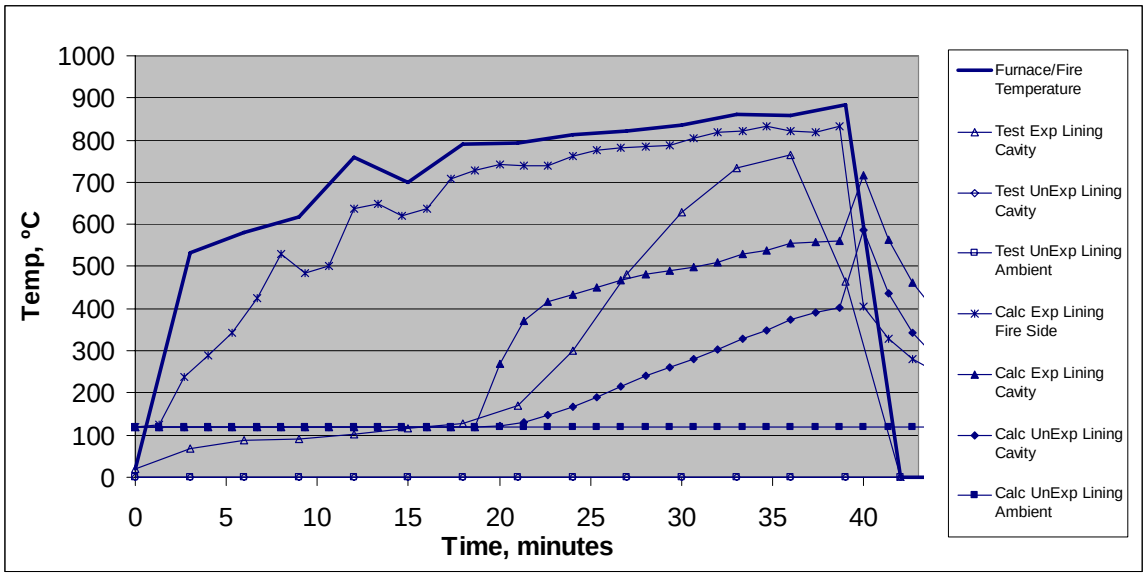

Figure A5.8 Jones Test FP2922

(ISO Furnace Test, 13 GIB® Standard on Steel studs)

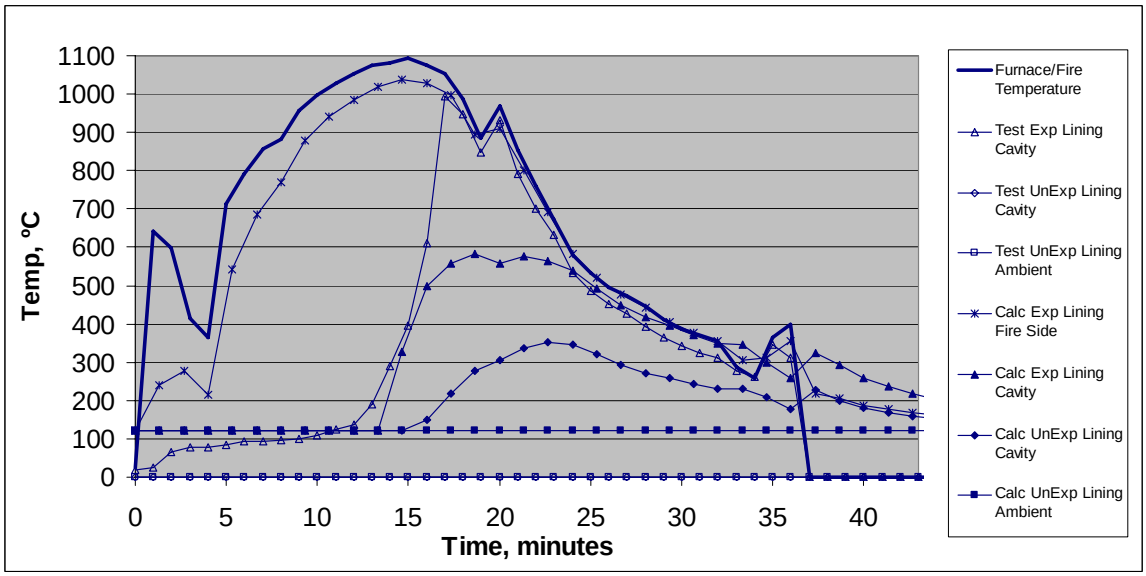

Figure A5.9 Jones Test FP2879

(Severe Furnace Test, 13 GIB® Standard on Steel studs)

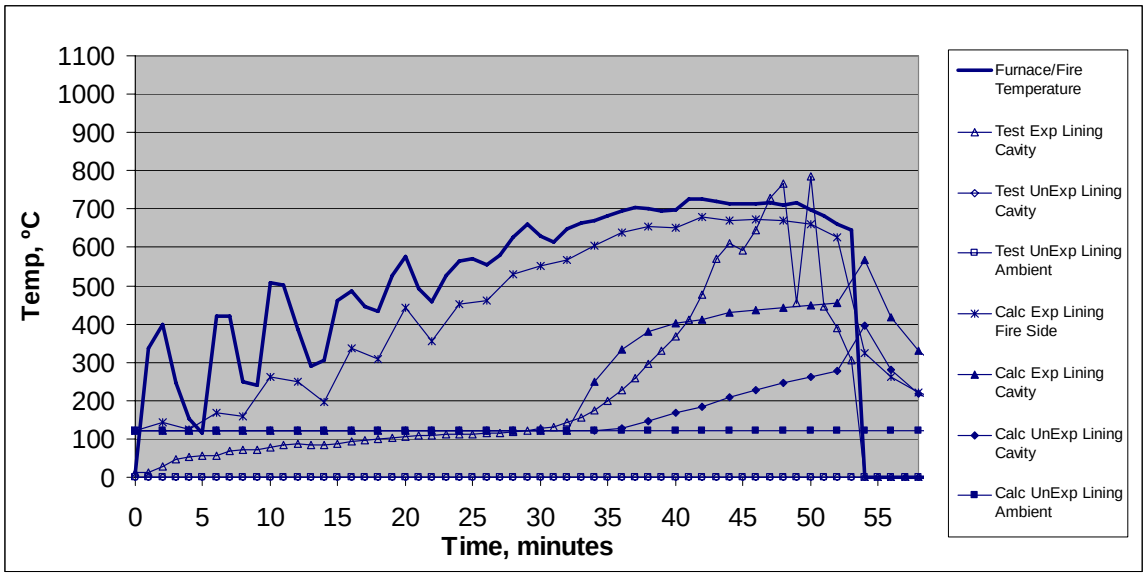

Figure A5.10 Jones Test FP2880

(Moderate Furnace Test, 13 GIB® Standard on Steel studs)

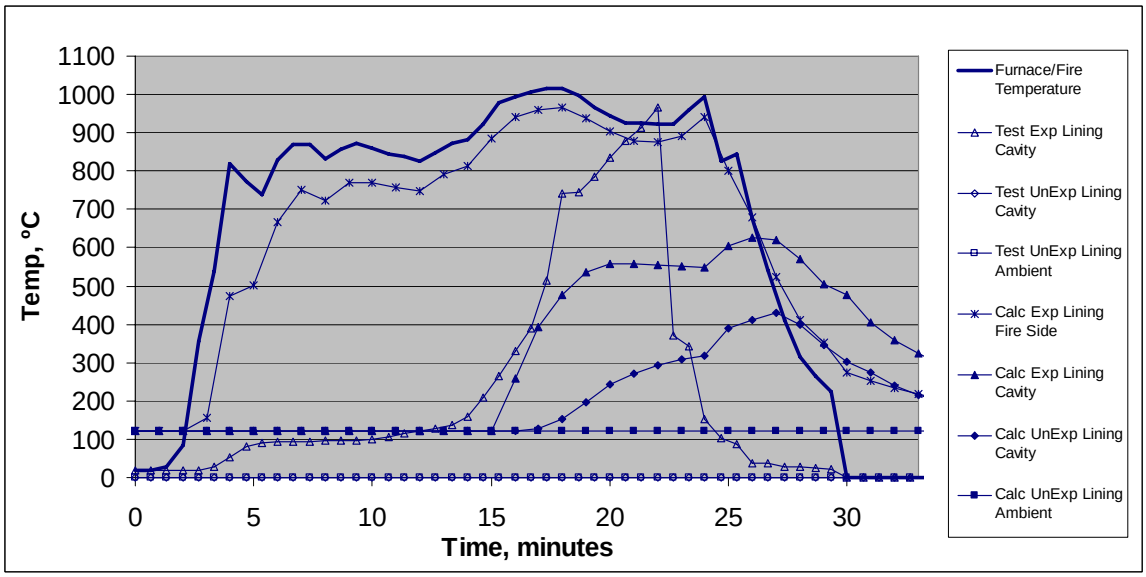

Figure A5.11 Nyman Test FQ0590_A

(Compartment Fire Test, 13 GIB® Standard on Steel studs)

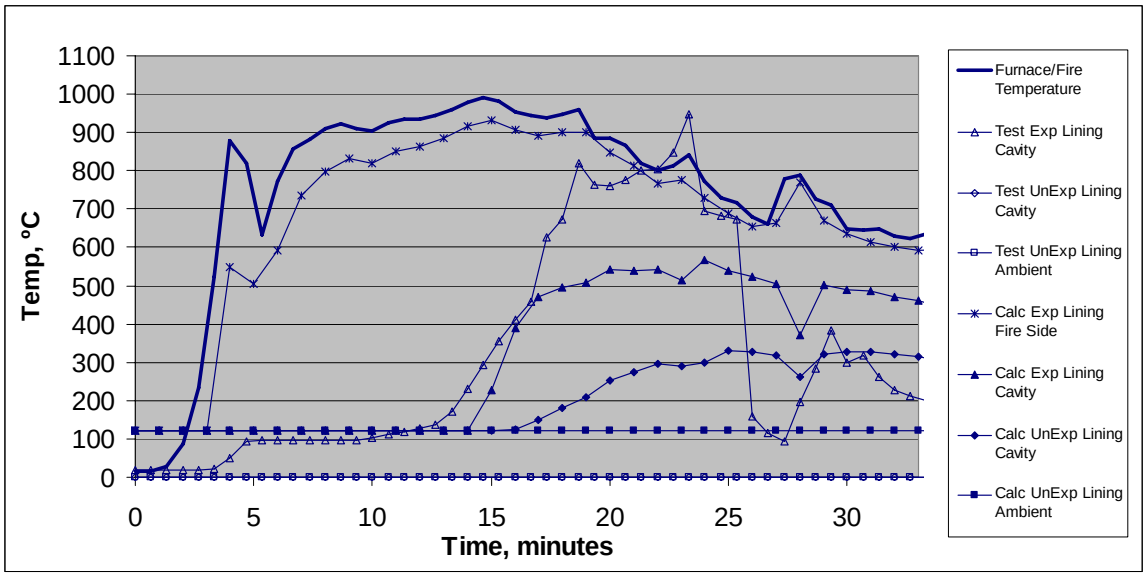

Figure A5.12 Nyman Test FQ0590_C

(Compartment Fire Test, 13 GIB® Standard on Steel studs)

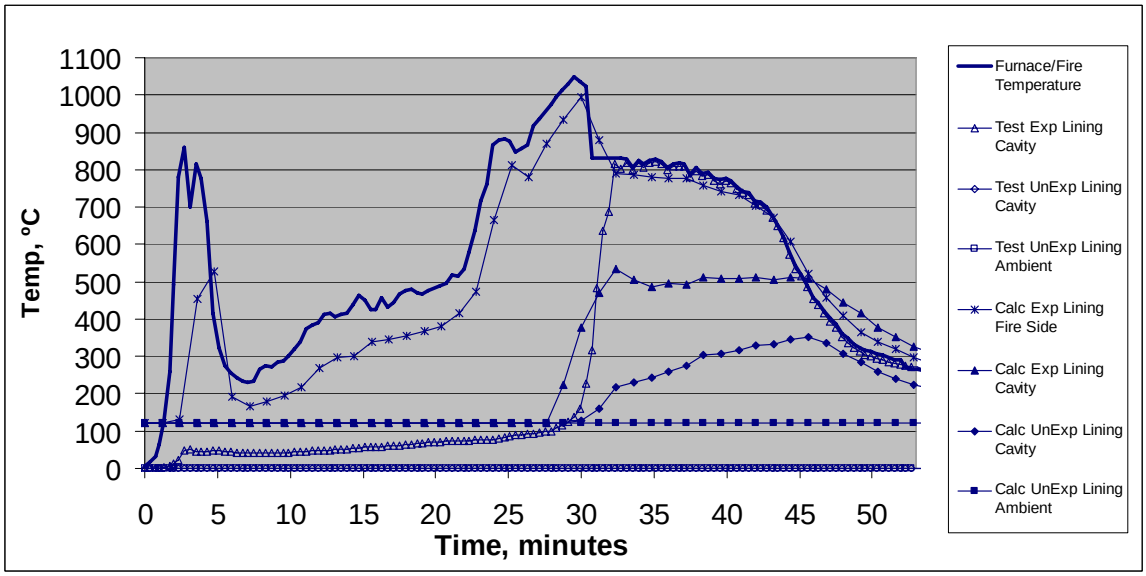

Figure A5.13 Brown Test FQ5013_1

(Compartment Fire Test, 13 GIB® Standard on Steel ceiling battens)

Test data from two 10mm GIB Fyreline® tests is also available. In the following graphs the material properties for 13mm GIB Fyreline® were changed in proportion to the relative densities. The enthaply was reduced by 7% and the thermal conductivity increased by 7%. The wallboard thickness was reduced to 0.010m.

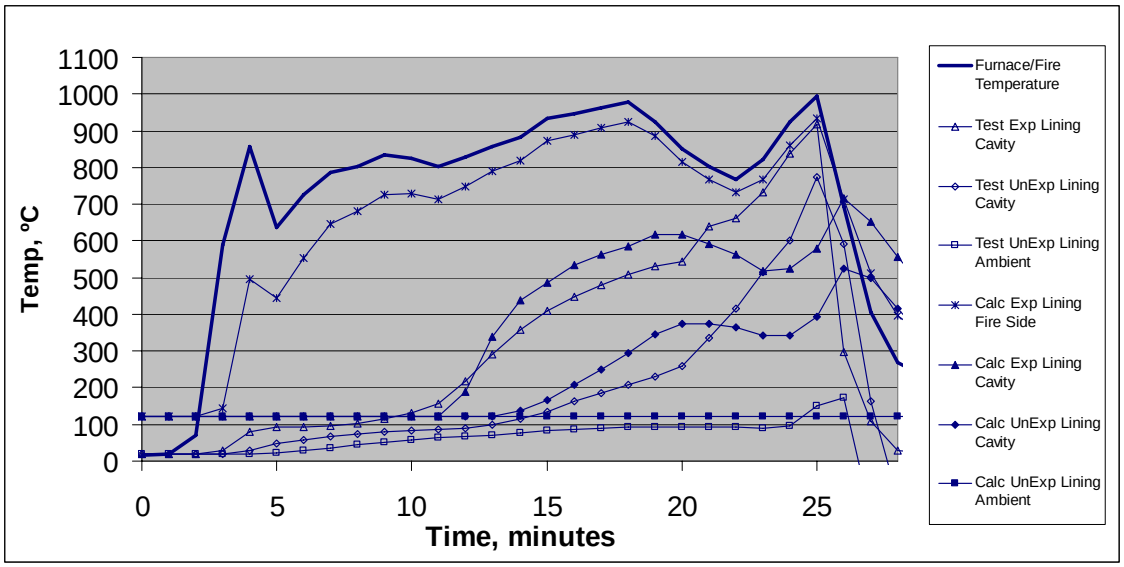

Figure A5.14 Nyman Test FQ0590_A

(Compartment Fire Test, 10 GIB Fyreline® on Timber Studs)

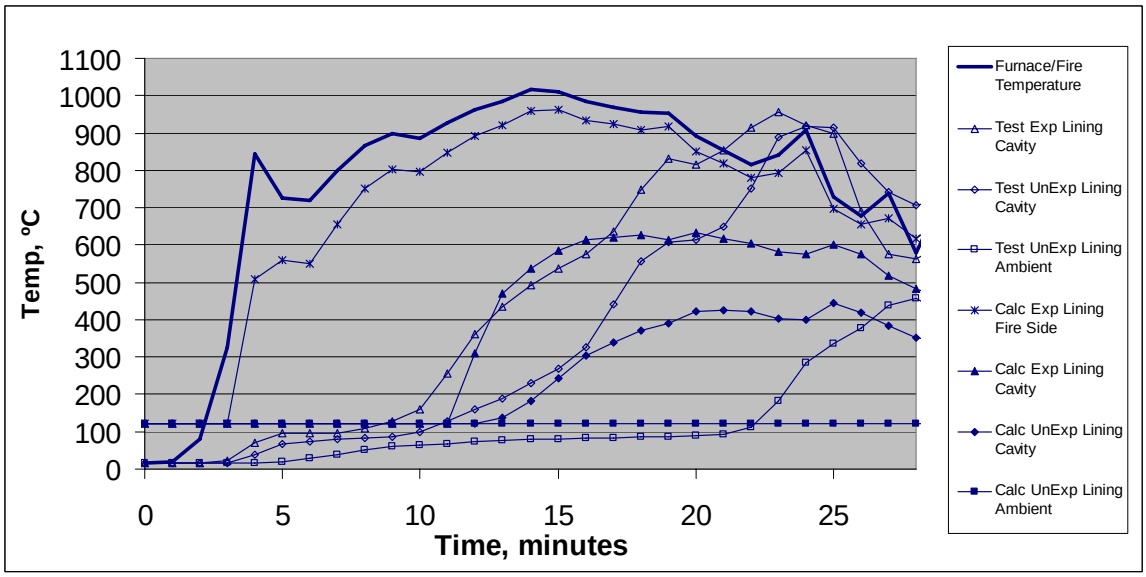

Figure A5.15 Nyman Test FQ0590_C

(Compartment Fire Test, 10 GIB Fyreline® on Timber Studs)